CHAPTER 7

Scenarios and Information for Policymakers

About the cover image:
The Montreal Protocol on Substances that Deplete the Ozone Layer has been ratified by every country on Earth – all 198 United Nations Member States.

Photo credit: MyCreative via Adobe Stock

CHAPTER 7

Scenarios and Information for Policymakers

Lead Authors : John S. Daniel
Stefan Reimann

Coauthors : Paul Ashford
Eric L. Fleming
Ryan Hossaini
Megan J. Lickley
Robyn Schofield
Helen Walter-Terrinoni

Contributing Authors : Laura McBride
Sunyoung Park
Martin N. Ross
Ross J. Salawitch
David Sherry
Susann Tegtmeier
Guus J. M. Velders

Review Editors : Lambert J. M. Kuijpers
Donald J. Wuebbles

CONTENTS

Chapter 7: Scenarios and Information for Policymakers

SCIENTIFIC SUMMARY

In its evaluation of future scenarios, this chapter uses reduced complexity models to calculate future impacts on ozone and climate. These models supplement the results from more complex models discussed in Chapters 3–6, with the added advantage that the simpler framework allows exploration of a greater number of scenarios and sensitivity experiments.

Post-Kigali Information of Interest

- **The Kigali Amendment to the Montreal Protocol, along with regional and national regulatory and voluntary actions taken before Kigali entered into force, is expected to substantially limit future climate forcing by HFCs.** Assuming global compliance with the Kigali Amendment, it is expected that HFCs will cause a peak radiative forcing of about 100 mW m^{-2} by mid-century. This may be compared to some past projections of forcing absent the Kigali Amendment or regulation under another convention, the highest being in excess of 400 mW m^{-2} in 2050, with substantial increases after that. Given the regional and national regulatory and voluntary actions taken before Kigali entered into force, and assuming global adherence to the Kigali Amendment to the Montreal Protocol, the contribution of HFCs to global annual average warming is projected to be 0.04 °C in 2100 (*Chapter 2*), with a continued decline after that time.
- **The elimination of all long-lived HFC emissions (including HFC-23) from 2023 onward represents an extreme example of the potential opportunities for future HFC reductions and would reduce the average radiative forcing over 2023–2100 by 79 mW m^{-2}**, with additional benefits continuing after 2100. This is more than twice the benefit of eliminating all controlled ODS emissions from the baseline scenario and would reduce the warming attributable to all HFCs to less than 0.01 °C by 2100. Of the 79 mW m^{-2}, 51 mW m^{-2} arises from future production and usage of long-lived HFCs (excluding HFC-23), 16 mW m^{-2} comes from future emissions from current banks, and 11 mW m^{-2} comes from emissions of HFC-23.
- **If emissions of HFC-23, a potent greenhouse gas, remain at the current relative level compared with HCFC-22 production, HFC-23 has the potential to cause about half of the climate forcing (30 mW m^{-2}) of all the other HFCs, combined, by 2100.** HFC-23 is emitted into the atmosphere mainly as a by-product from the production of HCFC-22. Its emissions relative to the amounts of HCFC-22 produced have not changed much in recent years and are higher than would be expected if state-of-the-art destruction had been performed during the HCFC-22 production process. While the Kigali Amendment to the Montreal Protocol requires that HFC-23 be "destroyed to the extent practicable," this requirement and the connected reporting of emissions went into effect only on 1 January 2020, and thus reporting is still incomplete and the global response is unclear. Through 2019, the emissions of HFC-23 as a fraction of HCFC-22 production indicate that a considerable part of the produced HFC-23 was still being released unabated into the atmosphere.
- **Other sources of HFC-23 emissions to the atmosphere may exist and could contribute to its atmospheric burden.** There could be contributions to HFC-23 abundances through formation and loss during the production of tetrafluoroethene (TFE) and from the incineration of HCFC-22. Furthermore, direct emissions could grow from the use of HFC-23 in low-temperature refrigeration, although it is not the only refrigerant used in this application.
- **The Kigali Amendment's control of high-GWP HFCs is expected to lead to overwhelmingly positive climate benefits. Nevertheless, there is a potential for certain negative side effects.** Hydrofluoroolefins (HFOs) are increasingly used for replacing high-global warming potential (GWP) HFCs in refrigeration, foam blowing, and various other applications. This replacement leads to less climate change. However, high-volume usage of CCl_4 (carbon tetrachloride) as a feedstock in the production of HFOs, a usage and production not controlled by the Montreal Protocol, could lead to sustained elevated abundances of CCl_4 if current techniques are continued and some fraction of feedstock production continues to be emitted. A second side effect is that HFO-1234yf emitted into the atmosphere will be fully converted to the stable trifluoroacetic acid (TFA; see below).
- **Trifluoroacetic acid (TFA), which is produced in the atmosphere from the degradation of HFCs, HCFCs, HFOs, and HCFOs, is not expected to harm the environment over the next few decades, although some regional concerns have been raised; periodic evaluation of this assessment is suggested, as important gaps in our understanding remain.** This assessment is based on updated estimates of the TFA formation from current atmospheric concentrations of HFCs and HCFCs (hydrochlorofluorocarbons) and their projected decline, as well as the expected increasing abundance of HFOs as HFC and HCFC replacements within the next years. With long-lived HFCs being replaced with high-TFA-producing, short-lived HFOs, more TFA will be formed in the atmosphere. Because of the shorter lifetime of HFOs, this TFA is expected to be deposited nearer to the location of emissions. Other anthropogenic sources of TFA, such as the incineration of polytetrafluoroethene (PTFE), could also contribute. In view of changing and potential unknown sources, concentrations of TFA should be monitored for changes in different parts of the environment, with a special focus on highly populated regions and on the remote ocean.

Updates on the Climate Impact of Gases Controlled by the Montreal Protocol

- **In the baseline scenario, future emissions of HFCs (excluding HFC-23), HFC-23, HCFCs, and CFCs contribute**

approximately 68, 11, 9, and 9 mW m^{-2} to radiative forcing, respectively, averaged over the 2023–2100 period. Of the 68 mW m^{-2} from HFCs, 51 mW m^{-2} arise from future production. For reference, CO_2 (carbon dioxide) emissions from fossil fuel usage over this time period are projected to contribute an average of about 3250 mW m^{-2} in the SSP2-4.5 scenario. The total radiative forcing from CFCs, HCFCs, and their HFC replacements is projected to continue to remain roughly constant for the next decade or two. After about 2040, the ODS and HFC restrictions of the Montreal Protocol, if adhered to, are expected to ensure a continued decline in the total RF from ODSs and their replacements. Previous expected increases in RF driven by projected HFC increases throughout the century are now mitigated by assumed compliance with the Kigali Amendment.

- **The effective radiative forcing of the halocarbons has been revised to encompass lower values due to a larger range of estimated negative forcing from the ozone depletion they cause.** This offset of the halocarbon direct radiative forcing remains highly uncertain.

Ozone-Depleting Substances (ODSs) and Their Replacements: Impacts on Ozone and Climate

Below, we discuss potential trajectories of equivalent effective stratospheric chlorine (EESC; a proxy for ozone depletion) and radiative forcing (a proxy for climate change) that result from our current understanding of the emissions of individual gases or groups of gases and the processes that lead to these emissions. We reference these potential changes to the so-called baseline scenario, which should be considered a plausible future pathway for these gases that is consistent with the controls of the Montreal Protocol. The specific assumptions made in the baseline scenario can be extremely important to the results. Note that the combined impact of changing assumptions is not always simply the addition of each of the changes. It is also important to recognize that the return date of EESC to 1980 levels is quite sensitive to any change in the EESC concentration because of the relatively small rate at which the EESC is projected to decline around the middle of this century. While a change in the return date to 1980 EESC levels measured in tenths of years or even a few years cannot be discerned in the atmosphere, primarily due to natural variability, this metric can be useful for comparing various alternative ODS scenarios.

It should also be noted that the EESC formalism adopted here is the same one that was applied in Appendix 6C of the 2018 Assessment and reflects our improved scientific understanding of EESC (see Section 7.3*). This alters the time evolution of EESC and dates when EESC returns to 1980 levels when compared with the older approach used in the main part of Chapter 6 of the 2018 Assessment, but it has little effect on the relative impacts of the various alternative future scenarios. If EESC comparisons are made with the 2018 Assessment, it is most appropriate to compare to those found in Appendix 6C rather than in Table 6-5 of that Assessment.*

- **Changes in the current baseline scenario lead to a delay in the return of mid-latitude and polar EESC to 1980 levels by 4 years and 7 years, respectively, compared with the baseline scenario in the previous Assessment. This is due mainly to a larger assessed CFC-11 bank, and to a lesser degree, to a larger assessed CFC-12 bank.** The larger bank for CFC-11 does not include any explicit increase due to unreported production over the past decade, as that amount is highly uncertain.
- **The unexpected emissions of CFC-11 declined after 2018. The continued elimination of this emission and the production that has caused it will prevent a substantial impact on ozone and climate.** Cumulative unexpected emissions over 2012–2019 have been estimated at 120–440 Gg. Since then, these annual emissions have diminished substantially from their peak amount. The integrated emissions over this period are calculated to lead to a delay in the return of mid-latitude EESC to 1980 levels by about one year and to cause an additional radiative forcing of 2 mW m^{-2} averaged over 2023–2100. It is unclear how much of the production that led to these emissions has gone into banks, as opposed to having already been emitted. If the unexpected emissions over 2012–2019 were associated with the production of insulating foams, it is estimated that they would have accounted for 25% to 45% of the unreported production, with the rest (146–1320 Gg) going into the CFC-11 bank. The impact of any increase in the bank can be estimated from knowing that a hypothetical 1000 Gg added to the 2020 bank delays the return of mid-latitude EESC to 1980 levels by almost four years and leads to an additional averaged radiative forcing over 2023–2100 of about 6 mW m^{-2}.
- **The hypothetical elimination of all future ODS emissions would bring forward the return of mid-latitude and polar EESC to 1980 levels by 16 years and 19 years, respectively, and increase the average of global stratospheric ozone levels in the period 2020–2070 by about 2 DU.** It would also reduce average radiative forcing by 31 mW m^{-2} averaged over 2023–2100. These emissions are dominated by the release from current banks, with a smaller contribution from future production of ODSs that is controlled by the Montreal Protocol and emissions associated with production intended for feedstock purposes. Estimates of bank sizes are highly uncertain though; the bank approach used in the scenarios here has resulted in substantially larger 2020 banks than estimated in the previous Assessment.
- **In the baseline scenario, future emissions from current CFC banks contribute more to EESC than do emissions from either HCFC banks or halon banks.** However, given the uncertainty in estimates of current bank sizes, these differences are likely not statistically significant. An elimination of the emissions from the CFC banks are calculated to bring forward the return of mid-latitude EESC to 1980 levels by about 5 years. In this chapter, there is no evaluation made regarding the accessibility of various banks in terms of recapture and destruction.
- **In the baseline scenario, future emissions from current HCFC banks contribute more to climate change than do future emissions from either CFC banks or halon banks.** However, the differences in the climate impacts between the banks of HCFCs and CFCs are likely not statistically significant. Again, there is no evaluation made regarding the accessibility of various banks in terms of recapture and destruction.

- **Elimination of future emissions of methyl bromide (CH_3Br) from quarantine and preshipment (QPS) applications, not controlled by the Montreal Protocol, would accelerate the return of mid-latitude and polar EESC to 1980 levels by about two years and would increase globally averaged total ozone by 0.2 DU when averaged over 2020–2070.** Production for QPS use has remained relatively stable over the last two decades and now constitutes almost 99% of reported production of CH_3Br, since emissions from other uses have declined dramatically. Non-QPS applications of CH_3Br were completely phased out in 2015, except for approved critical use exemptions (CUEs). These CUEs have declined by a factor of ~200 since 2005 and make up the remaining ~1% of reported production. CH_3Br has little direct impact on climate.
- **Otherwise controlled ODSs have increasingly been used as feedstocks. With estimated emission rates of 2–4% (4.3% for CCl_4) from the produced ODSs, this has resulted in estimated emissions associated with ODS feedstock applications of 37–59 Gg (15–19 ODP-Gg) in 2019. The influence on ozone of these emissions was dominated by emissions from the feedstock use of CCl_4. When compared to the baseline scenario, in which these emissions continue at current levels, an elimination of emissions associated with feedstock use would bring forward the return of mid-latitude and polar EESC to 1980 levels by about 4 and 5 years, respectively.** Between 2009 and 2019, the mass of ODSs used as feedstocks, which is not controlled under the Protocol, increased by 75%. When expressed in units of Gg ODP (Gg multiplied by the ozone depletion potential), the increase in feedstock-linked production was only 41% over the same period, as HCFC-22, with a relatively low ODP, was responsible for the highest growth. Eliminating all these emissions in the future would reduce averaged radiative forcing by 6 mW m^{-2} compared with the baseline scenario.
- **Of the feedstock production reported, estimated emissions from CCl_4 and HCFC production dominate the impact on climate over the coming decades. These two groups lead to an increased average radiative forcing over 2023–2100 of 5 mW m^{-2} in the baseline scenario.** The size of this climate effect is dependent on the assumptions made in the baseline scenario regarding feedstock production growth.
- **CCl_4 feedstock production and usage increased by a factor of about two within the last decade. If CCl_4 emissions associated with these allowed uses continue to grow through 2030 as they have been growing over the past decade, future CCl_4 atmospheric concentrations will decline more slowly and will be about twice as high (+20 ppt) in 2100 than in the baseline scenario, in which feedstock-related emissions remain constant.** As reported in the 2018 Assessment, CCl_4 emissions inferred from atmospheric observations continue to be considerably higher than those estimated from feedstock uses, as reported to the United Nations Environment Programme (UNEP), and other known sources. CCl_4 emissions related to its feedstock production and usage have been assessed to be 4.3% of the produced amount of CCl_4, with a relatively large associated uncertainty. Calculated as ODP-weighted emissions, the emissions from feedstock use of CCl_4 in 2019 was 11.2 ODP-Gg yr^{-1}, or 60–74% of all feedstock-related emissions. This is important, as the usage of CCl_4 is projected to continue to increase because of its application in the growing production of HFOs in the replacement of the long-lived HFCs. An elimination of all future CCl_4 emissions associated with feedstock usage would reduce radiative forcing by about 2 mW m^{-2} compared with the baseline scenario when averaged over 2023–2100.
- **In addition to CCl_4, the most important contributions to ODP-weighted emissions from other ODSs used as feedstock are from CFC-113 and CFC-114 (2.3–4.6 ODP-Gg), from HCFC-22 (0.5–1.1 ODP-Gg), and from the sum of other HCFCs (0.1–0.3 ODP-Gg), with the highest contribution from HCFC-142b.** These values are based on estimated emissions of 2–4% relative to the production amount. The increased use of HCFC-22 and other HCFCs as feedstocks for fluoropolymer production within the last decades is expected to continue into the future. On the other hand, the usage of feedstock chemicals for the production of HFCs will likely decline because of the Kigali Amendment.
- **The production and usage of short-lived chlorinated solvents is not controlled by the Montreal Protocol, and some are used in large amounts. Their impact on stratospheric ozone, and their ODPs, vary depending on the season and location of emissions and could grow in the future even as emissions from long-lived ODSs decline.** More than 1600 Gg of $CHCl_3$ (chloroform) are used as feedstock in the production of HCFC-22. Emissions from $CHCl_3$ used as a feedstock are comparable to its solvent emissions. CH_2Cl_2 (dichloromethane), TCE (trichloroethene), and PCE (perchloroethene) are also used as feedstock chemicals, although their emissions are dominated by emissive uses (e.g., from solvents).
- **Sustained increases in anthropogenic chlorinated very short-lived substance (VSLS) emissions, as seen for CH_2Cl_2 over the last two decades, would lead to more stratospheric ozone depletion in the future.** While observed growth rates of CH_2Cl_2 have been highly variable and future projections are believed to be highly uncertain, emissions have continued to increase since the last Assessment. If emission rates remain constant at their present level into the future, CH_2Cl_2 is projected to deplete 0.8–1.7 DU averaged over 2020 to 2070 compared to a case of zero future emissions. Any reduction in the production and consumption of CH_2Cl_2 would have a rapid impact on ozone, since this VSLS is both emitted soon after production and is cleansed out of the stratosphere within a few years.
- **A reduction in future N_2O emissions from that in the baseline scenario (SSP2-4.5) to that in the SSP scenario with the strongest N_2O mitigation (SSP1-1.9) results in a 0.5 DU increase in ozone averaged over 2020 to 2070, or about one-quarter of the impact of eliminating all emissions from controlled ODSs beginning in 2023.** This emission reduction also leads to a radiative forcing reduction of 43 mW m^{-2} averaged over 2023–2100. The magnitude of this N_2O reduction represents a decrease in anthropogenic N_2O emissions of 3% compared with the baseline scenario when averaged over 2020–2070.

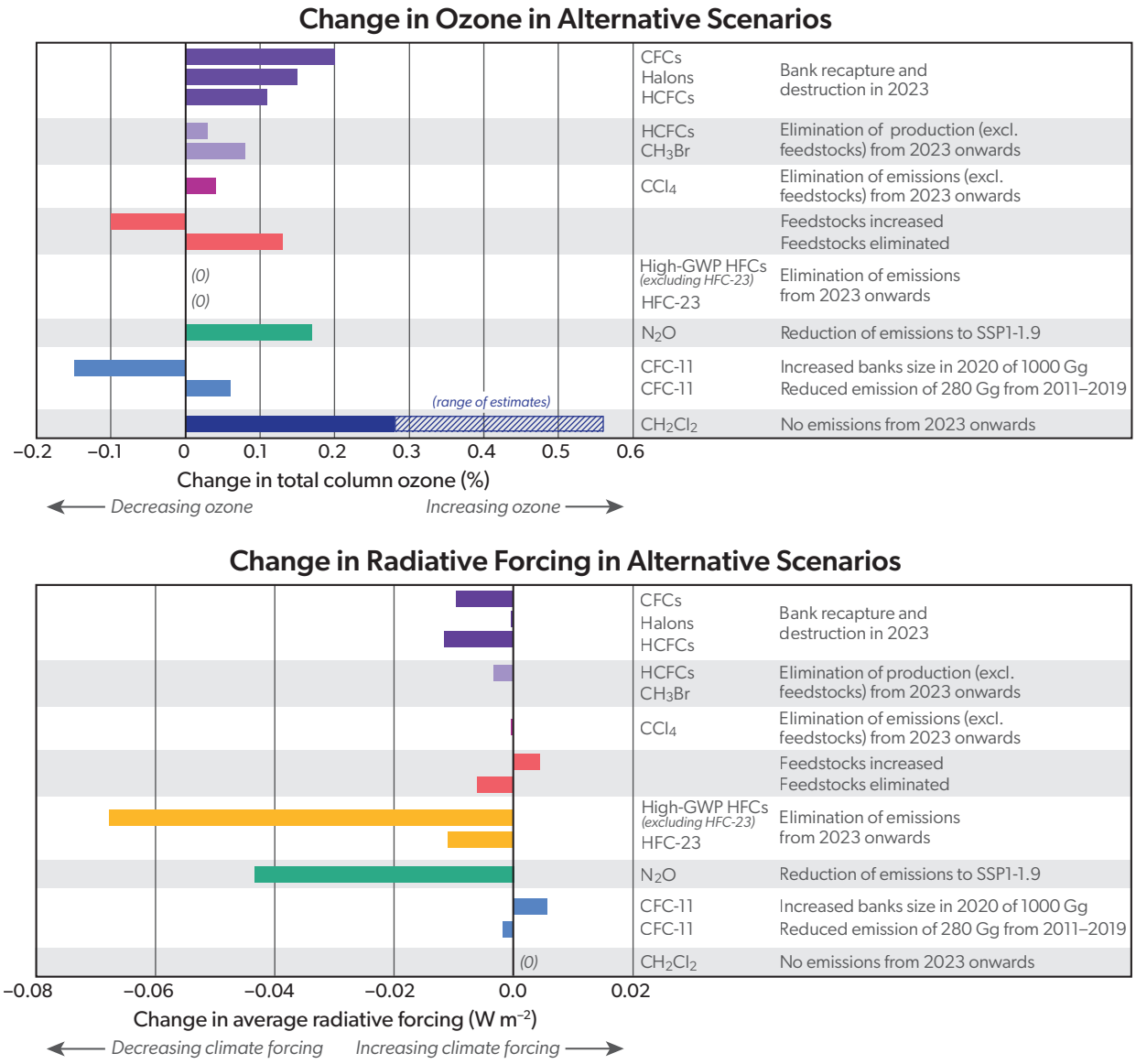

Figure 7-1. Impacts of various alternative scenarios and test cases on total column ozone (averaged over 2020 through 2070) and radiative forcing of climate (averaged over 2023 through 2100) compared with the baseline scenario. The scenarios and cases include reduced N_2O emissions (SSP1-1.9 scenario), elimination of emissions for HFCs, HFC-23, CH_2Cl_2, and CCl_4 (excluding emissions from feedstock production and usage) starting in 2023, elimination of future production of CH_3Br and HCFCs starting in 2023 (excluding feedstock production and usage), and elimination and destruction of banks of halons, HCFCs and CFCs in 2023. Also considered are the unexpected CFC-11 emissions over 2012–2019 (assumed to be 280 Gg in total), an additional 1000 Gg in the 2020 CFC-11 bank, elimination of all feedstock-related emissions starting in 2023, and a case in which feedstock-related emissions are allowed to grow at their current growth rates through 2030 and are then held constant. Potential climate benefits from improved energy efficiency in the refrigeration and air conditioning sector are not included here, and are thought to have the potential to have an impact much larger than that of any of the scenarios and cases considered here. For reference, current total column ozone depletion is about 2% when averaged over 60°S–60°N, and the current radiative forcing from CO_2 is about 2 W m^{-2}.

Impacts of Mitigation Options and Particular Scenarios

Figure 7.1 (also shown as Figure ES-8 in this document) shows the ozone and climate-relevant changes that would occur if various actions were to be taken. These changes are shown as the differences in global total column ozone averaged over 2020–2070 and in radiative forcing averaged over 2023–2100, both relative to the baseline scenario, which includes the Kigali Amendment controls for HFCs in Annex F, Group 1. The options available to hasten the recovery of the ozone layer are somewhat limited, mostly because past actions have already been very successful at reducing emissions of ODSs and their replacements.

- For the ODSs, the single most effective ozone depletion and climate change mitigation option, not considering technical feasibility, is bank recapture and destruction of the CFC banks; however, large uncertainties in the CFC-11 and CFC-12 banks have been reported in the literature, with the recent production associated with the unexpected emissions of CFC-11 further adding to uncertainties in the bank sizes. Furthermore, no assessment has been made here regarding the fraction of the banks that are accessible for capture or the fraction that are active.
- For CH_3Br, elimination of production for currently uncontrolled QPS applications is shown.
- For CCl_4, the impact of eliminating emissions from controlled production starting in 2023 is shown.
- For CH_2Cl_2, an uncontrolled ozone-depleting gas with an atmospheric lifetime of ~180 days, future emissions continue to have the potential to lead to more ozone depletion than emissions from many of the other alternative scenarios explored here. CH_2Cl_2 is emitted mainly from Asia, and emissions and concentrations have been growing steadily in recent years.
- For N_2O, the impacts of a strong mitigation scenario (SSP1-1.9) are compared to the base-line scenario (SSP2-4.5).
- For HFCs, the impact of a hypothetical complete global phaseout of production (excluding HFC-23) starting in 2023 is shown. An additional scenario is included in which HFC-23 emissions are reduced to virtually zero, consistent with the current best practice of incineration, rather than the assumed emissions rate of 1.6% of HCFC-22 production included in the baseline scenario, in order to show the effect of nearly eliminating by-product emissions.

Updates on Impacts of Greenhouse Gases and Other Processes on Future Stratospheric Ozone

In this section, we summarize potentially important impacts on the future of the ozone layer that could result from anthropogenic activity not associated with ODS or replacement production and consumption and that is not controlled by the Montreal Protocol. Net stratospheric cooling, which is projected in many scenarios due to increases in greenhouse gas concentrations, is predicted to lead to increases in upper-stratospheric ozone at all latitudes, with a more complex pattern of ozone changes in the lower stratosphere, including a decrease at tropical latitudes driven by changes in dynamics and transport; these processes are discussed in detail in Chapters 3 *and* 4*. Potential climate intervention activities that may affect ozone are discussed in* Chapter 6.

- **Our ability to accurately predict future changes in the ozone layer continues to be limited more by uncertainties in the future levels of CO_2, CH_4 (methane), and N_2O than by uncertainties in the levels of ODSs.** Global mean tropospheric warming, as well as stratospheric cooling, will drive ozone changes through both atmospheric circulation and chemistry, while changing CH_4 and N_2O will lead to further changes in the chemistry associated with stratospheric ozone. Future ozone levels depend on the path of greenhouse gas emissions and aerosol abundances, as well as the sensitivity of the climate system to these emissions.
- **Rocket launches presently have a small effect on total stratospheric ozone (much less than 0.1%). However, rocket systems using new propellants (e.g., hydrogen and methane) could exert a substantial influence in the future.** The future scenarios of space industry emissions consider the potential for a significant increase in launch rates, the adoption of new launch-vehicle propellants, and an increase in middle-atmosphere aerosol and the production of NO (nitrogen monoxide) by reentering space debris. Many of the impacts of rocket activity involve chemistry and radiative interactions that are poorly understood and, in some cases, not yet studied. Furthermore, the planned development of massive low-Earth orbit satellite constellations (megaconstellations) could cause particulates resulting from space debris reentry to become comparable to that from launch emissions; little is known about the impacts of reentry particles, and their accumulation in the stratosphere has not been modeled. The uncertainties in these processes and in any potential new emission sources limit the confidence level of predictions of present and future impacts of space industry emissions on stratospheric ozone. Periodic assessment and critical knowledge gap identification are warranted.
- **The influence of hydrogen as an energy carrier on stratospheric ozone remains uncertain.** Hydrogen-based energy will likely play a role in a future non- or reduced-fossil economy. However, if it is not a dominant energy carrier, it is unlikely that it will significantly affect ozone. This statement should be reevaluated periodically.
- **The impacts of supersonic aircraft on stratospheric ozone are discussed in *Chapter 4*.**
- **Climate intervention approaches that affect the stratospheric ozone layer are discussed in *Chapter 6*.**

7.1 INTRODUCTION

As documented by many prior WMO Ozone Assessments, control measures introduced under the Montreal Protocol and its Amendments have been resoundingly successful, as evidenced by the 99% reduction in the reported production of ODSs since the peak in the late 1980s. As the ozone-depleting substances (ODSs) have been successfully replaced by hydrofluorocarbons (HFCs) and through other measures (*Chapters 1* and *2*), indications of reduced ozone depletion are emerging (*Chapters 3* and *4*). While HFCs do not contribute to ozone depletion, they do contribute to climate change and were recently included in the Montreal Protocol through the Kigali Amendment.

This chapter provides an update to Chapter 6 of the 2018 Assessment. It focuses on possible options and sensitivity scenarios to support policymakers in decisions related to further protecting stratospheric ozone and minimizing effects on climate from ODSs and their replacements. As production and consumption of controlled ODSs have continued to decline, policy options for reducing their future emissions have become somewhat more limited; however, some options remain that have notable potential for ozone and climate protection. Some of these are related to ODSs and their replacements, and some are not.

Policy-relevant issues discussed in this chapter include: 1) climate and ozone depletion impacts of future ODS and HFC emissions from multiple sources, including continued production for use as feedstocks; 2) future climate and/or ozone depletion impacts from continued production and use of other short- and long-lived compounds not currently controlled; 3) other future environmental effects of ODSs, HFCs, and short-lived replacement compounds; and 4) potential impacts of future high-altitude transportation and satellite activities.

In the rest of this section, key points from WMO (2018) are summarized, followed by a description of the objectives and the contents of this chapter.

7.1.1 Summary of Findings from the Previous Assessment

The Kigali Amendment to the Montreal Protocol went into force on 1 January 2019, around the time the 2018 Ozone Assessment was published. Some of the key findings from that Assessment involved the Kigali Amendment. Specifically, the large expected climate benefit of that Amendment was assessed, and the benefits of faster and deeper controls on HFC production and consumption were explored. Other key findings in Chapter 6 of the previous Assessment (Carpenter, Daniel et al., 2018) included the following:

- A proposed N_2O mitigation option was highlighted as having a larger impact on CO_2-equivalent emissions over 2020–2060 than even the elimination of all emissions of controlled ODSs.
- Emissions of ODSs from the estimated banks were assessed to be slightly more important than future production for ozone depletion over the next four decades.
- CCl_4 emissions, as projected, continued to have the largest influence on future stratospheric ozone of all controlled ODSs.
- The importance of destroying HFC-23 (a by-product of the production of HCFC-22) to limit its future climate impact was underscored.
- The role of climate change, and specifically the influence of future CO_2 levels, on stratospheric ozone was highlighted.
- The existence of large gaps in our understanding of how future rocket activity might affect stratospheric ozone levels was raised.
- The continuing gaps in our understanding of the trifluoroacetic acid (TFA) budget were pointed out, along with the expectation that TFA would not rise to levels that would harm the environment over the next few decades.

7.1.2 Key Issues to Be Addressed in This Chapter

In this chapter, we describe updates to our understanding of actions related to the Montreal Protocol and its Amendments that could alter the recovery of the ozone layer and impact Earth's climate or other parts of the natural environment. In addition, other potential threats to and influences on the ozone layer are discussed. As in previous Assessments, we use equivalent effective stratospheric chlorine (EESC) as a proxy for the amount of stratospheric ozone depletion caused by ODSs that contain chlorine and/or bromine and reside in the atmosphere for more than a few months. The return of EESC to 1980 values is used as a metric to compare different future scenarios related to altered production, emissions, and banks of ozone-depleting ODSs on ozone layer recovery. The EESC formulation used here is based on Engel et al. (2017) and was described in Section 6.4.1 in Carpenter, Daniel et al. (2018), with scenario results shown in Appendix 6C of that chapter. This represents a different approach to calculating EESC than used in Ozone Assessments before 2018.

In addition to EESC, we use 2-D model simulations to estimate changes in future ozone depletion for various scenarios. The 2-D model is needed to quantify the effect of the various scenarios on ozone itself and to evaluate compounds that cannot be easily quantified with EESC or do not affect ozone through halogen chemistry (e.g., CO_2, CH_4, and N_2O). The 2-D model is used here in scenario evaluation rather than a 3-D model since it has been shown to capture the key necessary processes for emissions of long-lived source gases, including long-term changes in EESC, the Brewer-Dobson circulation (as reflected by the stratospheric age of air), and projections of future ozone (see, e.g., Appendix 6B of WMO, 2018). Thus, the substantially increased computational cost of running a 3-D model is deemed too great for the added benefit. The exception to this is when considering the short-lived CH_2Cl_2, for which we use published 3-D model calculations of ozone depletion potential (ODPs) to estimate the impact of future emissions scenarios on ozone depletion. Note that 3-D model projections of global and polar ozone and analyses of expected recovery dates are presented in *Chapters 3* and *4*. These 3-D model calculations and the 2-D model include changes in greenhouse gas levels and in atmospheric transport, and thus their recovery dates are not expected to be the same as the recovery dates determined from EESC alone.

Our ability to reasonably constrain future changes in the ozone layer continues to be limited more by uncertainties in the future levels of CO_2, CH_4, and N_2O than by uncertainties in the levels of ODSs, owing to the fact that the Montreal Protocol has highly constrained future ODS trajectories. Importantly, ozone levels in some regions of the atmosphere could exceed historic natural levels if CO_2 and CH_4 mixing ratios, in particular, continue

to increase in the future, with possible consequences to humans and natural ecosystems, assuming natural levels represent a desired balance. The influence of CO_2 on stratospheric ozone occurs primarily through its role in the climate system as a driver of change in stratospheric temperatures and atmospheric circulation. The influences of CH_4 and N_2O occur primarily through their roles as chemical reagents in the atmosphere. ODSs themselves are greenhouse gases, and their influence on climate and ozone layer depletion are intricately intertwined. We discuss these influences separately for clarity of presentation.

A foundational aspect of this chapter is the choice of scenarios used to assess future possible impacts on ozone depletion and climate change. These scenarios begin with a baseline scenario, against which others are compared. The baseline scenario is not a "most likely" scenario, nor is it a prediction. It consists of a plausible set of well-defined production or emissions assumptions, depending on the gas. The primary purpose of the baseline and alternative scenarios is to assess the impacts of various sources of future production and emissions on ozone depletion and climate change. Notice that the various actions associated with the alternative scenarios discussed later in this chapter affect future ozone to a much smaller degree than what has already been accomplished by the Montreal Protocol. Some of the specific activities that could be important to future ozone depletion and climate change are explored in this chapter through simulations and include the following:

- Using the latest atmospheric observations of ODS mixing ratios, latest current bank estimates, and latest global lifetimes to develop new ODS scenarios; these scenarios are used to explore the impacts of future emissions from banks and production on the return of EESC to 1980 levels, on ozone depletion itself, as well as on climate forcing. In addition to scenarios in the previous Assessment, emissions from feedstock production and use are explicitly included for several ODSs.
- Generating future scenarios for the emissions of HFC-23, which is closely associated with the production of HCFC-22.
- Incorporating future emissions scenarios for the other key HFCs, developed in *Chapter 2*, into the analysis of future climate impacts from anthropogenic activities.
- Developing an analysis for assessing the future contribution of HFOs and HFCs to TFA in precipitation and in sea water.
- Providing an updated assessment of the potential impact of very short-lived substances (VSLSs) on future ozone depletion.
- Assessing plausible impacts of the recent unexpected emission and associated production of CFC-11 on future ozone depletion and discussing the current status and remaining key uncertainties associated with this issue.
- Using the latest generation of climate scenarios, which include greenhouse gas emissions and mixing ratios, to reassess the potential future impact of CO_2, CH_4, and N_2O on ozone abundances.
- Including an expanded modeling capability to explore the future impact of revised CFC-11 and CFC-12 bank estimates (unrelated to the unexpected emissions issue).
- Briefly summarizing the potential gains that can be achieved through a focus on energy efficiency in air-conditioning and refrigeration applications as the world transitions away from long-lived HFCs. This is discussed in more detail in *Chapter 2*.
- Assessing the potential impact of a foreseeable large increase in future rocket launches, including possible changes in their propellants, as well as estimating the effect of a planned fleet of new supersonic airplanes on the ozone layer.

7.2 ISSUES OF POTENTIAL IMPORTANCE TO STRATOSPHERIC OZONE AND CLIMATE

7.2.1 ODSs Controlled Under the Montreal Protocol and VSLSs

In this section, current and future emissions of ODSs and VSLSs are discussed. As emissive uses of ODSs are increasingly controlled by the Montreal Protocol, emissions from the direct application of these substances are now largely restricted to hydrochlorofluorocarbons (HCFCs) mostly from Article 5 countries, and to exempted applications of methyl bromide (CH_3Br). However, emissions are ongoing from built-in ODSs (i.e., banks) and from the usage of ODSs and VSLSs as building blocks in the synthesis of other chemicals (i.e., feedstocks). Additionally, some unintended emissions of halogenated intermediates and undesired by-products, which arise during the production of halogenated compounds, are occurring.

7.2.1.1 Emissions from Usage

Production and consumption of CFCs, CCl_4 (carbon tetrachloride), and CH_3CCl_3 (trichloroethane, methyl chloroform) have been banned for emissive uses under the Montreal Protocol. Nevertheless, because of the perceived use of CFC-11 in foam blowing in eastern China and potentially other parts of the world, emissions of CFC-11 increased between 2012 and 2018, when compared with the preceding years. After Montzka et al. (2018) and Rigby et al. (2019) highlighted this increase, emissions dropped considerably in 2019 (*Chapter 1*). WMO (2021) estimates that cumulative emissions that originated from this associated production were 120–440 Gg over 2012–2019. There are still large ongoing emissions of CCl_4 and, to a minor degree, of several CFCs and CH_3CCl_3. Large-scale unreported production seems to be an unlikely source for these compounds, but emissions from banks (*Section 7.2.1.2*) and fugitive emissions from losses during production and usage of feedstocks (*Section 7.2.1.3*) could be playing an important role.

For HCFCs, the overall demand for emissive uses has been declining for several years due to increasingly stringent controls by the Montreal Protocol and adequate financial support by the Multilateral Fund for conversions. The significant remaining applications in Article 5 countries are in the refrigeration, air-conditioning, and foam sectors. For refrigeration and air-conditioning, there is still demand for HCFC-22 for the servicing of existing equipment, as a substantial part of the charged amount is emitted over time. In non-Article 5 countries, where the infrastructure exists, the remaining HCFC-22 demand in the air-conditioning sector is now met from recovered and reclaimed HCFC-22 or from recycled materials. In the USA, there is no specified end-date for the use of reclaimed or recycled HCFC-22 in air-conditioning equipment, so emissions will continue at some level until all HCFC-22-based equipment has reached the end of its

operational life. In Article 5 countries, recovery is less likely, as newly produced chemical material continues to be available and reclamation infrastructure is less well established.

For the foam sector, HCFC-141b remains the primary ozone-depleting blowing agent still in use in Article 5 countries, albeit with some HCFC-22 and HCFC-142b used as gaseous blowing agents in extruded polystyrene. However, most, if not all, of this use is limited to those Article 5 countries where HCFC Phaseout Management Plans (HPMPs) are still ongoing. For foams, there is no economical recovery route for recycling the HCFC-141b that is already incorporated into products. Hence, any remaining demand in Article 5 countries will have to be met from new supplies. The Montreal Protocol has set the phaseout date for all newly produced HCFCs in Article 5 countries as 2030, but most HPMPs at the country level foresee phaseouts of use ahead of that date. The remaining uses of HCFC-141b as a blowing agent tend to be in smaller enterprises where the investment to use alternative blowing agents is prohibitive. For example, in the case of polyurethane spray foam applications, the use of hydrocarbon blowing agents has not been adopted for safety reasons. At the point of in situ applications of these spray foams, emissions of around 15–20% of the blowing agents in question occur.

CH_3Br is globally banned from use in agriculture with only critical-use exemptions (CUEs) allowed. However, quarantine and pre-shipment (QPS) uses are not restricted, albeit production for these uses has to be reported. CUEs declined from nearly 20,000 t in 2005 to currently <30 t (TEAP, 2021a). This amount is insignificant in comparison with the usage in QPS of about 9000 t in 2019 (*Chapter 1*).

Halons are completely banned except for critical uses, such as in civil aircraft. Fire extinguisher refilling uses recycled halons, for which a global market exists, and emissions are restricted to maintenance and to usage during fire events.

7.2.1.2 Emissions from Banks

When equipment is produced that contains halocarbons, a part of the quantity used is emitted during the production, while the rest is contained within the equipment for its intended use and is subject to later release. This reservoir of stored halocarbons within equipment is referred to as halocarbon banks. Quantifying existing banks and their contribution to future emissions is key to interpreting the sources of ongoing halocarbon emissions and estimating future potential emissions. **Box 7-1** explains the characteristics of banks and their long-term behavior, as well as the ways that have been used to calculate the amounts of ODSs and replacement compounds stored in banks at a given time. As discussed in *Section 7.4*, accurate knowledge of the sizes of current banks is a key aspect in projecting future ODS mixing ratios and the resulting ozone depletion as well as climate forcing.

Box 7-1. Banks

In the context of ODSs, "banks" refers to equipment and applications that contain ODSs. These ODSs will eventually be released to the atmosphere if pre-emptive action of capturing and destroying them is not taken. Bank characteristics, such as magnitude and release rates, differ by compound and their respective uses. For example, compounds used in foam have long residence times within their banks (~2% yr^{-1} release rates), uses such as refrigeration and air-conditioning have moderate residence times (~10% yr^{-1} release rates), and compounds in applications such as for aerosol generation and use as solvents are emitted quickly (~50–100% yr^{-1} release rates) (Ashford et al., 2004). Release rates also vary depending on the life cycle phase. The technological ease of bank capture depends on the type of application and life cycle phase. Banks existing in products still in use are referred to as active banks, and once products have been decommissioned and reside in a landfill or in some other waste stream (TEAP, 2021b), these banks are referred to as inactive and are generally more difficult to capture and are likely to have different release rates.

Previously published bank estimates have varied widely due to the widespread use of ODSs and the associated difficulty in assessing the total amount of equipment and applications containing ODSs, as well as different modeling approaches and assumptions. International assessments prior to 2006 primarily relied on top-down analyses, where banks were estimated as the cumulative difference between production and emissions. Bank estimates in this approach are very sensitive to small biases in annual emissions and production estimates, with the resulting biases in bank estimates increasing over time (Velders, Daniel et al., 2014). Biases in emissions can be caused by biases in atmospheric mixing ratio observations and in ODS lifetime estimates. Biases in production can result from biases in production figures reported to the Ozone Secretariat, for example.

In bottom-up estimates (e.g. Ashford et al., 2004; IPCC/TEAP, 2005), the inventory of sales, by-product, or equipment type are carefully tallied along with estimated release rates by application use. While there are reasonable estimates for production and leakage rates of various equipment types, these estimates are also subject to uncertainties. Bottom-up methods are generally independent of observed atmospheric mixing ratios and the estimated lifetimes of the various ODSs.

Since 2006 and the publication of bottom-up bank estimates (IPCC/TEAP, 2005), international assessments have used a hybrid approach that starts with bottom-up bank estimates in a given year and uses the top-down method to propagate banks forward in time, using yearly reported production and observationally derived emissions. In the present Assessment, we adopt a Bayesian analysis of banks (Lickley et al., 2020, 2021, 2022). In the Bayesian method, banks are estimated by developing initial (prior) bank estimates where production is associated with the application and equipment type following the bottom-up method, relying on reported and published data, accounting for large uncertainties in production and leakage rates, and then finding the best (in a Bayesian sense) parameters that are statistically consistent with atmospheric mixing ratios. The result is a final (posterior) distribution of banks by equipment type, along with an updated estimate of release rates for each equipment type (Lickley et al. 2020, 2021, 2022).

7.2.1.3 Emissions from Feedstock Production and Usage

Although the produced quantities of ODSs used as feedstocks must be reported by the Parties to the Montreal Protocol, they are exempted from controls. This exemption was granted under the assumption that emissions during production and usage of feedstocks are small. In this section, the fugitive emissions of ODSs, HFCs, and VSLSs from production and uses of feedstock are evaluated. Many feedstock chemicals contain chlorine, some or all of which is displaced by fluorine by using HF (hydrofluoric acid) in the process of manufacturing the final halogenated product. **Table 7-1** and **Figure 7-2** summarize the most important chlorinated feedstocks, intermediates, by-products, and their halogenated products, which are most relevant for the Montreal Protocol and the Kigali Amendment. Whereas intermediates are substances that can be used further to produce the final product, undesired by-products are also produced in the process but cannot usefully react further and are therefore removed from the final product for destruction or potential release into the atmosphere. Feedstock-related emissions can occur during the production of the feedstock chemical, from its storage, and/or during transport (**Box 7-2**). Finally, emissions occur during the conversion to the final product, which may require several intermediate stages, consisting of fugitive leaks in the storage and/or transport processes, and possible trace residual levels in the ultimate products. In addition, the charging and discharging of cylinders or road/rail containers may also contribute to emissions.

Figure 7-2 provides an overview of the feedstocks used in the production of some key synthetic, fluorinated greenhouse gases. In the course of their production, different chlorinated substances (ODSs and uncontrolled chemicals) are fluorinated, which can result in their emissions and the formation of several ODSs as intermediates and by-products. Annual production rates of the most important ODS feedstock chemicals between 2000

Table 7-1. Regulated ODSs used as feedstocks, with their uses and annual production for feedstock applications in 2019 (UNEP, 2021). Calculated emissions are given in Gg and ODP-Gg (in parentheses). The relative contribution of feedstock emissions to global emissions is calculated against global emissions figures from *Chapter 1*.

Feedstock	Industrial Products[1]	Global Feedstock Production[2] [Gg]	Feedstock Emissions[3] [Gg] (ODP Emissions[4] [CFC-11-eq Gg])	Percentage of Feedstock Emissions Versus Global Emissions (2019)[5]
CCl_4	HFC-245fa HFC-365mfc HFC-236fa HFO-1234yf HFO-1234ze(E) HCFO-1233zd Tetrachloroethene	318	13.6 (11.2)	32%
1,1,1-trichloroethane	HCFC-142b HCFC-141b HFC-143a	84	1.7 (0.2)	78%
CFC-113 CFC-113a	CTFE (HFO-1113) HFC-134a HFO-1336mzz	108	2.2–4.3 (1.8–3.6)	43–87%
CFC-114 CFC-114a	HFC-134a	45	0.9–1.8 (0.5–1.0)	33–66%
HCFC-22	TFE, a monomer to PTFE, HFP, and other fluoropolymers. Isoflurane/desflurane anesthetics	713	14.3–28.5 (0.5–1.1)	4–8%
HCFC-124 HCFC-124a	HFC-125 HFC-134a	25	0.5–1.0 (0.01–0.02)	19-37%
HCFC-141b	HFC-143a	13	0.3–0.5 (0.03–0.05)	0.5–0.9%
HCFC-142b	HFO-1132a (VDF) monomer, HFC-143a	174	3.5–7.0 (0.2–0.4)	17–33%
Halon-1301	Fipronil	1.3	0.03–0.05 (0.5–1.0)	2–4%
Minor Chemicals[6]		11	0.2–0.4 (0.04–0.09)	
Total Gg of Regulated ODSs		1492	37.2–58.9	
Total ODP-Gg		558	15.0-18.7	

Notes:
[1] Feedstock usage from Montzka, Reimann et al. (2011), TEAP progress report (TEAP, 2020), Sherry et al. (2018), Table S2 of Chipperfield et al. (2020), and Andersen et al. (2021).
[2] Global feedstock production from UNEP (2021).
[3] Relative emissions from feedstock usage are estimated to be 2% for 1,1,1-trichloroethane, 4.3% for CCl_4, and 2–4% for all the other chemicals (**Box 7-2**).
[4] ODP values from **Table 7-4**.
[5] Global emissions in 2019: Average between 2018-2020 and NOAA/AGAGE from *Chapter 1*.
[6] Minor chemicals: HCFC-123, HCFC-133/133a, HCFC-225, methyl bromide, bromochloromethane (UNEP, 2021), characterized by an average ODP of 0.22, when weighted by production mass.

Box 7-2. Feedstock-Related Emissions

Emissions from the production and use of feedstock chemicals relative to their production volumes are summarized in **Table 7-1**. Feedstock emissions estimated in this section are used as input for the scenarios in *Section 7.4*. For 1,1,1-trichloroethane, relative emissions are assessed at 2%, related to the 2019 ratio of global emissions against reported global production (**Table 7-1**). 1,1,1-trichloroethane is an excellent tracer for generally estimating feedstock losses, because emissions from banks can be neglected, as it was historically used only as a solvent. For all other feedstock chemicals (except CCl_4; see below), emissions of 2–4% relative to their production were estimated, which covers the range between the 2% above and the Tier 1 default emissions factor of 4% for fluorochemical production (IPCC, 2019). Further evidence of real-world emissions from feedstocks comes from industry-based estimates of 1.5–3.3% of fugitive emissions during production of CFCs and HCFCs (Gamlen et al., 1986; Midgley and Fisher, 1993; Ashford et al., 2004) and additional emissions of 1% during the usage of feedstocks (as estimated for HCFC-22 by Midgley and Fisher (1993)). An additional rationalization of the upper margin of 4% is substantiated from estimated emissions of 4–6% during the historic production of CFC-11 (TEAP, 2021b), which, however, could have been as high as 15% in the case of small and poorly operated enterprises, as assessed during the recent surge in CFC-11 production in eastern China.

Feedstock-related emissions of CCl_4 are treated separately, as they have been specifically assessed in the past by SPARC (2016) and Sherry et al. (2018), by estimating that 0.4% of the global production of chloromethanes is emitted as CCl_4 and by adding process-specific emissions from the usage of CCl_4 as feedstock. In 2014, this resulted in estimated emissions of 15 Gg (i.e., 7.4% of the 203 Gg of CCl_4 produced that year). In this chapter, this number has been revised for 2019 by estimating that 2% (0.9–4.0%), or 6.4 Gg (2.9–12.7 Gg), of the produced amount of CCl_4 (318 Gg) is emitted during the production process and an additional fraction of 7.2 Gg (2.2–9.8 Gg) from its usage (**Figure 7-4**; update of Sherry et al., 2018). This results in a best estimate of 4.3% (13.6 Gg, 5.1–22.5 Gg) of feedstock-related emissions of CCl_4 in 2019 (i.e., combination of pathways C and D in **Figure 7-4**).

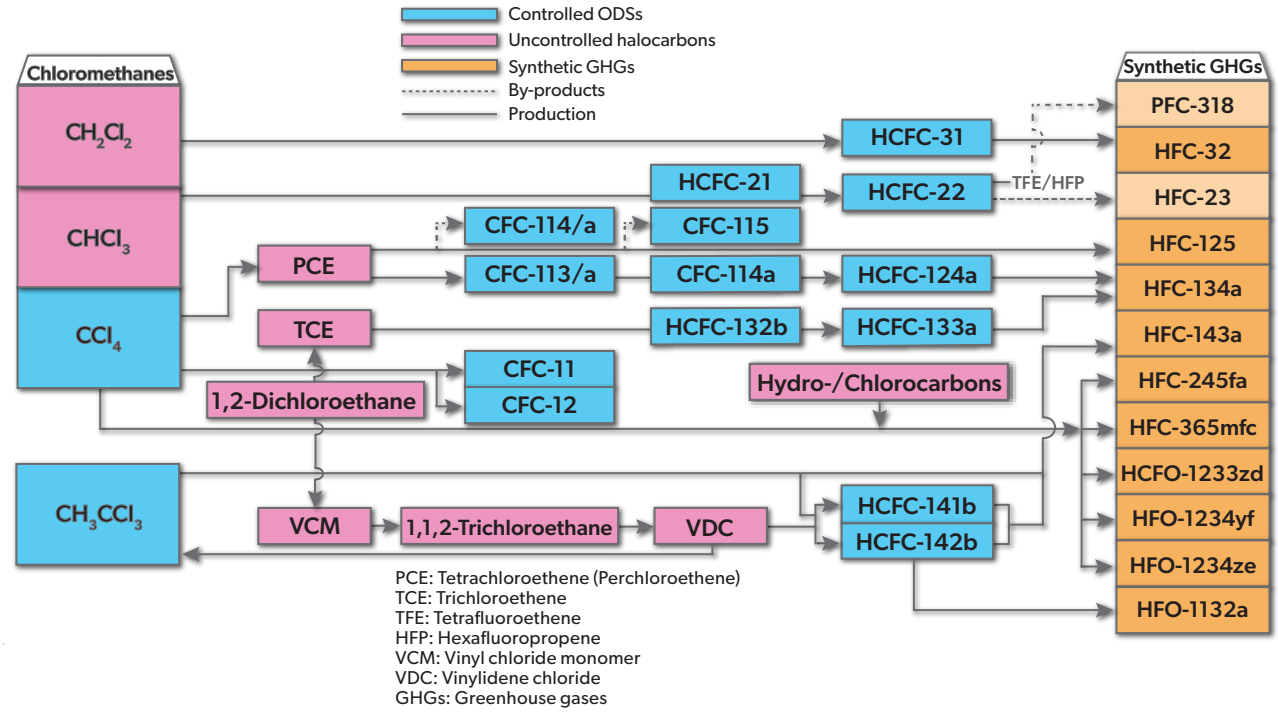

Figure 7-2. Controlled ODSs and uncontrolled halocarbons used as feedstocks for the production of controlled ODSs and synthetic greenhouse gases (GHGs). Uncontrolled halocarbons are shown in purple, controlled ODSs in light blue. Synthetic greenhouse gases, as the final products, are shown in orange. Intermediates are drawn in-line from the feedstock chemical to the final product; by-products are connected by a dotted line. HCFC-22 is mostly used for the synthesis of PTFE, (polytetrafluoroethene) with TFE (tetrafluoroethene) and HFP (hexafluoropropene) as intermediates. PFC-318 and HFC-23 are by-products but are also used to a smaller extent as final products, which are indicated by lighter orange.

and 2019 (UNEP, 2020) are shown in **Figure 7-3**. In addition, **Table 7-1** summarizes the amounts of ODSs that were used as feedstocks in 2019 and shows their estimated fugitive emissions, as well as the ratio of ODS emissions from this use to their global total, as an average between 2018–2020 (*Chapter 1*).

In 2019, a greater mass of HCFC-22 was produced in a single year than any other fluorocarbon in history, with a global production close to 1000 Gg. More than 700 Gg (>70%) of this is reported to be used as feedstock in the production of PTFE (polytetrafluoroethene), HFP (hexafluoropropene), and other fluorinated monomers. Production related to feedstock usage has increased by more than a factor of five from 2000 to 2019. More recently, HCFC-22 has also started to be used for the synthesis of HFO-1234yf. The usage of HCFC-22 as a feedstock chemical is expected to grow until market saturation of the produced fluoro-derivatives is reached or environmentally based restrictions are imposed. Current estimated feedstock-related emissions of 14–29 Gg yr^{-1} (**Table 7-1**) are less than 10% of the current global HCFC-22 emissions (*Chapter 1*), but this fraction is projected to increase, as emissions from refrigerants and foam-blowing agents are expected to decline.

At more than 300 Gg yr^{-1}, CCl_4 was the chemical with the second-highest mass production rate for feedstock usage in 2019. In recent decades, inexplicably high and ongoing global emissions have been calculated for CCl_4 using observationally-based methods. This issue has been highlighted in three previous Ozone Assessments (2006, 2010, 2014). The studies of SPARC (2016) and Sherry et al. (2018) show that emissions of CCl_4 from feedstock production and its use were higher than previously estimated. This finding significantly reduced the gap between top-down and bottom-up estimates of CCl_4 emissions. Historically, CCl_4 was used for producing CFC-11 and CFC-12, which, according to the Montreal Protocol, was due to cease for both production and consumption by 2010. However, with the renewed production of CFC-11 in eastern China and potentially elsewhere (WMO, 2021), a minimum of an additional 360 Gg of CCl_4 was estimated to have been produced (TEAP, 2021b) between 2012 and 2018 as feedstock for this application. These values are not included in the global sum of reported feedstock usages of CCl_4 in **Figure 7-3** and **Table 7-1**.

Production for allowed uses of CCl_4 increased by a factor of two in the last decade. Currently, CCl_4 is used in the production of tetrachlorethene and other base chemicals, as well as for the synthesis of HFC-245fa, HFC-365mfc, and the newly introduced HFO-1234yf, HFO-1234ze(E), and HCFO-1233zd. The specific hydrocarbons or chlorocarbons used to react with CCl_4 in the products, illustrated in **Figure 7-2**, determine the specific end product. For instance, the reaction of CCl_4 with ethene provides the chlorocarbon base for HFO-1234yf, whereas the selection of vinyl chloride monomer (VCM) as a reactant with CCl_4 provides the base for HFC-245fa. In the future, it is expected that the amounts of CCl_4 used for HFCs will decline due to the Kigali Amendment, whereas those for the production of HFOs are currently expected to increase steadily until economic saturation is reached.

In **Figure 7-4** the pathways of emissions of CCl_4 are compiled as an update of Sherry et al. (2018) (see explanation in **Box 7-2**). In 2019, emissions of feedstock production and fugitive emissions from usage are estimated at 13.6 Gg (5.1–22.5 Gg), or 4.3% (1.6–7.1%) of the produced CCl_4 (pathways C and D in **Figure 7-4**). In addition, another 5 Gg (2.5–7.5 Gg) are estimated to arise from inadvertent sources (i.e., the production of chlorine and base chemicals such as the production of VCM from 1,2-dichloroethane; pathway B) and around 5–10 Gg from legacy emissions (e.g., from landfills and contaminated soils; pathway A). In total, the best estimate of the sum of the contributions from these different sources, 26.1 Gg (12.6–40.0 Gg) in 2019, still leaves a considerable gap to the estimated global emissions of 43 Gg in 2019 from *Chapter 1*.

The third most produced feedstock is HCFC-142b, which is used for manufacturing fluoropolymers. In parallel to HCFC-22, its usage has increased continuously and reached around 170 Gg yr^{-1} in 2019. Emissions of HCFC-142b related to feedstock usage are estimated to have contributed 17–33% to its global emissions in 2019 (**Table 7-1**), with the remaining fraction from declining emissive uses from foam production and banks.

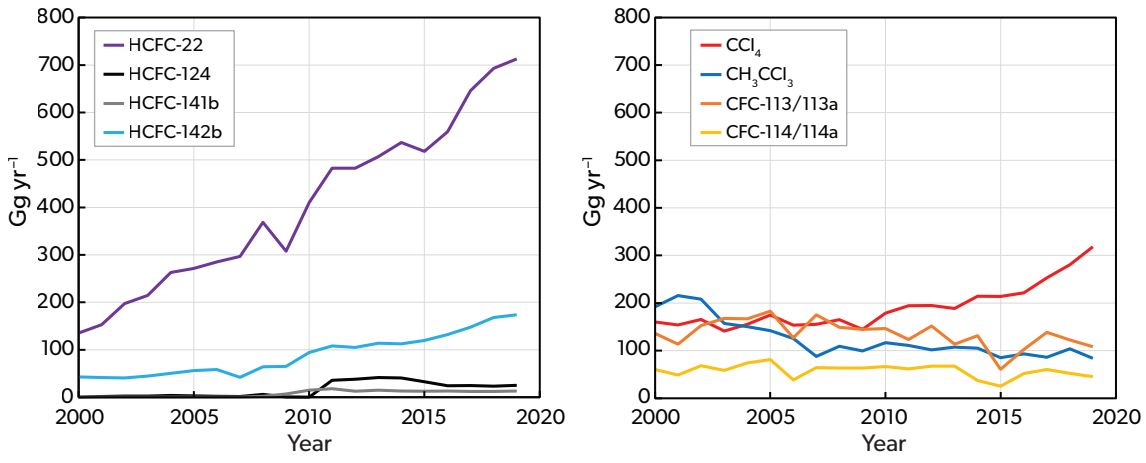

Figure 7-3. Global production of ozone-depleting substances for feedstock usage, which is exempted from the Montreal Protocol controls (UNEP, 2021).

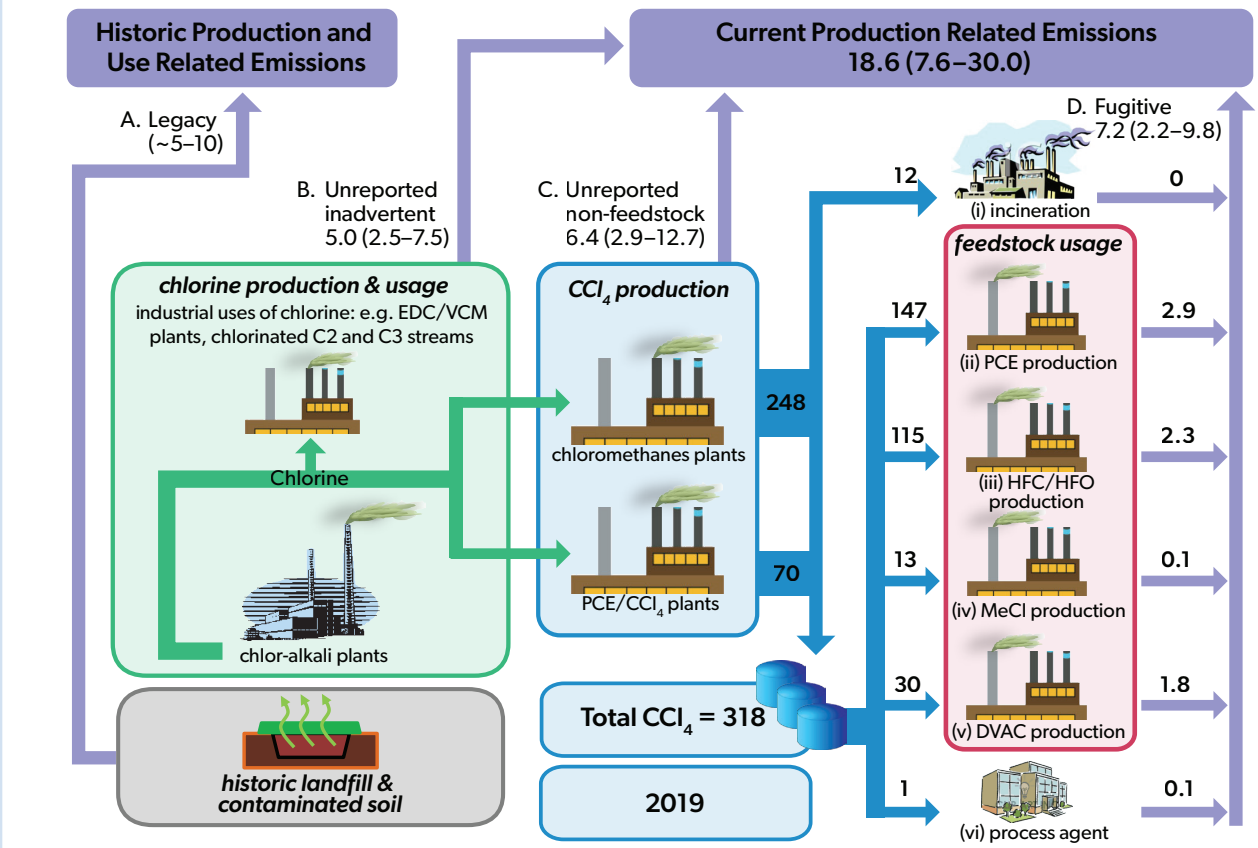

Figure 7-4. Update of CCl_4 (carbon tetrachloride) emission pathways from SPARC (2016) and Sherry et al. (2018). Emissions from each source are given in Gg for 2019.

Currently 1,1,1-trichloroethane (CH_3CCl_3), CFC-113/113a, and CFC-114/114a are nearly exclusively used as feedstock chemicals in the synthesis of widely used HFCs, HCFCs, and fluoropolymers (Table 7-1 and Figure 7-2). While the amounts used for the production of HFCs and HCFCs are still considerable, they are decreasing steadily, and, with the Kigali Amendment restrictions, the importance of these product compounds for emissive uses is projected to progressively decline. This tendency could be partly compensated for by an increased demand in the production of fluoropolymers, which would lead to a stabilization in emissions, albeit at potentially lower amounts than at present. Interestingly, the estimated feedstock emissions rate of 2–4% for CFC-113/CFC-113a and CFC-114/CFC-114a yields emissions that are lower than the measurement-based estimate of global emissions (*Chapter 1*). For CFC-114/CFC-114a, this could be explained by potential emissions as an undesired by-product in the production of HFC-125.

Declared feedstock usages of HCFC-124/124a and HCFC-141b are in principle related to their production as intermediates, but in some instances, they are also reported as feedstocks (see Box 7-2). As they are mainly used for the production of HFCs, their importance is also projected to decline.

In total, the recent usage of ODSs as feedstocks has been rising substantially. Between 2009 and 2019 the mass of ODSs used as feedstocks, which is not controlled under the Protocol, increased by 75% (Figure 7-3). When expressed as emissions in units of Gg ODP (Table 7-2), this increase in feedstock-linked production was 41%. This difference between absolute mass emissions and ODP-based emissions is due to the fact that HCFC-22, with a relatively low ODP, was responsible for the highest growth. If the original ODPs from the Montreal Protocol were used instead of the ODPs recommended in this Assessment (Table 7-2), the ODP-weighted increase would be 46% instead of 41%.

In addition to the ODSs and HFCs regulated by the Montreal Protocol, the nonregulated chlorinated VSLSs dichloromethane (CH_2Cl_2), chloroform ($CHCl_3$), trichloroethene (C_2HCl_3), and tetrachloroethene (C_2Cl_4) are also used in large amounts as feedstock chemicals (Chipperfield et al., 2020). In fact, Figure 7-2 shows that the usage of these VSLSs and 1,2-dichloroethane as feedstock is the starting point for the synthesis of either the ODS feedstock chemicals discussed above or provides an ODS-free feedstock route for the production of halogenated compounds. Because of their much lower ozone depletion potentials (ODPs), emissions during feedstock usage are generally of minor importance to the ozone layer. Nevertheless, a short discussion of their uses is included here.

About 96% of the nearly 1500 Gg of chloroform ($CHCl_3$) produced in 2016 was used as feedstock in the production

Table 7-2. Atmospheric lifetimes, fractional release factors (FRFs), and ODPs for long-lived halocarbons. FRFs are for mid-latitude conditions and are from Engel et al. (2017). Lifetime uncertainties are based on (SPARC, 2013) lifetimes as evaluated by Daniel, Velders et al. (2014). See *Chapter 1* for further discussion on atmospheric lifetimes and FRFs.

Halocarbon	Global Lifetime (yrs)	Lifetime Uncertainty (1σ)	Fractional Release Factors	ODPs	
				This Assessment's Recommendation	In Montreal Protocol
Annex A-I					
CFC-11	52	±22%	0.47	1.0	1.0
CFC-12	102	±15%	0.24	0.75	1.0
CFC-113	93	±17%	0.30	0.82	0.8
CFC-114	189	±12%	0.13	0.53	1.0
CFC-115	540	±17%	0.07	0.45	0.6
Annex A-II					
Halon-1301	72	±13%	0.32	17.0	10.0
Halon-1211	16	±29%	0.65	7.1	3.0
Halon-2402	28	±19%	0.66	15.6	6.0
Annex B-II					
CCl_4	30		0.56	0.82	1.1
Annex B-III					
CH_3CCl_3	5.0	±3%	0.61	0.12	0.1
Annex C-I					
HCFC-22	11.6	±16%	0.15	0.037	0.055
HCFC-123	1.4			0.02	0.02
HCFC-124	5.9			0.022	0.022
HCFC-141b	8.8	±15%	0.34	0.095	0.11
HCFC-142b	17.1	±14%	0.17	0.054	0.065
HCFC-225ca	1.9			0.025	0.025
HCFC-225cb	5.8			0.033	0.033
Annex E					
CH_3Br	0.8	±17%	0.60	0.57	0.6
Others					
Halon-1202	2.5	±33%	0.67	1.8	
CH_3Cl	0.9	±18%	0.44	0.015	

of HCFC-22 (Chipperfield et al., 2020). HCFC-22 production increased by 17% between 2016 and 2019 (UNEP, 2021), so the feedstock-related production of $CHCl_3$ is estimated to be around 1700 Gg in 2019. Assuming a loss rate of 2–4%, as for the other feedstock chemicals, implies emissions of 32–68 Gg yr^{-1}, which is comparable to the emissions from its use as a solvent (Chipperfield et al., 2020). This could partly explain the large increase in $CHCl_3$ emissions over the last decade (*Chapter 1*). In contrast, only around 15% of the ~1200 Gg of dichloromethane (CH_2Cl_2) produced was used as feedstock—mainly in the production of HFC-32, with the remainder being used and emitted as a solvent (Chipperfield et al., 2020). Next are trichloroethene (TCE) and tetrachloroethene (also named PCE, perchloroethene), whose usage as feedstocks in the production of HFCs is higher than the amounts used as solvents. Finally, 1,2-dichloroethane is used as a feedstock for the production of TCE and, via chloroethene (VCM, vinyl chloride) and 1,1,2-trichloroethane, for the production of 1,1-dichloroethene (VDC), which is then used to produce 1,1,1-trichloroethane, HCFC-141b, and HCFC-142b (**Figure 7-2**).

7.2.1.4 Emissions of Intermediates and Undesired By-Products

In addition to emissions from banks and feedstock usages, controlled substances (ODSs and HFCs) can also be lost to the atmosphere as chemical intermediates and undesired by-products during the production of a final product.

Generally, for intermediates and undesired by-products, relative emissions of 1% or smaller are estimated, relative to the produced final products. For HFC-23 as a by-product of HCFC-22 production, relative emissions of 1.6% are estimated, which is the average of the global HFC-23 emissions relative to the HCFC-22 production between 2014–18 (Stanley et al., 2020).

Emissions of intermediates can occur during their production and use on-site. The production and then consumption

of intermediates are not reported as feedstock use under the Montreal Protocol. It is only if intermediates are transported off-site that their usage has to be reported as feedstocks. A number of these intermediates have been detected recently in the atmosphere that are likely due to fugitive emissions during the synthesis of chemical products; these are summarized in *Chapter 1*. The most prominent examples are HCFC-31 from the production of HFC-32 (Schoenenberger et al., 2015), as well as HCFC-132b and HCFC-133a from the production of HFC-134a (Vollmer et al., 2021). In addition, CFC-114, CFC-114a, and CFC-115 are by-products in the production of HFC-125 (**Figure 7-2**). As the origin of these intermediates and by-products in the atmosphere is related to the production of HFCs, their importance is projected to decline in the future.

Further examples of undesired by-product formation are HFC-23 from the production of HCFC-22 (*Section 7.2.2.1*) and the formation of c-C_4F_8 (PFC-318) from the pyrolysis of HCFC-22 to manufacture TFE (tetrafluoroethene) and HFP (Mühle et al., 2022). In addition, atmospheric CFC-13 is potentially at least partly released as a by-product from the production of other fluorochemicals (Vollmer et al., 2018). Finally, CCl_4 is potentially emitted as a by-product during the use of chlorine in the production of several chlorinated chemicals, such as ethylene dichloride (EDC), vinyl chloride monomer (VCM), and other organic operations (**Figure 7-4**).

7.2.2 HFCs Controlled Under the Kigali Amendment of the Montreal Protocol

This section covers issues related to HFCs, which have recently become controlled under the Kigali Amendment. First, the future implications of the gap between reported emissions of HFC-23 from its by-product formation in the production of HCFC-22 and its actual measurement-based emissions are discussed. Then, the reported HFC feedstock uses are assessed, followed by a short discussion of the potential for energy efficiency improvements when equipment filled with HFCs is replaced. Decisions on which kind of foam-blowing agent or refrigerant should be used are policy relevant, and these issues are discussed in *Chapter 2* in conjunction with existing HFC usages; only a short summary on this topic is given in this section.

7.2.2.1 HFC-23

HFC-23 is predominantly released into the atmosphere as an undesired by-product from the production of HCFC-22 and from the subsequent production of tetrafluoroethene. Additional minor emissions occur from the electronics industry, from aluminum smelters, and from its usage in ultra-low refrigeration (e.g. Simmonds et al., 2018). The recent surge in demand for ultra-low-temperature cooling devices for storing vaccines could potentially increase emissions from this source, although other refrigerants are also used for these devices, and current emissions are estimated to be small in comparison with those related to the production of HCFC-22 (TEAP, 2021c). This potential new source is not included in the projections, as no information is yet available of this emerging market.

Technical solutions for destroying HFC-23, which is emitted in the production of HCFC-22, are available and economically viable (TEAP, 2018a). However, in contrast to the basket of other HFCs with an agreed phasedown schedule, restrictions on HFC-23 are prescribed only qualitatively in the Kigali Amendment as follows: "Each country manufacturing HCFC-22 or HFCs shall ensure that starting in 2020 the emissions of HFC-23 generated in production facilities are destroyed to the extent practicable using technology approved by the Montreal Protocol" (UNEP, 2016). The reporting of related emissions went into effect on 1 January 2020, so current reporting is still potentially incomplete.

As outlined in *Chapter 2* and related to the discussions by Stanley et al. (2020), abatement capacities seem to have been used only partially in recent years. If this continues to be true in the long term, compliance with the Kigali Agreement will not be met. In view of the uncertainty of the future development and the currently fragmentary documentation of HFC-23 destruction, two different scenarios have been developed to project future HFC-23 emissions within this Assessment. For both scenarios, production of HCFC-22 is assumed to increase by 5.8% yr^{-1} until 2030 (representing the average increase from 2014–2019) and to stabilize thereafter, with increasing feedstock usage compensating for a decrease in emissive applications. One scenario assumes full compliance with the Protocol, with emissions of only 0.08% relative to the produced HCFC-22. This scenario estimates an effective destruction capacity of 97% of the 2.8% (1.5–4.0%) of undesired HFC-23 produced per mass of HCFC-22 without incineration (McCulloch and Lindley, 2007). Remaining small emissions are related to failures and to maintenance work at the destruction systems. The other scenario, which is used as our baseline scenario, assumes a business-as-usual behavior, with an emissions rate of 1.6% relative to the HCFC-22 production (*Section 7.2.1.4*) and where destruction capacities are only partly exploited.

An additional contribution to the ongoing emissions could also be from the formation of HFC-23 in the pyrolysis reaction from HCFC-22 to TFE and HFP, used in fluoroplastics production, when fluorinated catalysts are used (Sung et al., 2006; Ebnesajjad, 2015). Furthermore, Ha et al. (2011) detected HFC-23 as the main product of the thermal treatment of HCFC-22, which could be important, as HCFC-22 from dismantled old air-conditioner systems is potentially incinerated. None of these additional potential sources has been included in the future scenarios related to the by-product formation from HCFC-22 production, but they could be key elements in closing the gap between known sources and measurement-based emissions, as discussed in *Chapter 2*.

7.2.2.2 Feedstock Usage of HFCs

To date, the amounts of HFCs used as feedstocks are much lower than those of ODSs. The submission of production and consumption data to the United Nations Environment Programme (UNEP), which is prescribed for feedstock usages of HFCs within the Kigali Amendment, is still incomplete, as not all countries with potential HFC feedstock usages have signed the treaty yet. Known applications are the use of HFC-152a and HFC-23 (TEAP, 2020). The dehydrofluorination of HFC-152a is the most broadly used chemical process for the production of vinyl fluoride, which means a considerable part of the produced HFC-152a is used as feedstock. HFC-23 is used as a minor feedstock (e.g., <1 Gg yr^{-1}) in the production of halon-1301, which is then used as feedstock in the production of fipronil (**Table 7-1**).

7.2.2.3 Energy Efficiency

An in-depth discussion on the potential for energy efficiency gains in connection with the future phasedown of HFCs used as

refrigerants in air-conditioning and refrigeration can be found in *Section 2.4.6*. In short, the replacement of old equipment containing HFCs with high Global Warming Potentials (GWPs) by new installations and low-GWP alternatives, as well as not-in-kind solutions, has the potential for multiple positive effects on climate change. For example, the emissions of low-GWP alternatives will directly reduce projected radiative forcing of climate. Also, and thought to have greater potential climate benefit, the transition to new refrigerants is an opportunity to implement design changes for achieving higher energy efficiency and therefore lowering greenhouse gas emissions from energy use.

7.2.3 Replacement Compounds of Controlled Halocarbons (HFOs and Others)

With the adoption of the Kigali Amendment, high-GWP HFCs as replacement compounds for ODSs are, themselves, supposed to be phased down. In **Figure 7-5**, historic and projected emissions of ODSs, high-GWP HFCs, and low-GWP alternatives are shown in Tg yr^{-1} and Pg CO_2-equivalents yr^{-1}, together with their influence on climate, expressed as radiative forcing (update of Figure 2-21 of Montzka, Velders et al. (2018), using data from Velders et al. (2022)). Whereas emissions of high-GWP HFCs are not projected to decline until after around 2025, ODS emissions are projected to continue their current steady decline. For both groups of compounds, emissions are expected to still occur in 2100, albeit at much lower levels than today. Due to the long lifetime of these compounds, their effect on climate, as measured by their radiative forcing (**Figure 7-5c**), will only slowly decrease after 2040 and is expected to still be around 50% of their maximum by 2100. Low-GWP alternatives to long-lived HFCs include both fluorinated alkenes (HFOs, HCFOs, HBFOs) and non-halogenated compounds, such as hydrocarbons, CO_2, and NH_3. These two groups are expected to constitute an important fraction of the low-GWP compounds in the future. Given the dynamics in the application markets, however, it is very difficult to estimate the future ratio of these halogenated alkenes relative to non-halogenated substitutes (*Section 7.2.3.3*). It can be expected that non-halogenated substitutes will comprise a substantial share of the low-GWP compounds. This assumption is substantiated, as historically after adoption of the Montreal Protocol, ODSs with large ODPs were also only partly replaced by HCFCs and HFCs. Therefore, it is estimated in this report that only 50% of the future low-GWP emissions (**Figure 7-5**) will be due to HFOs; this same assumption is also applied in the assessment of future trifluoroacetic acid (TFA) formation in *Section 7.2.5.1*.

7.2.3.1 Fluorinated Low-GWP Alkenes (HFOs, HCFOs, HBFOs)

HFOs (hydrofluoroolefins), HCFOs, (hydrochlorofluoroolefins), and HBFOs (hydrobromofluoroolefins) are fluorinated alkenes that are being introduced as low-GWP substitutes during the phasedown of HFCs (**Table 7-3**). Depending on their chemical and physical properties, they can be used in a similar way as the HFCs they replace. Their atmospheric lifetimes are small, and, therefore, their emissions do not contribute perceptibly to climate change. However, some of these compounds can

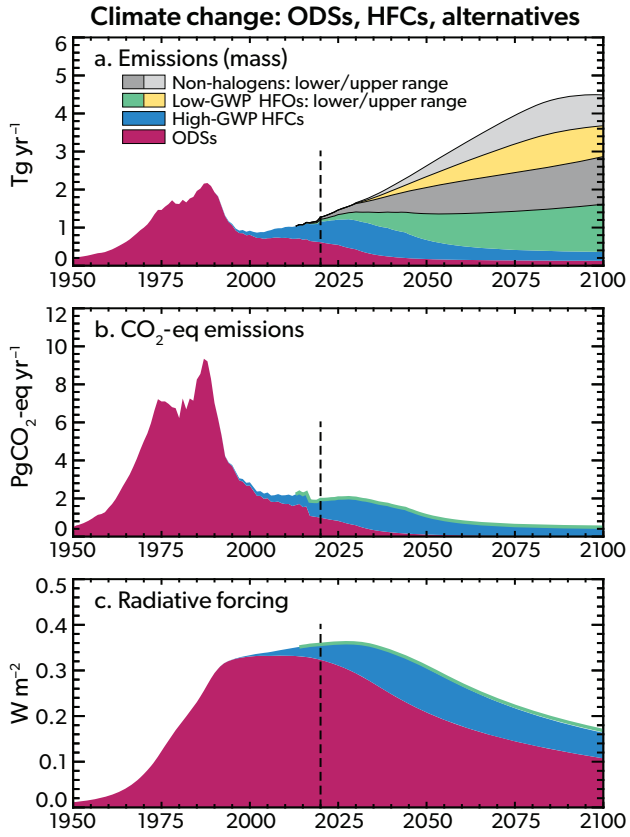

Figure 7-5. Historical and projected contributions to climate change from ODSs, high-GWP HFCs, low-GWP HFOs and non-halogenated alternatives, assuming full compliance with the provisions of the Montreal Protocol, including the Kigali Amendment [update of Figure 2-21 from Montzka, Velders et al., 2018]. Shown are (a) emissions by mass, (b) CO_2-eq emissions, and (c) direct radiative forcing. Only the direct GWP-weighted emissions and radiative forcing of the ODSs and HFCs are shown. The ODS emissions from around 1980 through 2020 are derived from atmospheric observations and after 2020 are from this scenario (distinction indicated by dashed vertical lines). The contributions of the low-GWP HFOs in panels b and c, are smaller than the thickness of the green curves. Not included here are contributions from HFC-23, indirect radiative effects from ozone depletion, and indirect effects associated with the energy used by equipment and the associated CO_2 emissions.

contribute to the formation of the stable compound TFA, as discussed in *Section 7.2.5.1*. An additional issue is the prevailing process for producing these compounds, some of which use CCl_4 as a feedstock, (*Section 7.2.1*) and therefore leads to ODS emissions (*Section 7.2.1.3*).

7.2.3.2 Non-halogenated Substitutes and Not-In-Kind Solutions

Several non-halogenated ODS substitutes have been used for decades in various applications. Hydrocarbons are the compounds of choice when considering alternatives, and in some countries are even mandatory (e.g., for use in domestic refrigeration and foam blowing). In addition, NH_3 and CO_2 are valid alternatives for large-scale cooling facilities. While CO_2 was also discussed as a replacement for HFC-134a in mobile air conditioners, HFO-1234yf was ultimately chosen, although CO_2 is still used in small quantities. Finally, so-called not-in-kind solutions are gaining increased attention, especially for cooling applications. Techniques such as solid-state cooling materials and Stirling coolers are discussed in, for example, Qian et al. (2016) and TEAP (2018b). All of these compounds and techniques have to be evaluated for their energy efficiency and integrative effects on climate (see *Section 7.2.2.3* and *Section 2.4.6* on energy efficiency).

7.2.3.3 Trifluoroiodomethane (CF_3I)

CF_3I, with an ODP of 0.008–0.016 (Youn et al., 2010), has been evaluated since the late 1990s as a replacement compound for halons in fire extinguishers, but it was never marketed as such (TEAP, 2018c). Recently, however, it has been proposed as an ingredient of low-GWP refrigerant blends in order to lower their flammability. Related to its ODP, Zhang et al. (2020) proposed using a new metric, called SODP (stratospheric ozone depletion potential), which includes only the fraction of ozone loss that takes place in the stratosphere. The SODP for CF_3I was determined to be essentially zero (within statistical error), as large fractions of CF_3I are destroyed in the troposphere, where the actual iodine-catalyzed ozone destruction occurs. It is too early to evaluate the general implications and acceptance of using SODP or ODP for assessing the ozone-depletion abilities for other VSLSs; historically, ODPs of these compounds have been calculated using a range of different methods (Zhang et al., 2020). If CF_3I were adopted in suggested blends and uses, the overall quantities of CF_3I potentially released could become significant.

7.2.4 Anthropogenic and Biogenic Very Short-Lived Substances (VSLSs)

VSLSs are not controlled under the Montreal Protocol. However, there is now strong evidence from observations and models that VSLSs contribute to stratospheric chlorine and bromine and therefore also to the ozone loss in this part of the atmosphere (see *Chapter 1*).

7.2.4.1 Chlorinated VSLSs

Currently, the most important chlorinated VSLSs in terms of their potential to deplete ozone are dichloromethane (CH_2Cl_2), chloroform ($CHCl_3$), 1,2-dichloroethane (CH_2ClCH_2Cl), trichloroethene (C_2HCl_3), and tetrachloroethene (C_2Cl_4). With the exception of chloroform, which also has significant natural sources, chlorinated VSLSs are largely of anthropogenic origin. They are emitted from their use as solvents and as feedstock chemicals in the production of HFCs and other chemicals (**Figure 7-2** and Chipperfield et al., 2020). As a group, chlorinated VSLSs contributed 3.5% to total tropospheric chlorine in 2020 (Chapter 1). While this contribution is still small, the relevance of VSLSs for stratospheric ozone depletion has increased over time (*Chapter 1* and Hossaini et al., 2017; Fang et al., 2019; Hossaini et al., 2019). Since the last Assessment, new studies have reported substantial increases in chlorinated VSLS emissions from Asia (Fang et al., 2019; Say et al., 2019; Claxton et al., 2020), and new information on the ODPs of chlorinated VSLSs has become available.

Dichloromethane (CH_2Cl_2) is a widely used VSLS whose atmospheric abundance and global emissions have both increased

Table 7-3. HFOs, HCFOs, and an HFBO currently in use and foreseen for future use, with their chemical formula, GWP, atmospheric lifetime, and main applications.

	Formula	GWP[1]	Atmospheric Lifetime[1]	Main Applications
HFO-1234yf	$CF_3CF=CH_2$	<1	12 days	Refrigerant Component of HFC-HFO blends
HFO-1234ze(E)	trans- $CF_3CH=CFH$	1	19 days	Refrigerant Component of HFC-HFO blends Aerosol propellant Insulation foam-blowing agent
HFO-1336mzz(Z)	cis-$CF_3CH=CHCF_3$	2	27 days	Refrigerant Fire extinguisher Insulation foam-blowing agent
HFO- 1336mzz(E)	trans-$CF_3CH=CHCF_3$	26	121 days	Refrigerant
HCFO-1233zd(E)	trans-$CHCl=CHCF_3$	4	42 days	Refrigerant Insulation foam-blowing agent Precision solvent
HCFO-1224yd(Z)	CF_3-$CF=CHCl$	<1	12 days	Refrigerant Polyurethane foam-blowing agent
HBFO-1233xfB	$CF_3CBr=CH_2$	<1	3.5 days	Fire extinguisher

Note:
[1] Atmospheric lifetimes and GWPs from *Annex*.

by more than a factor of two since the mid-2000s (*Chapter 1*). The issue of the growth of CH_2Cl_2 emissions was raised by Hossaini et al. (2017), who concluded that elimination of future CH_2Cl_2 emissions would have a substantial positive impact on total column ozone (see also Figure 6-1 of Carpenter, Daniel et al., 2018). CH_2Cl_2 is used in a wide range of solvent applications, notably as a process solvent in pharmaceutical processing, as a blowing agent in polyurethane foam production, and as an essential feedstock in HFC-32 production (Feng et al., 2018; Chipperfield et al., 2020; An et al., 2021). Around 90% of global CH_2Cl_2 emissions have been estimated to emanate from Asia (Claxton et al., 2020). Chloroform ($CHCl_3$), another prominent chlorinated VSLS, is used primarily (>95% of that produced) as a feedstock in HCFC-22 production and is also a by-product from water chlorination and from bleaching processes in the pulp and paper industry (e.g. McCulloch, 2003). Global $CHCl_3$ emissions have increased considerably within the last decade (*Chapter 1*), with regional inverse modeling showing that enhanced emissions from China are likely responsible (Fang et al., 2019).

A detailed examination of possible future industrial production of chlorinated VSLSs has yet to be performed. Hence, predictions of future VSLS emissions and ozone impacts are highly uncertain. Once HCFC-22 emissive applications are nearly phased out, which must occur by 2030 per the Montreal Protocol, $CHCl_3$ demand will likely be tied to the demand for HCFC-22 produced for feedstock usage, such as in the production of PTFE (*Section 7.2.1.3*). As $CHCl_3$ and CH_2Cl_2 are co-produced in chloromethane plants, supply and demand issues affecting one compound should invariably impact the other, although chloromethane plants have some flexibility to determine the extent to which one or the other compound is produced. By extrapolating recent trends, it is anticipated that Asian emissions will exert a dominant influence on the trajectory of global chlorinated VSLS emissions in the next decade. A bottom-up analysis (Feng et al., 2018) predicts that Chinese emissions will increase monotonically to the year 2030 under a business-as-usual scenario. This is substantiated by An et al. (2021), who estimated that CH_2Cl_2 emissions from China increased from 232 Gg in 2012 to 627 Gg in 2019, which practically covers the total global CH_2Cl_2 emissions increase in this period. Given the large uncertainties, we examine three scenarios to span a range of possibilities in *Section 7.4*: one in which the growth of CH_2Cl_2 emissions continues until 2022 and then stabilizes, one with the elimination of CH_2Cl_2 emissions beginning in 2023, and one in which emissions continue the increase as they have exhibited over the past five years through 2030, after which year they remain constant.

It has been well established that the ODP of a VSLS is dependent on the location and season of its emissions (e.g. Brioude et al., 2010; Pisso et al., 2010). However, to date, very few studies have considered the ODPs of the above chlorinated VSLSs. One recent analysis (Claxton et al., 2019) revealed that the ODPs of chlorinated VSLSs vary only slightly with the season of emissions but could differ by a factor of two to three depending on the source location. The highest ODP values were assessed for emissions from Tropical Asia and industrialized East Asia, which, in view of 1) the currently large regional emissions (e.g., Fang et al., 2019; Claxton et al., 2020) and 2) the existence of efficient regional transport pathways to the tropical upper troposphere (e.g. Oram et al., 2017), make it a significant finding.

7.2.4.2 Brominated and Iodinated VSLSs

In contrast to chlorinated VSLSs, brominated and iodinated VSLSs are predominantly produced naturally in the ocean. The most abundant brominated VSLSs are bromoform ($CHBr_3$) and dibromomethane (CH_2Br_2), with important source regions in coastal and shelf waters (e.g. Quack and Wallace, 2003). Natural production of $CHBr_3$ and CH_2Br_2 involves marine organisms such as macroalgae and phytoplankton, while the sea-air flux is driven by their oceanic abundance, temperature, and surface winds. The spatiotemporal variability of emissions and tropospheric transport processes are key factors controlling the contribution of brominated VSLSs to stratospheric bromine (Hossaini et al., 2013; Hossaini et al., 2016).

Atmospheric abundances of brominated VSLSs have not shown any trends (*Chapter 1*). However, oceanic production, sea-air fluxes, atmospheric lifetimes, and transport pathways of VSLSs are all sensitive to changing environmental conditions. Changes in VSLS emissions could occur due to changing irradiance and temperature affecting the production of halocarbons by macroalgae (e.g., Keng et al., 2020). In addition, climate change and ocean acidification will affect the distribution, abundance, and diversity of macroalgae itself, with further consequences for VSLS production. Thus, very large uncertainties exist in the prediction of future VSLS sources, as the responses of macroalgae toward environmental changes are highly species- and compound-specific. Sea-air fluxes of natural VSLSs have been predicted to increase throughout the 21st century due to changing physical forcings such as sea surface temperature and wind speed, assuming constant VSLS mixing ratios (Ziska et al., 2017). Recently quantified anthropogenic sources of $CHBr_3$ from power plants also have the potential to increase their total emissions over time (Maas et al., 2021). Finally, climate-driven changes to the troposphere's oxidizing power and to the troposphere-stratosphere transport may alter the contribution of VSLSs to the stratospheric halogen budget (Dessens et al., 2009; Hossaini et al., 2012; Falk et al., 2017). Overall, there is no clear picture of how brominated VSLS emissions and their contribution to stratospheric bromine will change in the future due to the large uncertainties associated with all these individual factors.

Iodinated VSLSs are present in the troposphere (*Chapter 1*), including methyl iodide (CH_3I). Like brominated VSLSs, organic iodine emissions from the ocean can be impacted by climate parameters (Keng et al., 2020). However, very little long-term data on tropospheric CH_3I trends exist, impeding future predictions of natural production and potential anthropogenic sources (Yokouchi et al., 2012; Zeng et al., 2020). Inorganic iodine emissions of hypoiodous acid (HOI) and iodine (I_2) from the ocean are driven by the reaction of ozone with iodide (I^-) at the ocean surface. Atmospheric iodine mixing ratios have tripled since 1950 (Cuevas et al., 2018), most likely because increased surface ozone leads to growing oceanic iodine emissions (Legrand et al., 2018).

Future inorganic iodine emissions will depend strongly on socioeconomic development and associated changes in anthropogenic ozone deposition and oceanographic changes impacting the sea-surface iodide abundance, among other factors (Iglesias-Suarez et al., 2020).

7.2.5 Breakdown Products from Anthropogenic Halocarbons

The atmospheric degradation of HCFCs, HFCs, and HFOs is initiated by their reaction with the hydroxyl radical (OH) leading to the formation of halogenated carbonyl compounds, which can further react to secondary products. Discussions in this section are related to trifluoroacetic acid (TFA) and carbon tetrafluoride (CF_4), which are both more stable in the environment than the primarily emitted halocarbons. Whereas TFA has some herbicidal properties, CF_4 is a strong greenhouse gas. In addition, degradation of halocarbons also contributes to the formation of tropospheric ozone, but mixing ratios of halocarbons are too small in comparison with other volatile organic compounds to make a considerable contribution.

7.2.5.1 Trifluoroacetic Acid (TFA)

TFA is a very strong acid with low to moderate toxicity for a range of organisms (Neale et al., 2021). It is found in many environmental compartments in varying concentrations, and its origin in these different parts of the environment is still an area of active research (*Chapter 2*; Joudan et al. (2021)). Here, the ranges of future TFA concentrations in precipitation and in ocean water are projected between 2020 and 2100. The model is restricted to the formation of TFA from the degradation of HFC-134a and HFO-1234yf, which, according to current knowledge, are expected to have the most significant influence on future TFA concentrations among those gases controlled by the Montreal Protocol or used as substitutes. Other fluorocarbons containing a CF_3 group also have the potential of being degraded to TFA in the atmosphere, albeit with a lower influence, as they currently have very small atmospheric mixing ratios and lower conversion rates to TFA (see also *Chapter 2*). Thus, the resulting TFA concentrations in different parts of the environment should be treated as lower-range projections. The contribution of HFC-134a is calculated by using its projected future mixing ratios, taken from Velders et al. (2022), with a lifetime of 14 years and a conversion rate to TFA of 7–20% (Wallington et al., 1994). For the short-lived HFO-1234yf, with a conversion rate to TFA of 100%, projected emissions are taken from the low and high scenarios of low-GWP alternatives shown in **Figure 7-5**. Thereby, it is assumed that 50% of the future emissions of the low-GWP alternatives (**Figure 7-5**) are related to HFOs, of which 50% is HFO-1234yf. The resulting projected annual TFA formation rates related to HFC-134a and HFO-1234yf are shown in **Table 7-4** for the years 2020, 2050, and 2100. In addition, the mass of deposited TFA from each and for the two together is given for the periods 2020–2050 and 2020–2100.

With an estimated total atmospheric formation and deposition of 31.5–51.9 Tg of TFA between 2020 and 2100 (**Table 7-3**), and subsequent transfer to the ocean, average TFA concentrations in sea water are projected to increase by 23–38 ng/L between 2020 and 2100, assuming a total ocean volume of 1.37×10^9 km^3. This would signify a substantial increase compared with the total ocean content of 61–205 Tg of TFA around the year 2000 reported in Scott et al. (2005), based on measuring varying concentrations in different ocean parts, or the 274 Tg of TFA reported in Frank et al. (2002), based on a measured constant concentration of 200 ng/L. The additional contribution of TFA related to the degradation of HFC-134a alone is estimated to be 1.0–2.9 Tg between 2020 and 2100.

With a total global precipitation volume of 5.5×10^{17} liters, and assuming that TFA will be deposited through wet deposition only, the degradation from HFC-134a and HFO-1234yf is projected to result in a global average TFA concentration in precipitation of 660–970 ng/L in 2050 and 1150–1910 ng/L in 2100. This would represent an increase of a factor of around two to three in 2050 and of around three to six in 2100, when compared to the precipitation-weighted average of 340 ng/L of TFA found in Germany in 2018–19 (Freeling et al., 2020).

The global average deposition rate of TFA from the combined degradation of HFC-134a and HFO-1234yf is projected to be 0.7–1.0 kg km^{-2} yr^{-1} and 1.2–2.1 kg km^{-2} yr^{-1} in 2050 and 2100, respectively. In the first period, these numbers are comparable to those in the regional projections for 2030 (Wang et al., 2018) and 2040 (David et al., 2021). While all these global averages in concentration and depositions are still far below the toxic values for aquatic organisms, as summarized by Solomon et al. (2016) and Neale et al. (2021), regional studies focused in highly populated and industrialized areas have projected regions of higher impact and high concentrations in precipitation and in the atmosphere (e.g. Henne et al., 2012; Wang et al., 2018; David et al., 2021; Holland et al., 2021). Understanding the TFA budget in the different environmental compartments is key for evaluating the future

Table 7-4. Projected annual TFA production rate due to atmospheric conversion of HFC-134a and HFO-1234yf in 2020, 2050, and 2100, as well as cumulative projected totals of deposited TFA mass between 2020 and 2050 and between 2020 and 2100, in Tg (1012 g).

	HFC-134a	HFO-1234yf	Sum
Annual TFA Formation			
2020	0.01–0.03 Tg yr^{-1}	0.03–0.03 Tg yr^{-1}	0.04–0.06 Tg yr^{-1}
2050	0.02–0.05 Tg yr^{-1}	0.34–0.49 Tg yr^{-1}	0.36–0.54 Tg yr^{-1}
2100	0.01–0.02 Tg yr^{-1}	0.63–1.03 Tg yr^{-1}	0.64–1.05 Tg yr^{-1}
Sums of Deposited TFA			
2020–2050	0.5–1.5 Tg	5.3–6.6 Tg	5.8–8.1 Tg
2020–2100	1.0–2.9 Tg	30.5–49.0 Tg	31.5–51.9 Tg

Note:
The calculation of the formation of TFA from HFC-134a is based on its expected mixing ratio of HFC-134a (Velders et al., 2022) and its lifetime of 14 years. Conversion rates from the destroyed HFC-134a amounts to TFA were 7–20%. For HFOs, it is assumed that 50% of the future emissions of low-GWP alternatives (**Figure 7-5**; Velders et al., 2022) are related to HFOs, from which it is assumed that 50% is HFO-1234yf, with a conversion rate of 100% to TFA.

environmental impacts of anthropogenic TFA. Of specific interest in this respect is the uncertainty in the natural background of TFA found in the ocean (Frank et al., 2002; Scott et al., 2005; Joudan et al., 2021).

In addition, other sources of TFA in the atmosphere could also gain in importance. An increasing bank of fluoropolymers raises the possibility of TFA formation from the thermic destruction of fluoropolymers (Ellis et al., 2001; Cui et al., 2019), such as in waste incinerators or from uncontrolled burning.

7.2.5.2 Carbon Tetrafluoride (CF_4)

CF_4 is a very strong greenhouse gas that is emitted by various industrial sources (*Chapter 1*). In addition, Jubb et al. (2015) found that CF_4 is formed from the UV photolysis of trifluoroacetylfluoride ($CF_3C(O)F$), which itself is an atmospheric degradation product of several halocarbons (e.g., 13% of HFC-134a and 100% of HFO-1234yf; see *Section 7.2.5.1*). However, the relative production of CF_4 from $CF_3C(O)F$ is extremely small, as formation of CF_4 from $CF_3C(O)F$ is only possible in the presence of UV wavelengths found in the stratosphere and above. For 2100, Jubb et al. (2015) estimated a contribution of 9 t for HFC-134a. For the very short-lived HFO-1234yf the contribution is expected to be even smaller. This is insignificant relative to the global CF_4 emissions, currently around 15 Gg yr^{-1} (*Chapter 1*).

7.2.6 The Key Climate Gases: Carbon Dioxide, Methane, and Nitrous Oxide

The most important drivers of climate change over the last century are the well-mixed greenhouse gases (GHGs) carbon dioxide (CO_2), methane (CH_4), and nitrous oxide (N_2O). The atmospheric abundances and associated radiative forcings of climate from these gases have increased substantially in the industrial era (see *Chapters 1*, *3*, and *5*). Their future increase will depend on policy actions related to curbing climate change. Future changes in halogen mixing ratios will take place against the backdrop of the changing chemical, radiative, and climatic conditions caused by these GHGs, and future stratospheric ozone levels will be strongly dependent on their future emissions and mixing ratios. The continuing increase of these GHGs has important effects on stratospheric ozone through cooling of the stratosphere, which slows the ozone chemical loss rates. The resulting climate change from increasing GHGs also strengthens the stratospheric Brewer-Dobson circulation, which will redistribute ozone (see *Chapter 5*). In addition, CH_4 and N_2O are also key chemical gases affecting the ozone layer directly. The breakdown of N_2O in the stratosphere enhances nitrogen oxides (NO_x) and depletes ozone, while increases in CH_4 lead to ozone changes that vary with altitude, with net production in total column ozone.

For this Assessment, the new Shared Socioeconomic Pathway (SSP) scenarios are used for future projections of the major GHGs. These replace the previous Representative Concentration Pathway (RCP) scenarios used in the last Assessment. The SSPs are designed based on socioeconomic and technological development and adapt the future climate radiative forcing outcomes used for the RCPs, while providing more detail in the variety of climate outcomes that can be obtained (Gidden et al., 2019; Meinshausen et al., 2020; Chen, Rojas, Samset et al., 2021).

Section 7.4.3.1 examines how the changing mixing ratios of CO_2, CH_4, and N_2O under selected SSPs could affect future changes in stratospheric ozone relative to the changing emissions and mixing ratios of halogenated compounds. The nine selected scenarios include updates of the four RCPs having the same radiative forcing levels of 2.6, 4.5, 6.0, and 8.5 W m^{-2}, as well as five scenarios that fill gaps not covered in the RCPs (Gidden et al., 2019). These SSPs include five high-priority scenarios from the Sixth Assessment Report of the Intergovernmental Panel on Climate Change, including a lower-bound 1.9 W m^{-2} scenario (Rogelj et al., 2018), which corresponds to the most optimistic interpretation of Article 2 of the Paris Agreement and comes closest to holding the global temperature increase to below 1.5 °C.

7.2.7 Deliberate Climate Intervention

Chapter 6 provides a comprehensive analysis of the influence of deliberate climate interventions on the stratospheric ozone layer.

7.2.8 Other Potential Influences on Stratospheric Ozone

In this section, the potential impact of future anthropogenic emissions from a large-scale rocket economy, potential new supersonic airplanes, and a hydrogen-based energy system is discussed. In addition, the current knowledge of the impact of volcanoes and wildfires is summarized.

7.2.8.1 Influence of a Growing Spaceflight Industry

Emissions from rockets and their effect on stratospheric ozone have been the subject of research since the 1970s. Since the previous Assessment, significant launch growth has occurred and more satellites have been launched into low-Earth orbit than during the previous 60 years, an increase entailing larger rockets and greater launch rates.

The greatest part of this growth has come from kerosene-fueled rockets, from which black carbon (BC) emissions have doubled in the past four years (Miraux, 2022). Emissions from solid-fuel rockets have increased only slightly, and this trend is likely to continue. On the other hand, hydrazine-fueled rocket launches have decreased during this period because of propellant toxicity concerns. The number of hydrogen-fueled launches has been approximately constant, representing only a small fraction of all launches. Methane-fueled rockets, in advanced testing, are expected to play a significant role in the future, although the rate at which methane replaces existing rocket fuel is uncertain.

Rocket propulsion systems typically combine the exhaust from several of the four primary propellant types during a single launch (by fuel: kerosene, ammonium perchlorate, hydrazine, and hydrogen). Mixed rocket emissions into the stratosphere are mostly (>90% of about 8 Gg yr^{-1}) a combination of CO_2, CO, H_2O, NO, and OH with the exact amounts depending on propellant and altitude. None of these gas-phase emission components have a significant effect on stratospheric ozone, except at implausibly larger launch rates (Larson et al., 2017; Ryan et al., 2022). NO_x emissions (<1%) from some rocket types can affect ozone (Ross et al., 2004), although to a lesser degree than solid fuel chlorine emission.

Direct ozone loss caused by chlorine emissions (0.2 Gg yr^{-1}) from solid fuel rockets into the stratosphere is well understood.

Models generally agree on the amount and distribution of ozone loss (Voigt et al., 2013; Ryan et al., 2022). Alumina emissions from solid fueled rockets (0.4 Gg yr^{-1}) cause ozone loss by heterogeneous Cl_y (inorganic chlorine) activation reactions; this is less well bounded because of uncertainties in the alumina surface area density, extent of sulfate coating, and reaction coefficients (Danilin et al., 2003). In situ plume data suggest that ozone loss from alumina could be larger than the loss from chlorine (Danilin et al., 2001), and this question remains unresolved.

Indirect ozone loss caused by the absorption and scattering of solar radiation by rocket BC and alumina particles in the stratosphere have not yet been comprehensively investigated. General principals of stratospheric processes suggest that rocket BC and alumina increase heating rates and temperature in the stratosphere and cause ozone loss (Lee et al., 2021). This is confirmed by new models of rocket BC emissions (Maloney et al., 2022; Ryan et al., 2022), which show ozone loss from rocket BC is comparable to ozone loss from rocket chlorine emissions (per propellant mass), consistent with models of climate change mitigation using stratospheric BC (Weisenstein et al., 2015).

With a very large number of 100,000 projected hydrogen-fueled reusable small rocket launches per year, H_2O emissions from space travel has been estimated to enhance stratospheric water by up to 9%, leading to a 20% increase in polar stratospheric clouds (PSCs) in both hemispheres (Larson et al., 2017). An even larger effect of hydrogen-based space travel is through anticipated increases in stratospheric NO_x, which, combined with HO_x cycle perturbations, leads to 0.5% loss of the globally averaged ozone column, with column losses in the polar regions exceeding 2%.

The effect on ozone of stratospheric aerosols generated by destruction of space debris during reentry is a new area of research (Boley and Byers, 2021; Ryan et al., 2022). It is expected that spaceflight architectures that assume disposal of space debris into the mesosphere via destructive reentry will take on greater importance in coming years (Ross and Jones, 2022). Reentry vaporization and lower mesosphere particle production and sedimentation presents a source of stratospheric particles that could exceed those from present-day launches by 2030 (Boley and Byers, 2021). Very little is known about the composition, sizes, and steady state distribution of reentry particles or their possible impact on stratospheric ozone. Nitrogen oxide (NO) produced during heating of the atmosphere during reentry reduces mesospheric ozone (Ryan et al., 2022), though reentry NO production rates are poorly quantified.

In view of the rapid growth of rocket launches, rocket fuels, spacecraft in orbit, and the anticipated increase in space debris reentries these knowledge gaps suggest further assessments are warranted.

7.2.8.2 Influence of a New Fleet of Supersonic Airplanes

Early research on the environmental effect of supersonic airplanes warned of potential adverse effects on stratospheric ozone, mainly through their emissions of NO_x into the stratosphere (e.g., Crutzen, 1972). This concern was reinforced by later studies (e.g., Johnston et al., 1989). To date, this potential source of ozone loss has not been realized, since the first generation of supersonic passenger planes was decommissioned in 2003. However, hypothetical concepts for a new generation of supersonic airplanes are now again being developed. The potential influence of supersonic and hypersonic aircrafts on stratospheric ozone are discussed in *Section 4.2.5.3*.

7.2.8.3 Influence of a Potential Future Hydrogen Economy

Hydrogen fuel cells could play a role in future clean energy supply systems if produced using renewable energy sources. If their use is widespread, it will potentially lead to elevated atmospheric hydrogen mixing ratios because of leakages during storage and usage. With an atmospheric lifetime of two years (Paulot et al., 2021), surface emissions of hydrogen can at least partly reach the stratosphere. Further, direct emissions into the upper troposphere and lowermost stratosphere are expected if planned hydrogen-fueled airplanes and rockets are realized (*Section 7.2.8.1*).

In both the troposphere and stratosphere, hydrogen is oxidized to water vapor. The influence will be small in the troposphere because the water vapor perturbation is minimal compared with the background. In the stratosphere, additional hydrogen increases H_2O concentrations. However, it is generally concluded that the effect of future surface emissions from an economy that is only partly reliant on hydrogen as an energy carrier will be too small to have a substantial effect on stratospheric ozone (e.g. Warwick et al., 2004; van Ruijven et al., 2011; Vogel et al., 2011; Wang et al., 2013). If hydrogen were to play a major role in future energy policy, a potential influence, e.g., via the enhanced production of PSCs, has been modeled (Tromp et al., 2003).

7.2.8.4 Impact of Volcanoes and Wildfires

Volcanoes are well known to have an intermittent effect on stratospheric ozone through their input of aerosols and sulfur dioxide (SO_2) into the stratosphere (e.g., Langematz, Tully et al., 2018). Recently, the effect of wildfires has also been discussed (*Sections 3.2.1.3* and *4.3.5.3*). Strong Siberian wildfires (2019–2020) were responsible for a layer of dust in the lower stratosphere and could have contributed to very low stratospheric ozone concentrations over the Arctic during the same period of time (Ohneiser et al., 2021). In addition, strong Australian bushfires may also have contributed to very low ozone levels in the Antarctic in the spring of 2020 (Rieger et al., 2021) and have an at least sporadic negative effect also on mid-latitude ozone (Solomon et al., 2022). If intense fires in the temperate to subpolar regions increase, then these fires could have a potential long-term influence on stratospheric ozone.

7.3 METRICS FOR CHANGES IN OZONE AND CLIMATE

7.3.1 Metrics for Changes in Ozone

As in past Ozone Assessments, one key metric used to evaluate the ability of various ozone-depleting substances to destroy stratospheric ozone is their contribution to equivalent effective stratospheric chlorine (EESC; for a detailed description of this metric, see Box 5-2 of Harris, Wuebbles et al. (2014)). The other primary metric used in *Section 7.4* is the globally averaged ozone

depletion as calculated by a two-dimensional model. Semi-empirical ODPs are updated but are no longer used to evaluate the relative differences among the various presented scenarios. In calculating EESC, there have been minor changes in the adopted fractional release factors (FRFs), which represent the fractions of ODSs that have been broken down from their organic forms into inorganic molecules that can then be converted to molecules that can deplete ozone. These FRFs are consistent with the adopted EESC approach, which is used in *Chapter 1* of this document and was discussed in Section 6.4.3.1 and Appendix 6C of Carpenter, Daniel et al. (2018). The adopted FRF values are shown in **Table 7-2** along with the resulting semi-empirical ODPs, which are almost identical to those given in Carpenter, Daniel et al. (2018). For comparison, the ODPs used in the Montreal Protocol are also shown in the table. In evaluating the various scenarios discussed in *Section 7.4*, we use the integrated EESC differences over the time period from the year 2023 through the year when EESC returns to the 1980 level for each particular scenario. Consistent with no longer using GWP-weighted emissions as a metric to evaluate the climate impact (see *Section 7.3.2*), we do not compare scenarios using cumulative ODP-weighted emissions as was done in the previous Assessment. As discussed in *Chapter 1*, there have been some updates to the ODS lifetimes used in this Assessment. These lifetime updates are included in the *Annex*.

A more substantial change to the analysis of the ODSs in this chapter relative to the main section of Carpenter, Daniel et al. (2018) arises from using the revised EESC approach of Engel et al. (2017). The new approach used to calculate EESC leads to a larger effective stratospheric age of air compared with the previously assumed 3 years at mid-latitudes and 5.5 years in polar regions and was discussed in detail in Section 6.4.1 of Carpenter, Daniel et al. (2018). The effective increase in the age of air, combined with the fact that the EESC slope is steeper with time around 1980 than the projected slope when EESC returns to 1980 levels, leads to a delay of more than a decade in the projected time for mid-latitude EESC to return to 1980 levels with the Engel et al. (2017) EESC approach relative to that used in the main chapter of Carpenter, Daniel et al. (2018). The advantages of this newer approach were recognized in the 2018 Assessment, which is why both were discussed in Carpenter, Daniel et al. (2018) and scenario results of the Engel et al. (2017) approach were shown in Appendix 6C. If the scenario results of this chapter are to be fairly compared with those of Carpenter, Daniel et al. (2018), the results here should be compared with those of Table 6C-1 in Appendix 6C of Carpenter, Daniel et al. (2018) and not the results shown in their Table 6-5. Unfortunately, the change in EESC approach also inhibits straightforward comparisons with scenario results (using EESC) from Ozone Assessments before 2018. It should be noted that because nearly all of the source gases have almost fully dissociated by the time they make it to the polar vortexes, the difference between the two EESC approaches is substantially smaller in polar regions than it is at mid-latitudes. It should also be noted that in regions where full dissociation has not occurred, the move to the approach of Engel et al. (2017) introduces another potentially significant model sensitivity relating to atmospheric transport. Given this, when future comparisons of EESC are made with different models, it would be important to indicate which differences are due to model differences and which are due to ODS scenario differences.

7.3.2 Metrics for Changes in Climate

The climate metrics used in Carpenter, Daniel et al. (2018) were global warming potentials (GWPs), global temperature change potentials (GTPs), and radiative forcing (RF). A description of these metrics can be found in Box 5-3 of Harris, Wuebbles et al. (2014), and a discussion of radiative forcing can be found in **Box 5-3** of this Assessment. A search for better metrics continues in the scientific and policy community, with the most appropriate metric dependent on the particular purpose. Recently, Forster, Storelvmo et al. (2021) have discussed two new metrics that are demonstrably better when the goal is to have similar temperature change outcomes from similar metric-weighted emissions trajectories; these are GWP* and combined global temperature change potential (CGTP). Both approaches require that gases be divided into long-lived ones, which behave like CO_2 in that the amount of warming depends on the cumulative emissions, and short-lived ones, whose warming depends on changes in emissions. The GWP* approach, for example, has frequently been used to compare warming from CO_2 (long-lived) with that from CH_4 (short-lived). However, when there are important gases with intermediate lifetimes, this categorization is ambiguous and imperfect. In this chapter, for example, the way in which CCl_4 and CFC-11 are categorized have significant effects on the relative comparisons of the scenarios. Because of this and the shortcomings identified in using the traditional GWP-weighting to equate the climate impact of GHG emissions with substantially different lifetimes (see, e.g., Chapter 7 of the Working Group I contribution to IPCC AR6: Forster, Storelvmo et al., 2021), in this chapter, we compare the climate impact of various scenarios by using the averaged radiative forcing over the period 2023–2100.

In calculating the radiative forcing of the scenarios discussed in *Section 7.4*, the radiative efficiency (RE) factor estimates that have changed the most significantly since the previous Assessment are for CFC-11 and CFC-12. Hodnebrog et al. (2020b) have estimated that tropospheric feedbacks of these compounds imply their REs should be increased by 13% and 12%, respectively, and they have been changed accordingly.

Additional terminology that is relevant to the calculation of indirect GWPs in this section is effective radiative forcing (ERF). A detailed discussion of ERF and how it compares with RF is found in **Box 5-3**. The ERF of the halocarbons includes the offsetting radiative forcing due to the ozone depletion they cause, which is the dominant response, as well as to other adjustments such as tropospheric responses including cloudiness and circulation changes. In a case where the various atmospheric responses to an increase of a specific ODS mixing ratio completely offsets its direct radiative forcing, the ERF of that ODS would be zero. Three studies have been published since the previous Assessment that estimated the ERF of the combined ODSs (Morgenstern et al., 2020; O'Connor et al., 2021; Thornhill et al., 2021), and another has updated radiative efficiency estimates of the halocarbons as well as the resulting GWPs (Hodnebrog et al., 2020a). One of the ERF studies (Morgenstern et al., 2020) has attempted to remove the effect of the large variation among models in their calculated ozone depletion by constraining their modeled ERF estimate using observed depletion amounts. In their assessment of these studies, Forster, Storelvmo et al. (2021) suggest an ERF for all ODSs plus the HFCs in 2019 (relative to 1850) of 0.01 to 0.40 W m^{-2}, when including the responses in ozone depletion as well as in stratospheric water vapor and atmospheric methane mixing ratios. While the

radiative efficiencies for the key ODSs have changed little over the last four years (see, e.g., *Annex*), the uncertainty range for the ERF of the ODSs now encompasses smaller values; i.e., the offset through responses could be larger than previous Ozone and IPCC Assessments have suggested. Despite modeling improvements and a new approach constraining the ERF estimates with observations, the uncertainty in the ERFs remains substantial, as discussed in *Section 5.3.1.1.* The uncertainty range implies that the forcing offsets range between approximately no offset to a complete offset of the ODS direct radiative forcing. These ERFs, which include the radiative impact of ozone depletion resulting from ODSs, are used only in the calculation of indirect GWPs in this chapter. The comparison of the various scenarios presented in **Table 7-6** and the figures that show radiative forcing do not consider the radiative impact of ozone depletion.

The direct and indirect GWPs are shown in **Table 7-5**. The direct GWPs capture only the direct radiative effect of the ODSs themselves, including stratospheric temperature adjustment and, for CFC-11 and CFC-12, tropospheric adjustments. The offsetting radiative effects of ozone responses, as well as the smaller effects of methane and water vapor responses, to changes in ODS mixing ratios are given by the indirect GWPs (**Table 7-5**). The sum of the direct and indirect GWPs therefore approximately capture the full radiative effect of an ODS's emissions. The indirect GWPs given in **Table 7-5** incorporate the midrange of the new ERF in their calculation, using the same EESC-scaling approach described Daniel et al. (1995) and in previous Assessments (e.g., Carpenter, Daniel et al., 2018). The full uncertainty range varies between roughly 0 and twice the indirect GWP quoted. When compared with the equivalent Table 6-3 of the WMO (2018) Assessment, the slightly more negative indirect GWPs are apparent. As in previous Assessments, the relative magnitudes of the direct and indirect GWPs vary widely across the different ODSs, with key factors including whether the compound has a bromine atom instead of chlorine (since bromine is roughly 60 times more effective than chlorine at depleting ozone), the number of halogen atoms, and the radiative efficiency of the ODS. While HFCs do not cause chemical ozone depletion, they do alter stratospheric temperatures, which in turn leads to stratospheric ozone changes (Hurwitz et al., 2015; Dupuy et al., 2021). These changes are, however, minimal and are not considered in our indirect GWP calculations.

This ERF revision to the ozone forcing in response to the ODSs is also important for understanding the climate forcing role of the ODSs collectively. We do not include the offset of the ozone response in evaluating the scenarios later in this chapter but do point out that if the lower ERF estimates prove to be accurate, this would imply that the phasedown of the ODSs by the Montreal Protocol would have a smaller globally averaged climate impact than previously estimated, at least from a strictly global radiative point of view. Again, however, it is important to note the large uncertainty in determining this offsetting radiative

Table 7-5. Indirect GWPs from ozone depletion compared with direct GWPs for select ODSs. We calculate the "indirect" GWP using the radiative effect of the responses in ozone, methane, and stratospheric water vapor to the ODS. This indirect GWP calculation approach follows Daniel et al. (1995) and assumes that, as with ozone, all three indirect responses track EESC. The radiative forcing due to ozone depletion from 1979 to 2000 is updated to –0.17 W m^{-2}; this is 50% of the direct forcing from the ODSs and HFCs and is in approximately the middle of the range of this same ratio in Szopa, Naik et al. (2021). The relative uncertainty in this radiative forcing offset response (IPCC, 2021) translates directly to the same relative uncertainty in indirect GWPs. Notice that the number of significant figures shown for both indirect and direct GWPs are not meant to represent the level of uncertainty; instead, they are shown so changes relative to past studies and future studies can be more easily tracked.

Gas	Direct GWP 100-yr	Indirect GWP 100-yr
CFC-11	6410	–4390
CFC-12	12,500	–3490
CFC-113	6530	–3600
CFC-114	9450	–1490
CFC-115	9630	–355
HCFC-22	1910	–133
HCFC-123	91	–43
HCFC-124	596	–55
HCFC-141b	808	–302
HCFC-142b	2190	–219
HCFC-225ca	137	–45
HCFC-225cb	557	–69
CH_3CCl_3	164	–366
CCl_4	2150	–3460
CH_3Br	2	–1400
Halon 1211	1990	–25,400
Halon 1301	7430	–75,800
Halon 2402	2260	–64,400

forcing from ozone depletion (see *Section 5.3.1.1*) and to note that this remains an active area of research. We also reiterate that the issue of a potential ozone forcing offset does not apply to HFCs and thus will not alter estimates of the radiative forcing benefit of the Kigali Amendment.

7.4 SCENARIOS AND SENSITIVITY ANALYSES

7.4.1 Tools Used in Analyses of Ozone and Climate Effects

As in recent Ozone Assessments, the foundation for the ODS scenarios generated in this chapter are observed atmospheric mixing ratios of the ODSs and their replacements, as well as their global lifetimes, reported production to UNEP, and estimates of ODS banks (**Box 7-1**). The historical mixing ratios to which all the scenarios are tied, and from which annual emissions are estimated, are taken from a combination of the Advance Global Atmospheric Gases Experiment (AGAGE) and National Oceanic and Atmospheric Administration (NOAA) observational networks (*Chapter 1*). The production data are taken from what the Parties have reported to the Ozone Secretariat, aggregated into Article 5 and non-Article 5 country groups. The lifetimes for the ODSs considered in this chapter have been updated from those in the 2018 Assessment and are presented in the *Annex* of this Assessment as well as in **Table 7-2**.

We continue to use the 1-box model that has been used in the past several Ozone Assessments. In this model, banks are prescribed for a given starting year, chosen here to be 2020, and from these are calculated going forward from that year by adding projected annual production and subtracting projected annual emissions. It is important to recognize that the temporal evolution of these banks is performed in a relatively simplistic manner, with only a single bank for each compound. Thus, that bank can contain a mix of accessible and inaccessible banks as well as active and inactive banks, for example. In the previous three Assessments (WMO 2011, 2014, 2018), 2008 bank values were projected forward from estimates from UNEP (2009). Here, bank starting values are taken using a Bayesian approach described in Lickley et al. (2020, 2021, 2022). These banks represent the most recent comprehensive estimate of banks that has been peer-reviewed. Nonetheless, there are substantial uncertainties associated with these estimates. One contributing factor to uncertainties in both the Lickley approach and the previously used approach is uncertainties in global lifetimes, which lead to a bias in the emissions estimated from atmospheric concentration observations. Any biases in either production or emissions can have a significant impact on the bank size estimated for the present and moving into the future. A discussion of the potential impacts of these alternative bank estimates for ozone and climate is found in *Section 7.4.3*.

The Technology and Economic Assessment Panel (TEAP) has also performed a model analysis of CFC-11 banks. In their approach, they use estimates of release rates that vary over the bank's life cycle (WMO, 2021). These bank size estimates are consistent with the values calculated by Lickley et al. (2020), giving further credibility to their use in this chapter.

As in the previous Assessment, the GSFC 2-D model, described in Appendix 6B of Carpenter, Daniel et al. (2018) and in Fleming et al. (2020), is used to evaluate the ozone response for the scenarios developed here. The use of this 2-D model will again allow us to evaluate the impact of future projections of CO_2, CH_4, and N_2O.

7.4.2 Baseline Scenario

Future scenarios are derived in this chapter for the long-lived ODSs, CH_2Cl_2 (dichloromethane), and HFC-23. Projections for the other HFCs are described in *Chapter 2* and are incorporated here. HFC-23 scenarios are developed in this chapter because of the close association of HFC-23 emissions with HCFC-22 production. Beyond the ODSs, various scenarios of future mixing ratios of CO_2, CH_4, and N_2O are also examined with the 2-D model to show their influence on future ozone levels.

The scenario chosen to be the baseline scenario for non-ODS GHGs is SSP2-4.5. Of the five SSP narratives, this comes closest to representing a middle-of-the-road pathway, with social, economic, and technological trends projected to be not substantially different from what has occurred in the past. In addition, this is the baseline scenario used in the Chemistry-Climate Model Initiative (CCMI) model calculations, which are used elsewhere in this Assessment.

In general, the key assumptions that determine future ODS mixing ratios are 1) their global lifetimes, 2) projections of future production, 3) current banks, and 4) release rates from production, including production intended for feedstock use and from banks. For production intended for emissive uses (i.e., non-feedstock uses), it is assumed that all halon and CFC production has ceased globally, along with HCFC production in non-Article 5 countries. In Article 5 countries, future HCFC production is held constant at 2020 levels until 2025, after which it phases down in steps according to the Protocol controls. An important difference between the baseline scenario used here and the baseline scenarios in previous Assessments is that we include some emissions from feedstock production for the compounds CFC-113/CFC-113a, CFC-114/CFC114a, HCFC-22, HCFC-141b, HCFC-142b, CH_3CCl_3, CH_3Br, and CCl_4 and allow these emissions to continue into the future. The emissions from feedstocks are uncertain, and we conservatively make the assumption that 2% of production associated with feedstock usage is emitted in the year of production (see **Box 7-2** for a discussion of feedstock-related emissions) for all compounds except CCl_4, for which it is assumed to be 4.3% (see *Section 7.2.1.3* and **Figure 7-4**). These CCl_4 emissions arise from a combination of emissions from its production (i.e., unreported, non-feedstock emissions in **Figure 7-4**) and from the feedstock usage. Note that this 4.3% has been revised downward from that given in the SPARC CCl_4 report (SPARC, 2016). There are substantial increasing feedstock production trends over at least the past few years for HCFC-22 and CCl_4 (**Figure 7-3**). Nevertheless, in our baseline scenario, we assume that future production for feedstock use remains fixed at the 2020 levels. As discussed in **Box 7-2**, CCl_4 projections are calculated differently than the projections for other ODSs due to the large uncertainty in the sources of recent and current emissions. We assume that the current emissions are made up of a feedstock-related emissions component, an inadvertent component related to other industrial sources, and emissions related to historic production (e.g., from landfills; see **Figure 7-4**). It is assumed that emissions from this historic production are linearly phased out between 2021 and 2030, after which they remain zero, and the only continuing

emissions are associated with feedstock production and use as well as inadvertent production losses.

For the banks considered, including CFC-11, CFC-12, HCFC-22, HCFC-141b, HCFC-142b, halon-1211, and halon-1301, the Lickley approach (Lickley et al., 2022) is used to estimate banks at the beginning of 2020. These 2020 banks, along with historical emissions and reported production values are used to estimate banks back to 2015. Then, over the 2015–2020 time period, a single average annual percentage release rate from the bank is calculated for each compound and assumed to remain constant into the future. This uniquely determines future emission scenarios for each of the banked compounds, with annual production added to and annual emissions subtracted from the bank each year.

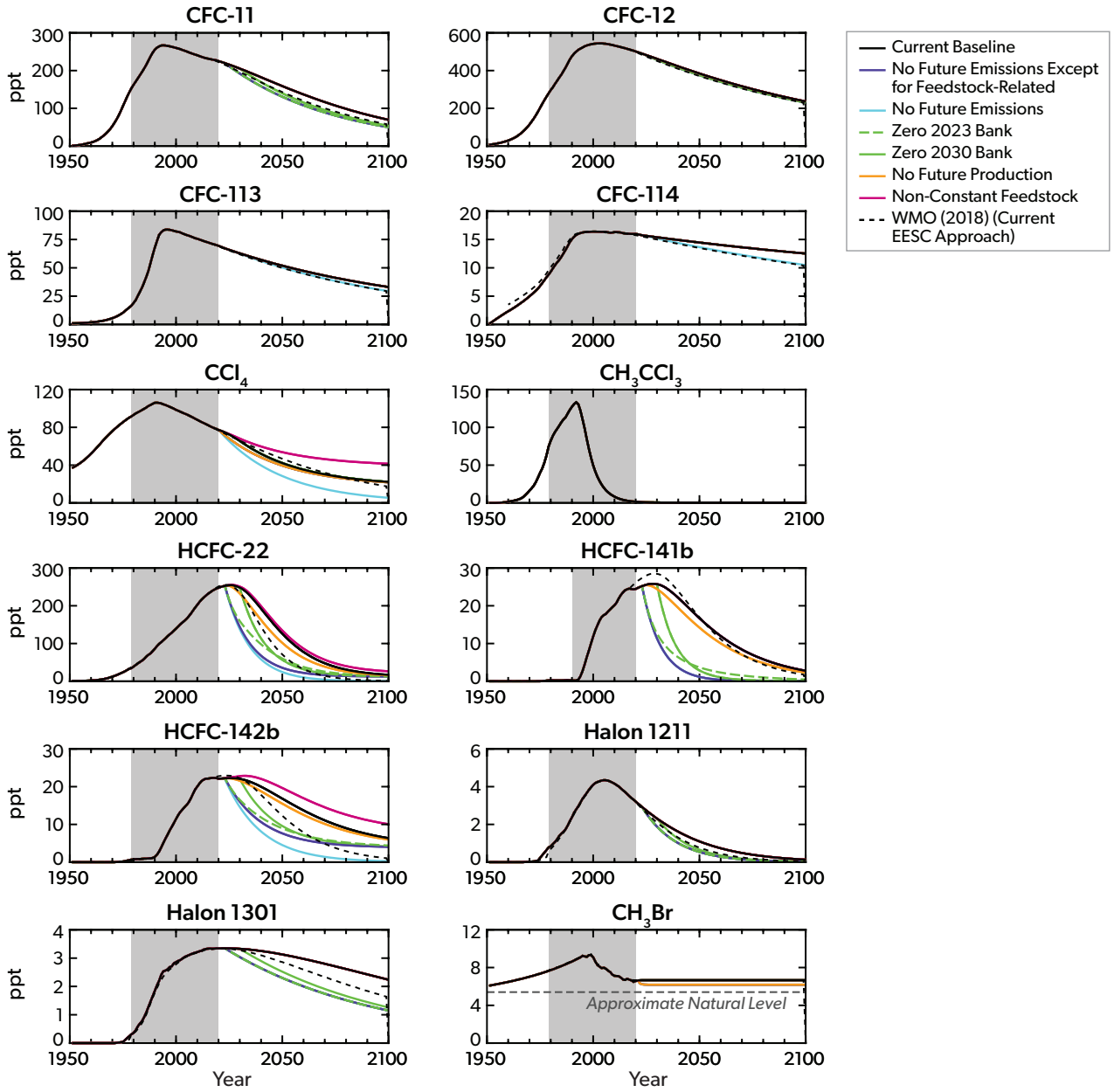

Figure 7-6. Comparison of mixing ratios from the current baseline scenario (solid black curves) with those of the alternative scenarios described in *Section 7.4.3* and those of the baseline scenario from the 2018 Assessment (dashed black curves). Alternative scenarios shown include the elimination of the banks in 2023 and 2030 (dashed and solid green curves, respectively), elimination of production from 2023 onward (orange curves), elimination of emissions from 2023 onward except for emissions associated with feedstock production (dark blue curves), elimination of all emissions from 2023 onward (light blue curves), and a "non-constant" feedstock production scenario in which feedstock production continues to increase or decrease in the future at the rate experienced over the past decade (described in the text; magenta curves).

CH_3Br is assumed to have no further controlled production globally, and continuing emissions arise from assumed constant ongoing production for critical use exemptions (CUEs) and quarantine and pre-shipment (QPS) uses consistent with what has been reported for 2020. Halon-1202 and halon-2402 are assumed to have no future emissions, and the mixing ratio of CH_3Cl remains at 539.5 ppt, a level assumed to be consistent with no further anthropogenic activity; while some anthropogenic emissions are likely to continue (see *Section 7.2*), these are not expected to significantly affect the conclusions of this chapter and thus are not considered here.

We also include in the discussion below the impact of CH_2Cl_2 on ozone, as calculated from 3-D model studies. We do not include this compound in our 2-D model calculations because of the dependence on the time of year and location of emissions (both latitude and longitude) in determining how much reaches the stratosphere. It is accepted that 3-D models are required to accurately calculate the transport of short-lived compounds from the surface to the stratosphere.

Finally, we develop a baseline scenario for HFC-23, including only its relationship to production of HCFC-22. HFC-23 is considered only in the climate forcing calculation since it has no chlorine, bromine, or iodine in it, and the change in ozone from its temperature impact would be minimal in our scenarios. While the HCFC-22 production intended for emissive uses is controlled by the Montreal Protocol, future feedstock production is uncontrolled. We assume that the emissions of HFC-23 are equal to 1.6% of the HCFC-22 production, where destruction capacities are only partly employed (*Section 7.2.1.4*). For the HFC-23 scenario, we assume that the HCFC-22 feedstock production increases through 2030 at the recently reported rate and remains constant thereafter. The baseline scenario for the other HFCs is developed and described in *Chapter 2*.

The ODS mixing ratios for the baseline scenario are shown in **Figure 7-6** and are tabulated in **Appendix Table 7A-1**. HFC-23 mixing ratios are also included in **Appendix Table 7A-1** starting in 2018. Many of the ODS projections are very similar to those of the baseline scenario from the 2018 Assessment. The biggest differences arise from the upward revision of bank estimates and, for some compounds, from including future emissions associated with feedstock production. HCFC-22 mixing ratios show the largest increases in the coming decades when compared with the previous Assessment, with values from 2042 to 2056 more than 50 ppt larger in the present projections. CFC-11 and CFC-12 both are larger by more than 10 ppt compared with the 2018 Assessment for periods in the future.

7.4.3 Alternative Future Scenarios

The primary alternative ODS scenarios are designed to assess the relative contributions of various sources of emissions to future ozone depletion and climate change. Specifically, we develop some scenarios that include the elimination of all emissions or production of certain compounds beginning in 2023 and some that eliminate banks that are projected to exist in 2023 or 2030. The purpose of examining two separate years for the elimination of banks is to provide some estimate of the benefit of quick action; however, this comparison depends on how quickly the ODSs are released from the banks and thus likely has more uncertainty associated with it than some of the other scenario comparisons. As stated earlier, there is also no differentiation of bank type in this chapter, which would be useful information if one wished to determine the practicality of capturing a bank. By grouping all banks into a single bank, we do not differentiate between active and inactive banks or the type of equipment in which the banked compound resides, nor can we comment on the accessibility of any bank. HFCs are also evaluated for their impact on climate under future scenarios in which all emissions, production, or banks are eliminated from 2023 onward.

Other alternative ODS scenarios performed are meant to estimate the impact of the unreported production and associated emissions of CFC-11 over the past decade, as well as the potential impacts of future emissions associated with uncontrolled production intended for feedstock applications. To quantify the impact of feedstock usage, we include a scenario in which all emissions associated with feedstock applications are eliminated beginning in 2023. We include an additional scenario that is identical to the baseline scenario except that through 2030, feedstock production for each compound considered is allowed to continue increasing or decreasing at the same rate as exhibited over the 2010–2020 period. Of course, changes after 2030 would further affect any conclusion, but we hold production constant after 2030 due to the speculative nature such projections would entail. It is important to recognize that the feedstock results presented in this chapter are specifically dependent on the ODS emissions that are assumed to be associated with feedstock activity in the baseline scenario.

Future ODS projections for selected alternative scenarios are included in **Figure 7-6** for comparison with the baseline scenario of this chapter and the baseline scenario of WMO (2018).

For CH_2Cl_2, we estimate the impact of future emissions if they are allowed to grow through 2030 at the rate exhibited over the past five years, after which emissions are held constant. Furthermore, we also estimate the effect of the elimination of all CH_2Cl_2 emissions after 2023.

For CO_2, CH_4, and N_2O, we examine eight alternative SSP scenarios that range from substantially lower (SSP1-1.9) to substantially higher (SSP5-8.5) greenhouse gas radiative forcing by the end of the century. We examine the impact of these different concentrations collectively and individually to show the specific effect that each compound has on future ozone levels.

The specific scenarios discussed above are evaluated for their impacts on stratospheric ozone and climate in **Table 7-6**.

7.4.3.1 Stratospheric Ozone Implications

The mid-latitude EESC evolution for selected key ODS scenarios is shown in **Figure 7-7**. This shows that in the baseline scenario, mid-latitude EESC returns to its 1980 levels at the beginning of 2066, about six years later than in the baseline scenario of the 2018 Assessment (cf. Appendix 6C of Carpenter, Daniel et al. (2018)). This is primarily due to the higher concentrations of CFC-11 and CFC-12 that result from the larger bank estimates used here compared with the previous Assessment. Polar EESC returns to 1980 levels in 2087, about nine years later than in Carpenter, Daniel et al. (2018). Slight changes in the age spectrum function used in the EESC calculation also contribute about one and two years to these mid-latitude and polar delays, respectively. In Carpenter, Daniel et al. (2018), the function describing the age spectrum for use in the Engel et al. (2017) approach, assumed a width to mean age ratio of 0.5 as suggested in Newman et al.

Table 7-6. *See caption on facing page.*

Scenario	Change in Integrated EESC[1] Relative to Baseline Scenario for the Mid-latitude Case		Year When EESC is Expected to Drop Below 1980 Value *(year x)*		Change in Average Radiative Forcing 2023–2100 (mW m^{-2})	Change in Integrated O_3 Depletion: 2020–2070 (%)
	$\int_{1980}^{year\ x} EESC\ dt$	$\int_{2023}^{year\ x} EESC\ dt$	Mid-latitude	Antarctic Vortex		
A1: Baseline scenario	0.0	0.0	2066.0	2086.6	0.0	0.0
Elimination of production for emissive uses[2]:						
All ODSs	–3.2	–9.6	2063.2	2084.1	–3.7	–0.15
HCFCs	–0.5	–1.5	2065.6	2086.3	–3.3	–0.03
CCl_4	–0.9	–2.6	2065.5	2086.3	–0.4	–0.04
CH_3Br for QPS and CUE	–1.9	–5.6	2064.1	2084.7	–0.0	–0.08
HFCs (except HFC-23)					–51.4	
Elimination of emission for emissive uses[3]:						
All Controlled ODSs	–10.1	–30.1	2052.9	2072.1	–25.1	–0.60
CFCs	–3.3	–10.0	2061.2	2080.7	–9.5	–0.20
Halons	–3.1	–9.3	2062.1	2082.0	–0.4	–0.12
HCFCs	–2.6	–7.7	2063.9	2085.1	–14.8	–0.14
CCl_4	–0.9	–2.6	2065.5	2086.3	–0.4	–0.04
CH_3CCl_3	0.0	0.0	2066.0	2086.6	0.0	–0.00
CH_3Br for QPS	–1.9	–5.6	2064.1	2084.7	0.0	–0.08
All ODS emissions, including related to feedstock use	–11.3	–33.8	2050.5	2068.1	–31.1	–0.71
HFCs (except HFC-23)					–67.7	
HFC-23					–10.9	
Entire 2023 bank captured and destroyed:						
All ODSs	–7.7	–22.9	2055.6	2074.7	–21.5	–0.46
All CFCs	–3.3	–10.0	2061.2	2080.7	–9.5	–0.20
All halons	–3.1	–9.3	2062.1	2082.0	–0.4	–0.15
All HCFCs	–2.1	–6.3	2064.4	2085.4	–11.6	–0.11
HFCs (except HFC-23)					–16.2	
Entire 2030 bank captured and destroyed:						
All ODSs	–4.7	–13.9	2057.7	2076.6	–15.7	–0.29
All CFCs	–1.8	–5.5	2062.5	2082.1	–6.1	–0.11
All halons	–1.9	–5.6	2062.8	2082.6	–0.3	–0.10
All HCFCs	–1.5	–4.6	2064.2	2085.2	–9.3	–0.09
Other scenarios:						
Continuing feedstock trend through 2030	2.3	6.8	2070.3	2092.1	+4.4	+0.10
Additional 1000 Gg bank of CFC-11 in 2021	3.0	9.0	2069.7	2090.3	+5.6	+0.15
Reduced CFC-11 of 280 Gg over 2012–2019	–1.2	–3.7	2065.2	2085.9	–1.7	-0.06
N_2O mitigation (uses SSP1-1.9 for N_2O)					–43.4	–0.17
No future CH_2Cl_2 anthropogenic emissions						–0.28 to –0.56
CH_2Cl_2 emissions increasing through 2030, then constant						+0.06 to +0.12

Note:
[1]EESC is calculated according to the approach described in Engel et al. (2017); this change accounts for a delay in the return of mid-latitude EESC to 1980 levels of more than a decade when compared with Table 6-5 of WMO (2018).
[2]Production scenarios all allow for non-emissive uses, such as those associated with feedstock usage.
[3]Emission scenarios allow for continued emission associated with non-emissive uses.

Table 7-6. Comparison of scenarios and test cases, showing the year when EESC[1] drops below the 1980 value for both mid-latitudes and in the Antarctic vortex, as well as integrated mid-latitude EESC differences relative to the baseline scenario; the integral is performed from 1980 or 2023 through the time when mid-latitude EESC returns to 1980 levels (denoted as "year x"). Also shown are changes in average radiative forcing over 2023–2100 and average global ozone depletion over 2020–2070. Future changes in CH_4 and CO_2 may also significantly alter ozone levels and radiative forcing, likely by amounts larger than any of the cases considered in this table (see, e.g., text in *Section 7.4.3.1*). Average radiative forcing from the ODSs in the baseline scenario, against which other scenarios are compared, is 0.22 W m^{-2} (220 mW m^{-2}); for HFC-23 it is 0.02 W m^{-2}, and for the other HFCs it is 0.08 W m^{-2}. For comparison, the current radiative forcing of CO_2 is about 2 W m^{-2}.

(2007); here we assume the ratio of the square of the width to the age is 0.7 yr, taken form Engel et al. (2017).

Figure 7-8 and **Figure 7-9** compare the impact of selected scenarios on globally averaged total column ozone, respectively, as calculated with the 2-D model. As expected, the ozone response exhibits a roughly inverse relationship with the EESC curves. While the subsequent discussion specifically refers to ozone and ozone depletion, EESC generally responds in a consistent manner with ozone depletion across the various scenarios shown in these figures as well as in **Table 7-6**.

Elimination of all halogenated ODS emissions starting in 2023 increases future global ozone above the baseline, with a 0.71%[11] increase in globally averaged column ozone averaged over 2020–2070 (**Table 7-6**), and it moves the date when EESC returns to 1980 levels forward by 16 years for mid-latitudes and 19 years for polar regions. Elimination of all ODS emissions represents the lowest future EESC that can be achieved with the lifetimes assumed here; these global lifetimes determine how quickly the various ODS atmospheric mixing ratios decline. CFCs, halons, HCFCs, CH_3Br, and CCl_4 (including emissions from production and use in feedstock applications) all contribute notably to future ODS emissions in the baseline scenario.

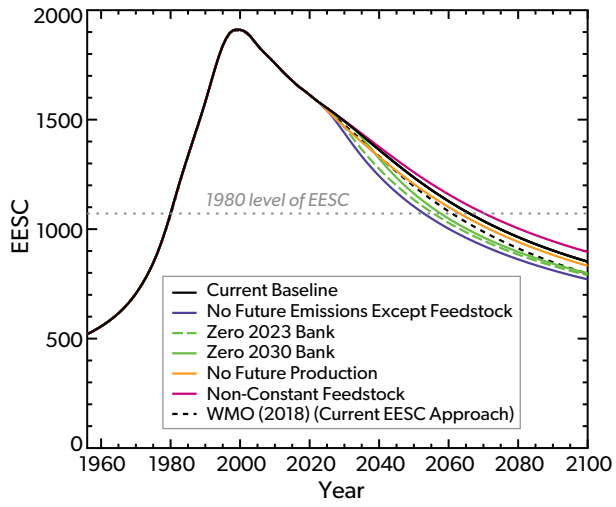

Figure 7-7. Mid-latitude EESC time series for the scenarios shown in **Figure 7-6**. The 2018 Assessment EESC values have been calculated using the approach adopted in this chapter and applied to the mixing ratios of that baseline scenario to obtain a consistent comparison.

In the baseline scenario, future feedstock-related emissions lead to a 0.11% decrease in globally averaged total ozone averaged over 2020 through 2070 and an increase in radiative forcing of 6 mW m^{-2} when averaged over 2023–2100. If feedstock emissions continue to change through 2030 at the same rate as over the past decade and are held constant thereafter, this would decrease total ozone averaged over 2020 through 2070 by an additional 0.10% and increase averaged radiative forcing by an additional 4 mW m^{-2} when averaged over 2023 through 2100.

The scenarios that assume hypothetical full capture and destruction of ODS banks in 2023 or 2030 (**Figure 7-9**) have a much larger effect on reducing future ozone depletion than does the scenario in which production of all ODSs is eliminated starting in 2023. As stated above, however, it should be recognized that there are substantial uncertainties in the current bank size estimates. The Lickley et al. (2022) bank values are generally higher than those projected for 2020 when starting with the 2008 values of IPCC/TEAP (2005); this is also the case for projections from the IPCC/TEAP (2005) banks estimated for 2002. It is our assessment that the uncertainties in bank values remain large at this time, with commensurate uncertainties in the extent to which capture and destruction of the banks could benefit climate and ozone.

Using the results from WMO (2021), we can put the potential impacts of the unreported production of CFC-11 over the past decade into context with the results above. We evaluate the impact of the unexpected emissions over the 2012–2019 period by assuming emissions associated with unreported production of 280 Gg, the middle of the range (120–440 Gg) given in WMO (2021). We also examine the impact of an additional 1000 Gg in the CFC-11 bank in 2020. While the increase in the CFC-11 bank from the unreported production is uncertain, this value of 1000 Gg can be used to approximately scale other potential bank increases if more certainty is eventually gained as to how much of the recent unreported production went into applications relative to how much has already been emitted. A CFC-11 bank increase of this size (1000 Gg) is projected to lead to about a 0.15% decrease to global column ozone averaged through 2070. This can be compared with the emissions through 2019 (280 Gg) associated with the unreported production causing an additional 0.06% depletion averaged over 2020–2070. It is thought likely that the observed

[11] Ozone change percentages modeled in this chapter are calculated with the simplifying assumption of a background globally averaged column ozone level of 300 DU. Thus, a 1% change represents a 3 DU change

emissions over this time period were associate with foam production, and historically it is found that about 25%–45% of the production is emitted through the foam production process. This would imply an increase in the CFC-11 bank of 146–1320 Gg. This range is comparable to another recent estimate of the increase in CFC-11 banks of 90 to 725 Gg due to this unreported production (Montzka et al., 2021).

To explore further how future emissions of other climate-relevant gases could affect ozone, **Figure 7-10** shows the range in future global total ozone associated with nine selected SSP scenarios (1-1.9, 1-2.6, 2-4.5, 3-7.0, 3-7.0-low NTCF [near-term climate forcer], 4-3.4, 4-6.0, 5-3.4 overshoot (OS), and 5-8.5). The influences of CO_2, CH_4, and N_2O are shown in combination (top panel), as well as individually (lower three panels), where the latter are calculated by varying each gas individually while using the baseline SSP2-4.5 scenario for the other two gases. The baseline ODS scenario is used in all runs. The processes responsible for the ozone impacts of these greenhouse gases (GHGs) are discussed in *Chapter 3* and in past Assessments. When compared with **Figures 7-8** and **7-9**, it is apparent that the variations of each of these three GHGs across the SSP scenarios lead to a substantially wider range of possible future ozone levels than from the ODS scenarios alone. For example, the difference in global ozone in 2100 between the baseline ODS scenario and a scenario with no ODS emissions from 2023 is 0.6% (**Figure 7-8**). This contrasts with a range of 6% across the SSP scenarios due to the combined impact of the three GHGs, and ranges of 3%, 4%, and 1.5% due to the individual ranges of CO_2, CH_4, and N_2O concentrations, respectively. Thus, policies that affect the future evolution of these three GHGs in particular will be important for predicting how ozone will change. The impacts of N_2O and ODS mitigation through the 21st century are also directly compared in **Figure 7-8**.

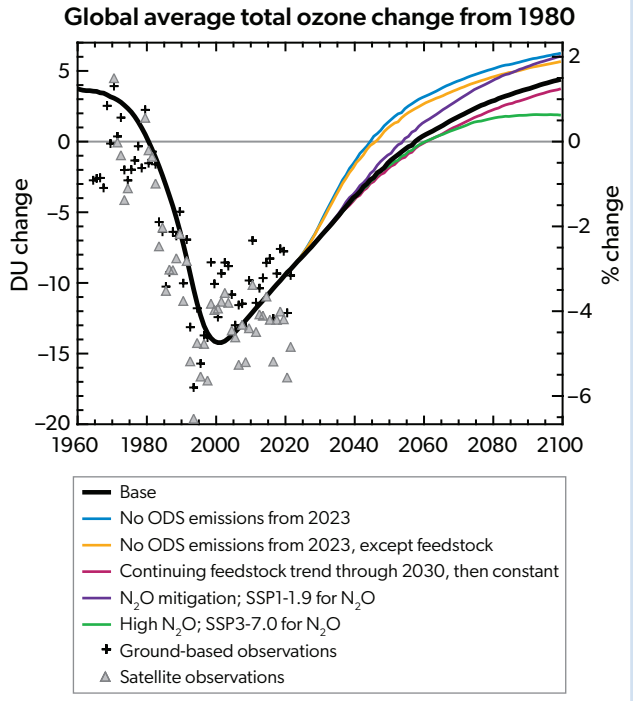

Figure 7-8. Influence of selected scenarios on globally averaged (90°S–90°N) total ozone relative to that in 1980. The scenarios include the baseline scenario; no long-lived ODS emissions from 2023 onward; no long-lived ODS emissions from 2023 onward except for feedstock uses; feedstock emission changes continuing at the same rate experienced over the past decade through 2030, then held constant; an N_2O mitigation scenario in which the low SSP1-1.9 projection is used for future N_2O mixing ratios; and a high N_2O scenario in which the high SSP3-7.0 projection is used for future N_2O mixing ratios, with all other assumptions following the baseline scenario. Calculations are from the GSFC 2-D model. The figure also shows observed global and annually averaged total ozone relative to the 1979–1981 average, from ground-based (black plus signs) and satellite (grey triangles) observations.

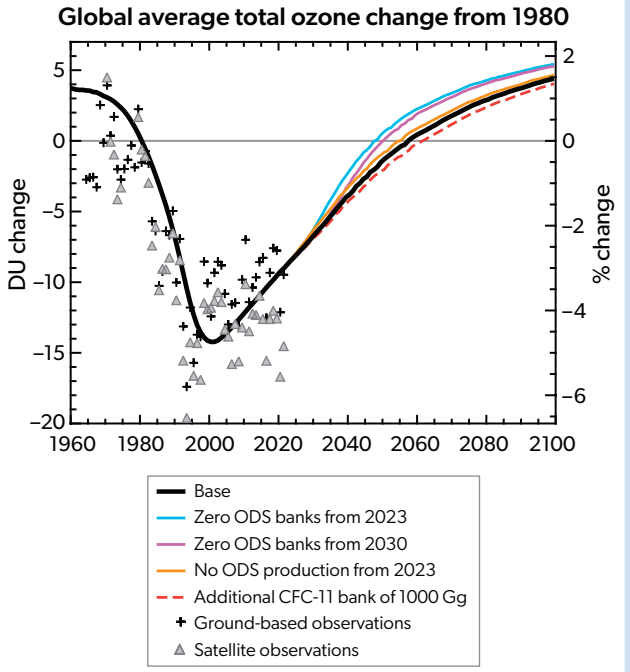

Figure 7-9. Same as in **Figure 7-8** but for additional scenarios. These scenarios include the baseline scenario; full capture and destruction of the ODS banks in 2023 but allowing continued production; full capture and destruction of the ODS banks in 2030 but allowing continued production; no ODS production from 2023 onward; and an additional 1000 Gg in the CFC-11 bank in 2020, with all other assumptions following the baseline scenario. Calculations are from the GSFC 2-D model. The figure also shows observed global and annually averaged total ozone relative to the 1979–1981 average, from ground-based (black plus signs) and satellite (grey triangles) observations.

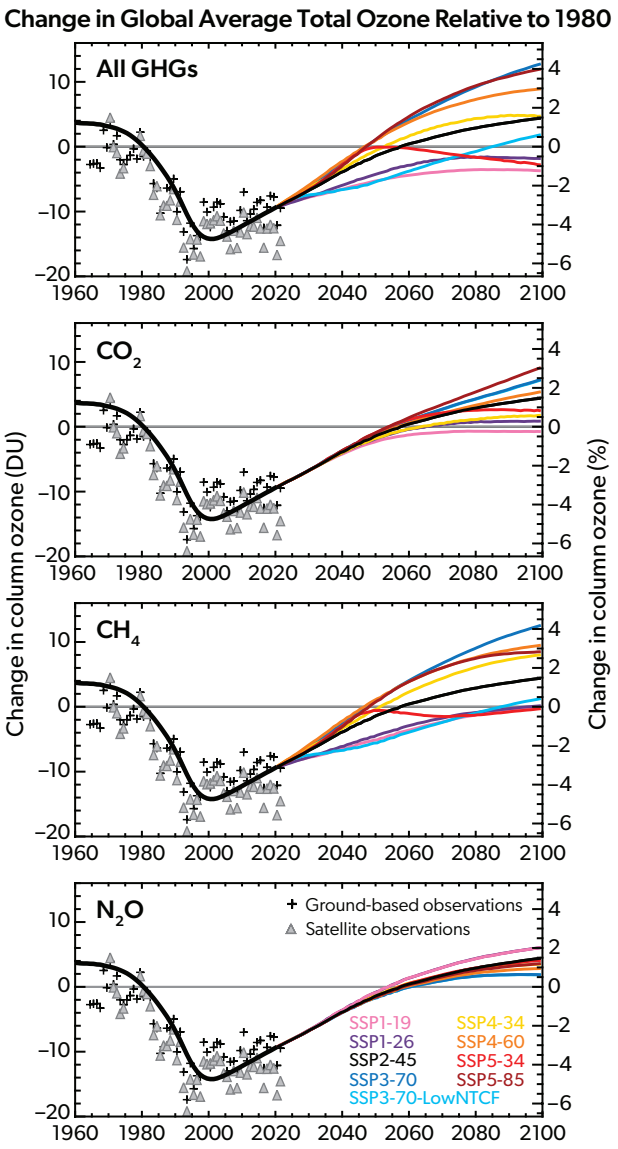

Figure 7-10. As in **Figure 7-9**, but showing global total column ozone responses to a range of future CO_2, CH_4, and N_2O emissions scenarios in the presence of decreasing ODSs. The colored lines depict the range in projected ozone for the nine SSP scenarios listed in the bottom panel, due to future changes in all three GHGs combined (*top panel*), and individually by varying each gas while using the baseline SSP2-4.5 scenario for the other two gases. For CO_2 and CH_4, the highest and lowest assumed emissions correspond to the highest and lowest ozone curves, respectively, while the opposite is true for N_2O. All simulations use the baseline ODS scenario. Calculations are from the GSFC 2-D model, which compares well with 3-D models, including for the CH_4 and N_2O perturbations (see WMO-2018, Appendix 6B).

Finally, two alternative scenarios are examined for CH_2Cl_2, namely (1) continued strong growth in emissions until 2030, with constant emissions thereafter, and (2) immediate cessation of emissions. Ozone impacts of these scenarios are shown in **Table 7-6**. Unlike the CFCs, CH_2Cl_2 has a short lifetime and thus responds rapidly to changes in emissions. If emissions quickly decrease in the future, the delivery of CH_2Cl_2 to stratospheric chlorine will also fall rapidly. Under scenario (1), a range of 3-D model ODP values (Claxton et al. 2019) implies that integrated global ozone depletion over 2020–2070 (shown in the final column of **Table 7-6**) would increase by a rather small amount (0.06%–0.12%). However, the continuing large variability in its surface abundances makes estimates of future concentrations highly uncertain and hinders evaluation of the plausibility of this scenario. If, on the other hand, all anthropogenic emissions of CH_2Cl_2 were to cease in 2023, the reduction in average ozone depletion from 2020–2070 relative to the baseline scenario would be more significant (0.28–0.56%). The amount of reduction in ozone depletion would be dependent on the regional variation of emissions sources, with the largest depletion reduction being for emissions sources in tropical Asia. The effect on average ozone depletion from 2020–2070 would be about 40–80% of the effect of eliminating all ODS emissions in 2023.

7.4.3.2 Climate Implications

The radiative forcing time series for ODSs in the baseline scenario and selected alternative scenarios are shown in **Figure 7-11**. As mentioned previously (*Section 7.3.2*), the forcing from these compounds due to ozone destruction is not included in this figure, in **Table 7-6**, or in our discussion below. Even with the extreme scenario that assumes no additional emissions of ODSs

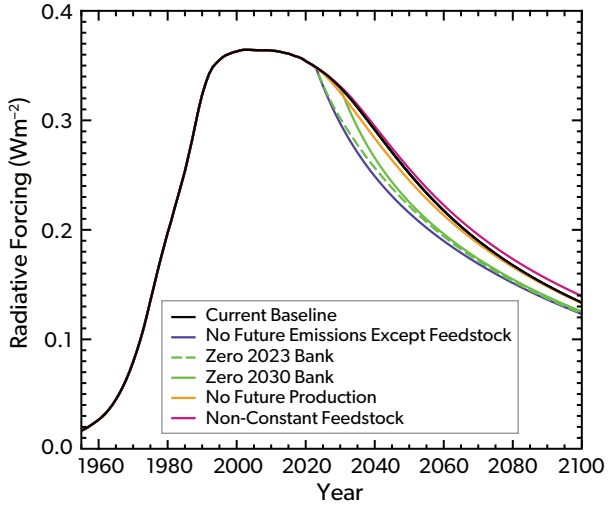

Figure 7-11. Direct radiative forcing (RF) from the combination of compounds and scenarios shown in **Figure 7-6**. The climate impacts of ozone depletion, resulting from the presence of these ODSs, is not included in this forcing. As indicated by the negative Indirect GWPs in **Table 7-5**, inclusion of the ODS impact on ozone would result in lower effective radiative forcing (ERF), although the extent to which it would be lower remains highly uncertain.

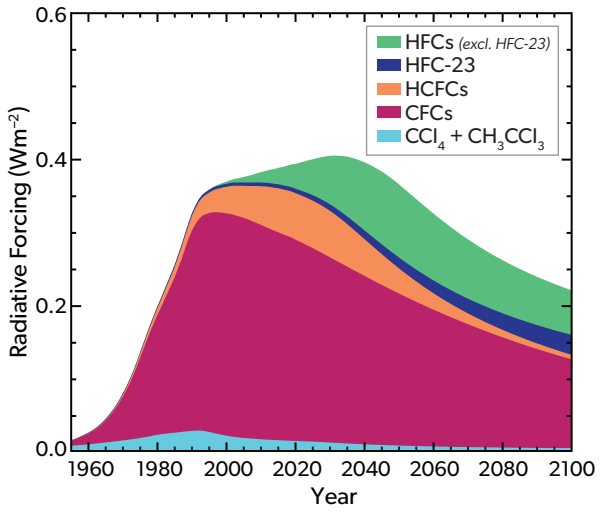

Figure 7-12. Contributions of various groups of ODSs and HFCs to direct radiative forcing for the baseline scenario. The light blue area represents forcing from CCl_4 and CH_3CCl_3, combined. CFC, HCFC, HFC-23, and other HFC (excluding HFC-23) contributions are then progressively stacked on top.

from 2023 onward, climate benefits are limited when compared with the forcing due to compounds already in the atmosphere. Compared to the baseline scenario, the average radiative forcing reduction arising from the elimination of all ODS emissions from 2023 onward (excluding feedstocks), from the capture and destruction of the 2023 ODS banks, and from the elimination of ODS production from 2023 onward is 25.1, 21.5, and 3.7 mW m^{-2}, respectively, when averaged over 2023–2100 (**Table 7-6**). If emissions associated with feedstocks were also assumed to be eliminated from 2023 onward, the average radiative forcing reduction would be 31.1 mW m^{-2} rather than 25.1 mW m^{-2}. A breakdown of the contribution from individual compounds or compound groups to the radiative forcing values is shown in **Figure 7-12** for the baseline scenario.

Using the assumptions described earlier in this section for the magnitude of emissions arising from unreported production of CFC-11 over the past decade, we estimate an average radiative forcing impact of 1.7 mW m^{-2} over 2023–2100 from these emissions. As stated in *Section 7.4.3.1*, it is unclear how much recent unreported production has contributed to the global CFC-11 bank. Thus, any additional contribution from any augmentation to the CFC-11 bank from unreported production remains highly uncertain and is not included in this estimate. As in *Section 7.4.3.1*, we can calculate the potential impact of an additional 1000 Gg added to the 2020 CFC-11 bank. This would lead to an additional 5.6 mW m^{-2} averaged over 2023–2100 and can be scaled to other CFC-11 bank sizes. These radiative forcing estimates also do not include any impact from potential co-emissions of CFC-12 or, to a lesser extent, CCl_4, that might have been associated with the recent, unreported CFC-11 production.

Figure 7-12 includes additional radiative forcing contributions of HFC-23 and the other HFCs calculated for the baseline scenario. The impact of potentially reducing future HFC emissions is strongly dependent on the assumption underlying the baseline scenario. For example, if the baseline scenario overestimates the future radiative forcing compared with what will happen under existing controls, the benefit of a hypothetical elimination of future emissions or production would also be overestimated. As was seen in Figure 6-7 of the 2018 Assessment, HFC forcing remains relatively constrained and does not increase sharply in the future because global adherence to the Kigali Amendment is assumed in the baseline scenario. **Figure 7-12** also shows that if HFC-23 emissions progress as assumed in the baseline scenario, its forcing continues to increase through the end of the century, even as the forcing from other HFCs will have begun to decline. Because of its long lifetime, any potential future declines in HFC-23 mixing ratios after 2100, or even before, could only happen slowly. In the baseline scenario, in which it is assumed that the destruction rate of HFC-23 relative to HCFC-22 production is not increased, its radiative forcing in 2100 is projected to be about half of all the other HFCs together (**Figure 7-12**). If destruction were maximized, consistent with current technical abilities, forcing from HFC-23 would remain minor. As shown in **Table 7-6**, elimination of HFC-23 emissions beginning in 2023 would reduce average radiative forcing over 2023–2100 by 11 mW m^{-2}. Elimination of the other HFC emissions in 2023 would reduce average radiative forcing by 68 mW m^{-2}, with future production accounting for about three-quarters of this total.

Not shown in the previous figures, but noted in **Table 7-6**, is that the reduction of N_2O emissions from our baseline scenario (SSP2-4.5) to the SSP1-1.9 scenario reduces average radiative forcing by 43 mW m^{-2}. SSP1-1.9 is the scenario considered with the greatest N_2O emissions mitigation; this anthropogenic reduction in emissions is about 3% when compared with the baseline scenario and averaged over 2020–2070.

To provide some context for the previous forcing values, the average radiative forcing by CO_2 over the 2023–2100 period in our baseline scenario (SSP2-4.5) is about 3250 mW m^{-2}.

Appendix Table 7A-1. Atmospheric mixing ratios (in ppt) of the ODSs considered in the baseline scenario. Values are for the beginning of the corresponding year. Values represent a combination of AGAGE and NOAA networks for years when those observations are available (see *Chapter 1*). Projection assumptions are discussed in *Sections 7.4.1* and *7.4.2*.

Year	CFC-11	CFC-12	CFC-113	CFC-114	CFC-115	CCl_4	CH_3CCl_3	HCFC-22
1955	3.3	14.3	1.3	1.1	0.0	42.3	0.1	1.0
1956	4.3	16.7	1.3	1.4	0.0	44.0	0.2	1.1
1957	5.6	19.4	1.4	1.6	0.0	45.9	0.4	1.3
1958	6.9	22.6	1.6	1.9	0.0	47.8	0.7	1.5
1959	8.2	25.9	1.7	2.1	0.0	49.9	1.0	1.7
1960	9.5	29.5	1.9	2.3	0.0	52.1	1.5	2.1
1961	11.1	33.9	2.0	2.6	0.0	54.4	2.0	2.4
1962	13.3	38.8	2.3	2.8	0.0	56.8	2.4	2.9
1963	16.1	44.4	2.5	3.0	0.0	59.3	3.2	3.4
1964	19.5	51.1	2.8	3.3	0.0	61.8	3.9	4.1
1965	23.5	58.8	3.1	3.5	0.0	64.4	4.7	4.9
1966	28.1	67.5	3.5	3.8	0.0	66.9	5.8	5.9
1967	33.1	77.3	3.9	4.1	0.1	69.3	7.6	7.1
1968	38.8	88.3	4.4	4.4	0.1	71.6	10.1	8.5
1969	45.3	100.6	4.9	4.7	0.1	73.8	13.0	10.3
1970	52.8	114.3	5.5	5.0	0.2	75.9	16.3	12.1
1971	61.3	129.3	6.3	5.3	0.2	78.0	19.1	14.1
1972	70.6	145.3	7.1	5.6	0.3	80.0	22.7	16.2
1973	81.1	162.8	8.1	6.0	0.4	81.9	27.4	18.6
1974	93.0	182.2	9.1	6.3	0.5	83.7	33.5	21.3
1975	106.1	203.1	10.4	6.8	0.7	85.5	40.0	23.8
1976	118.5	223.2	11.9	7.3	0.9	87.2	45.5	26.6
1977	130.9	242.6	13.5	7.8	1.1	88.8	53.1	29.8
1978	142.5	261.2	15.0	8.3	1.3	90.4	62.5	33.2
1979	153.2	279.0	16.6	8.8	1.5	91.6	74.7	34.8
1980	162.3	296.7	19.0	9.3	1.8	93.2	82.2	38.9
1981	170.7	311.4	21.5	9.9	1.9	94.8	88.8	43.1
1982	179.3	329.4	25.3	10.5	2.1	96.0	93.8	47.1
1983	187.6	345.3	28.9	11.0	2.4	97.1	97.9	50.9
1984	196.3	362.5	32.6	11.4	2.7	98.4	102.2	54.8
1985	205.5	378.0	37.3	11.9	3.1	99.6	106.8	59.1
1986	215.5	397.2	42.1	12.6	3.5	101.0	110.5	65.0
1987	226.6	416.0	47.5	13.2	4.0	102.6	113.3	70.1
1988	237.7	437.6	54.5	13.8	4.4	103.7	118.5	73.8
1989	247.4	458.7	61.3	14.5	4.8	104.9	123.2	79.6
1990	255.1	476.2	67.8	15.1	5.3	106.1	127.3	86.3
1991	260.5	489.6	73.5	15.5	5.7	106.2	131.0	92.8
1992	263.9	500.8	79.2	15.8	6.1	105.8	133.1	98.9
1993	266.4	510.1	81.4	16.0	6.5	105.3	130.5	103.5
1994	266.9	516.1	83.0	16.1	6.8	104.4	122.2	108.6
1995	266.3	522.2	83.7	16.2	7.2	103.7	110.6	113.5
1996	265.2	528.5	83.8	16.3	7.5	102.8	98.2	119.2
1997	264.3	533.2	83.6	16.3	7.7	101.8	84.0	124.1
1998	262.9	536.3	83.2	16.3	7.9	100.8	71.1	128.9
1999	261.5	539.1	82.7	16.4	8.0	99.7	59.5	134.3

HCFC-141b	HCFC-142b	Halon-1211	Halon-1202	Halon-1301	Halon-2402	CH_3Br	CH_3Cl	HFC-23
0.0	0.0	0.00	0.00	0.00	0.00	6.3	491.3	
0.0	0.0	0.00	0.00	0.00	0.00	6.3	495.1	
0.0	0.0	0.00	0.00	0.00	0.00	6.3	498.8	
0.0	0.0	0.00	0.00	0.00	0.00	6.4	502.6	
0.0	0.0	0.00	0.00	0.00	0.00	6.4	506.4	
0.0	0.0	0.00	0.00	0.00	0.00	6.5	510.3	
0.0	0.0	0.00	0.00	0.00	0.00	6.5	514.2	
0.0	0.0	0.00	0.00	0.00	0.00	6.6	517.9	
0.0	0.0	0.00	0.00	0.00	0.00	6.6	521.5	
0.0	0.0	0.00	0.00	0.00	0.00	6.7	524.9	
0.0	0.0	0.00	0.00	0.00	0.00	6.7	528.1	
0.0	0.0	0.00	0.00	0.00	0.00	6.8	531.0	
0.0	0.0	0.00	0.00	0.00	0.00	6.9	533.6	
0.0	0.0	0.01	0.00	0.00	0.01	6.9	536.0	
0.0	0.0	0.01	0.00	0.00	0.01	7.0	538.0	
0.0	0.0	0.02	0.00	0.00	0.02	7.0	539.9	
0.0	0.0	0.03	0.00	0.00	0.02	7.1	541.4	
0.0	0.1	0.04	0.00	0.01	0.03	7.2	542.8	
0.0	0.1	0.06	0.00	0.02	0.04	7.2	544.0	
0.0	0.1	0.09	0.00	0.03	0.05	7.3	544.9	
0.0	0.2	0.23	0.01	0.04	0.06	7.4	545.8	
0.1	0.3	0.37	0.01	0.11	0.08	7.4	546.5	
0.1	0.4	0.50	0.01	0.18	0.09	7.5	547.1	
0.2	0.6	0.64	0.01	0.24	0.11	7.6	547.6	
0.2	0.7	0.78	0.01	0.31	0.14	7.7	548.0	
0.2	0.8	0.84	0.01	0.36	0.15	7.7	548.4	
0.2	0.8	0.96	0.01	0.46	0.17	7.8	548.6	
0.3	0.8	1.07	0.01	0.59	0.19	7.9	548.9	
0.2	0.8	1.21	0.01	0.69	0.20	8.0	549.1	
0.2	0.9	1.39	0.01	0.78	0.22	8.1	549.3	
0.3	1.0	1.51	0.01	0.92	0.25	8.2	549.4	
0.3	1.0	1.61	0.01	1.09	0.27	8.3	549.5	
0.3	1.0	1.74	0.02	1.28	0.29	8.3	549.6	
0.3	1.0	1.94	0.02	1.47	0.32	8.4	549.7	
0.3	1.1	2.17	0.02	1.65	0.35	8.5	549.8	
0.3	1.4	2.38	0.02	1.84	0.38	8.6	549.8	
0.2	2.0	2.63	0.02	2.04	0.41	8.8	549.9	
0.2	2.8	2.80	0.02	2.19	0.43	8.9	549.9	
0.4	3.9	2.96	0.03	2.41	0.44	9.0	549.9	
1.3	5.1	3.16	0.03	2.53	0.46	9.1	550.0	
2.7	6.2	3.36	0.03	2.56	0.47	9.3	562.5	
4.5	7.3	3.52	0.04	2.60	0.47	9.2	546.4	
6.5	8.4	3.67	0.04	2.68	0.48	9.1	536.5	
8.2	9.4	3.84	0.04	2.71	0.49	9.3	556.9	
10.1	10.4	3.98	0.04	2.82	0.49	9.3	566.4	

Year	CFC-11	CFC-12	CFC-113	CFC-114	CFC-115	CCl_4	CH_3CCl_3	HCFC-22
2000	259.9	541.2	82.1	16.4	8.1	98.6	49.7	139.3
2001	258.4	542.9	81.8	16.4	8.2	97.6	41.5	144.9
2002	256.7	543.6	81.2	16.4	8.2	96.6	34.5	150.7
2003	254.5	543.6	80.4	16.4	8.3	95.6	28.8	155.7
2004	252.6	543.4	79.6	16.4	8.3	94.6	24.0	160.6
2005	250.4	542.7	78.9	16.4	8.4	93.7	20.0	165.9
2006	248.3	541.8	78.4	16.4	8.4	92.7	16.7	172.0
2007	246.1	539.8	77.7	16.3	8.4	91.5	14.0	179.1
2008	244.1	537.4	76.9	16.2	8.4	90.4	11.7	187.4
2009	242.2	535.3	76.1	16.2	8.4	89.1	9.9	195.2
2010	240.4	532.3	75.7	16.3	8.4	87.9	8.3	202.5
2011	238.3	529.5	75.0	16.3	8.4	86.8	6.9	210.0
2012	236.3	526.9	74.4	16.3	8.4	85.6	5.8	216.0
2013	234.4	523.9	73.7	16.2	8.4	84.6	4.8	221.5
2014	232.8	520.9	73.0	16.1	8.4	83.5	4.0	226.5
2015	231.6	518.3	72.5	16.1	8.5	82.4	3.3	231.6
2016	230.2	514.9	71.8	16.1	8.5	81.2	2.8	235.3
2017	229.1	511.4	71.2	16.0	8.5	80.1	2.4	239.3
2018	228.3	508.6	70.7	16.0	8.6	79.2	2.1	242.6
2019	227.2	505.1	70.1	16.0	8.7	78.4	1.8	245.5
2020	225.0	500.8	69.4	16.0	8.7	77.3	1.5	247.5
2021	223.3	497.1	68.7	15.9	8.7	76.5	1.3	249.7
2022	221.5	493.4	67.9	15.8	8.7	75.6	1.1	251.4
2023	219.7	489.6	67.2	15.8	8.6	74.6	1.0	252.6
2024	217.8	485.8	66.6	15.7	8.6	73.6	0.9	253.5
2025	215.8	481.9	65.9	15.7	8.6	72.5	0.8	254.1
2026	213.8	478.0	65.3	15.6	8.6	71.2	0.7	254.4
2027	211.7	474.0	64.7	15.6	8.6	69.9	0.7	253.8
2028	209.6	470.1	64.0	15.5	8.6	68.6	0.6	252.5
2029	207.4	466.1	63.4	15.5	8.6	67.1	0.6	250.6
2030	205.3	462.1	62.8	15.4	8.5	65.6	0.5	248.1
2031	203.1	458.1	62.2	15.4	8.5	64.1	0.5	245.2
2032	200.8	454.1	61.6	15.3	8.5	62.5	0.5	241.3
2033	198.5	450.2	61.0	15.3	8.5	61.1	0.5	236.7
2034	196.3	446.2	60.5	15.2	8.5	59.6	0.4	231.4
2035	194.0	442.2	59.9	15.2	8.5	58.3	0.4	225.6
2036	191.6	438.2	59.3	15.1	8.4	56.9	0.4	219.4
2037	189.3	434.2	58.7	15.1	8.4	55.6	0.4	212.9
2038	187.0	430.3	58.2	15.0	8.4	54.4	0.4	206.2
2039	184.6	426.4	57.6	15.0	8.4	53.2	0.4	199.3
2040	182.3	422.4	57.1	14.9	8.4	52.0	0.4	192.4
2041	179.9	418.5	56.5	14.9	8.4	50.9	0.4	185.5
2042	177.6	414.7	56.0	14.8	8.4	49.8	0.4	178.5
2043	175.2	410.8	55.5	14.8	8.3	48.7	0.4	171.5
2044	172.9	407.0	55.0	14.7	8.3	47.7	0.4	164.6
2045	170.5	403.2	54.4	14.7	8.3	46.7	0.4	157.8
2046	168.2	399.4	53.9	14.7	8.3	45.8	0.4	151.2
2047	165.9	395.6	53.4	14.6	8.3	44.8	0.4	144.7

HCFC-141b	HCFC-142b	Halon-1211	Halon-1202	Halon-1301	Halon-2402	CH_3Br	CH_3Cl	HFC-23
11.8	11.4	4.10	0.05	2.86	0.49	9.1	554.2	
13.5	12.5	4.20	0.05	2.90	0.49	8.6	541.2	
14.8	13.3	4.25	0.04	2.93	0.49	8.3	537.0	
16.1	13.9	4.29	0.04	2.98	0.49	8.1	542.5	
17.0	14.6	4.32	0.04	3.04	0.49	7.9	539.6	
17.5	15.2	4.34	0.04	3.08	0.48	8.0	541.6	
17.9	15.9	4.34	0.03	3.10	0.48	7.9	538.5	
18.5	16.9	4.32	0.03	3.14	0.47	7.7	542.1	
19.1	18.1	4.27	0.03	3.17	0.47	7.5	544.8	
19.6	19.3	4.22	0.03	3.19	0.46	7.3	543.2	
20.1	20.0	4.16	0.02	3.21	0.46	7.1	541.1	
20.9	20.8	4.08	0.02	3.24	0.45	7.1	534.8	
21.9	21.5	4.01	0.02	3.26	0.44	7.1	535.8	
22.8	21.8	3.91	0.02	3.30	0.44	6.9	542.6	
23.5	22.1	3.81	0.02	3.33	0.43	6.7	538.9	
24.1	22.1	3.71	0.02	3.34	0.42	6.7	546.0	
24.4	22.2	3.60	0.01	3.34	0.42	6.8	555.4	
24.6	22.3	3.50	0.01	3.34	0.41	6.7	549.3	
24.4	22.3	3.40	0.01	3.34	0.41	6.6	539.5	30.0
24.4	22.3	3.31	0.01	3.35	0.40	6.5	539.5	31.2
24.4	22.1	3.21	0.01	3.34	0.40	6.6	539.5	32.4
24.7	22.1	3.11	0.01	3.35	0.38	6.6	539.5	33.7
25.0	22.2	3.02	0.00	3.35	0.37	6.7	539.5	35.0
25.2	22.2	2.92	0.00	3.35	0.36	6.7	539.5	36.3
25.4	22.2	2.83	0.00	3.35	0.34	6.7	539.5	37.7
25.6	22.2	2.74	0.00	3.35	0.33	6.7	539.5	39.2
25.7	22.3	2.65	0.00	3.34	0.32	6.7	539.5	40.6
25.8	22.2	2.56	0.00	3.34	0.31	6.7	539.5	42.0
25.8	22.2	2.48	0.00	3.34	0.30	6.7	539.5	43.5
25.8	22.1	2.40	0.00	3.33	0.29	6.7	539.5	45.1
25.7	22.0	2.32	0.00	3.33	0.28	6.7	539.5	46.8
25.6	21.9	2.24	0.00	3.32	0.27	6.7	539.5	48.4
25.4	21.8	2.16	0.00	3.32	0.26	6.7	539.5	50.0
25.1	21.7	2.08	0.00	3.31	0.25	6.7	539.5	51.6
24.8	21.5	2.01	0.00	3.31	0.24	6.7	539.5	53.2
24.4	21.3	1.94	0.00	3.30	0.23	6.7	539.5	54.8
24.0	21.0	1.87	0.00	3.29	0.22	6.7	539.5	56.4
23.6	20.8	1.80	0.00	3.28	0.22	6.7	539.5	58.0
23.1	20.5	1.74	0.00	3.27	0.21	6.7	539.5	59.5
22.6	20.3	1.68	0.00	3.26	0.20	6.7	539.5	61.1
22.1	20.0	1.61	0.00	3.25	0.19	6.7	539.5	62.6
21.6	19.7	1.56	0.00	3.24	0.19	6.7	539.5	64.2
21.1	19.4	1.50	0.00	3.23	0.18	6.7	539.5	65.7
20.5	19.1	1.44	0.00	3.22	0.17	6.7	539.5	67.2
20.0	18.8	1.39	0.00	3.21	0.17	6.7	539.5	68.7
19.4	18.5	1.34	0.00	3.19	0.16	6.7	539.5	70.2
18.9	18.1	1.29	0.00	3.18	0.16	6.7	539.5	71.7
18.3	17.8	1.24	0.00	3.17	0.15	6.7	539.5	73.2

Year	CFC-11	CFC-12	CFC-113	CFC-114	CFC-115	CCl_4	CH_3CCl_3	HCFC-22
2048	163.5	391.9	52.9	14.6	8.3	43.9	0.4	138.3
2049	161.2	388.2	52.4	14.5	8.2	43.1	0.4	132.1
2050	158.9	384.5	51.9	14.5	8.2	42.2	0.4	126.1
2051	156.6	380.8	51.4	14.4	8.2	41.4	0.4	120.4
2052	154.4	377.2	51.0	14.4	8.2	40.6	0.4	114.8
2053	152.1	373.6	50.5	14.3	8.2	39.9	0.4	109.4
2054	149.8	370.0	50.0	14.3	8.2	39.2	0.4	104.2
2055	147.6	366.5	49.6	14.3	8.2	38.4	0.4	99.3
2056	145.4	363.0	49.1	14.2	8.1	37.8	0.4	94.5
2057	143.2	359.5	48.6	14.2	8.1	37.1	0.4	90.0
2058	141.0	356.0	48.2	14.1	8.1	36.5	0.4	85.7
2059	138.9	352.6	47.7	14.1	8.1	35.8	0.4	81.5
2060	136.7	349.2	47.3	14.0	8.1	35.2	0.4	77.6
2061	134.6	345.9	46.9	14.0	8.1	34.7	0.4	73.9
2062	132.5	342.5	46.4	14.0	8.0	34.1	0.4	70.3
2063	130.4	339.2	46.0	13.9	8.0	33.6	0.4	66.9
2064	128.4	335.9	45.6	13.9	8.0	33.0	0.4	63.7
2065	126.4	332.7	45.2	13.8	8.0	32.5	0.4	60.7
2066	124.3	329.5	44.8	13.8	8.0	32.0	0.4	57.8
2067	122.4	326.3	44.4	13.8	8.0	31.6	0.4	55.1
2068	120.4	323.1	43.9	13.7	8.0	31.1	0.4	52.5
2069	118.4	320.0	43.5	13.7	7.9	30.7	0.4	50.0
2070	116.5	316.9	43.2	13.6	7.9	30.2	0.4	47.7
2071	114.6	313.8	42.8	13.6	7.9	29.8	0.4	45.6
2072	112.8	310.8	42.4	13.6	7.9	29.4	0.4	43.5
2073	110.9	307.7	42.0	13.5	7.9	29.0	0.4	41.6
2074	109.1	304.8	41.6	13.5	7.9	28.6	0.4	39.8
2075	107.3	301.8	41.2	13.4	7.9	28.3	0.4	38.0
2076	105.5	298.9	40.9	13.4	7.8	27.9	0.4	36.4
2077	103.7	296.0	40.5	13.4	7.8	27.6	0.4	34.9
2078	102.0	293.1	40.1	13.3	7.8	27.3	0.4	33.5
2079	100.3	290.2	39.8	13.3	7.8	26.9	0.4	32.1
2080	98.6	287.4	39.4	13.2	7.8	26.6	0.4	30.9
2081	96.9	284.6	39.1	13.2	7.8	26.3	0.4	29.7
2082	95.3	281.8	38.7	13.2	7.8	26.0	0.4	28.5
2083	93.7	279.1	38.4	13.1	7.7	25.8	0.4	27.5
2084	92.1	276.4	38.0	13.1	7.7	25.5	0.4	26.5
2085	90.5	273.7	37.7	13.1	7.7	25.2	0.4	25.6
2086	88.9	271.0	37.4	13.0	7.7	25.0	0.4	24.7
2087	87.4	268.4	37.0	13.0	7.7	24.7	0.4	23.9
2088	85.9	265.8	36.7	12.9	7.7	24.5	0.4	23.2
2089	84.4	263.2	36.4	12.9	7.7	24.3	0.4	22.4
2090	83.0	260.6	36.1	12.9	7.6	24.1	0.4	21.8
2091	81.5	258.1	35.8	12.8	7.6	23.8	0.4	21.1
2092	80.1	255.6	35.4	12.8	7.6	23.6	0.4	20.6
2093	78.7	253.1	35.1	12.8	7.6	23.4	0.4	20.0
2094	77.3	250.6	34.8	12.7	7.6	23.2	0.4	19.5
2095	76.0	248.2	34.5	12.7	7.6	23.1	0.4	19.0

HCFC-141b	HCFC-142b	Halon-1211	Halon-1202	Halon-1301	Halon-2402	CH_3Br	CH_3Cl	HFC-23
17.8	17.5	1.19	0.00	3.16	0.15	6.7	539.5	74.7
17.3	17.2	1.14	0.00	3.14	0.14	6.7	539.5	76.2
16.7	16.8	1.10	0.00	3.13	0.14	6.7	539.5	77.7
16.2	16.5	1.06	0.00	3.11	0.13	6.7	539.5	79.1
15.7	16.2	1.02	0.00	3.10	0.13	6.7	539.5	80.6
15.2	15.9	0.98	0.00	3.08	0.12	6.7	539.5	82.1
14.7	15.6	0.94	0.00	3.07	0.12	6.7	539.5	83.5
14.2	15.2	0.90	0.00	3.05	0.11	6.7	539.5	84.9
13.7	14.9	0.87	0.00	3.04	0.11	6.7	539.5	86.4
13.3	14.6	0.83	0.00	3.02	0.11	6.7	539.5	87.8
12.8	14.3	0.80	0.00	3.01	0.10	6.7	539.5	89.2
12.4	14.0	0.77	0.00	2.99	0.10	6.7	539.5	90.6
12.0	13.7	0.74	0.00	2.97	0.09	6.7	539.5	92.1
11.6	13.4	0.71	0.00	2.96	0.09	6.7	539.5	93.5
11.2	13.1	0.68	0.00	2.94	0.09	6.7	539.5	94.9
10.8	12.9	0.65	0.00	2.92	0.09	6.7	539.5	96.2
10.4	12.6	0.63	0.00	2.91	0.08	6.7	539.5	97.6
10.1	12.3	0.60	0.00	2.89	0.08	6.7	539.5	99.0
9.7	12.1	0.58	0.00	2.87	0.08	6.7	539.5	100.4
9.4	11.8	0.55	0.00	2.85	0.07	6.7	539.5	101.8
9.0	11.6	0.53	0.00	2.84	0.07	6.7	539.5	103.1
8.7	11.3	0.51	0.00	2.82	0.07	6.7	539.5	104.5
8.4	11.1	0.49	0.00	2.80	0.07	6.7	539.5	105.8
8.1	10.8	0.47	0.00	2.78	0.06	6.7	539.5	107.2
7.8	10.6	0.45	0.00	2.76	0.06	6.7	539.5	108.5
7.5	10.4	0.43	0.00	2.75	0.06	6.7	539.5	109.8
7.3	10.2	0.41	0.00	2.73	0.06	6.7	539.5	111.2
7.0	10.0	0.39	0.00	2.71	0.06	6.7	539.5	112.5
6.8	9.8	0.38	0.00	2.69	0.05	6.7	539.5	113.8
6.5	9.6	0.36	0.00	2.67	0.05	6.7	539.5	115.1
6.3	9.4	0.35	0.00	2.65	0.05	6.7	539.5	116.4
6.1	9.2	0.33	0.00	2.63	0.05	6.7	539.5	117.7
5.8	9.0	0.32	0.00	2.61	0.05	6.7	539.5	119.0
5.6	8.8	0.31	0.00	2.60	0.04	6.7	539.5	120.3
5.4	8.7	0.29	0.00	2.58	0.04	6.7	539.5	121.6
5.2	8.5	0.28	0.00	2.56	0.04	6.7	539.5	122.8
5.0	8.3	0.27	0.00	2.54	0.04	6.7	539.5	124.1
4.8	8.2	0.26	0.00	2.52	0.04	6.7	539.5	125.4
4.7	8.0	0.25	0.00	2.50	0.04	6.7	539.5	126.6
4.5	7.9	0.24	0.00	2.48	0.04	6.7	539.5	127.9
4.3	7.7	0.23	0.00	2.46	0.03	6.7	539.5	129.1
4.2	7.6	0.22	0.00	2.44	0.03	6.7	539.5	130.4
4.0	7.5	0.21	0.00	2.43	0.03	6.7	539.5	131.6
3.9	7.3	0.20	0.00	2.41	0.03	6.7	539.5	132.8
3.7	7.2	0.19	0.00	2.39	0.03	6.7	539.5	134.1
3.6	7.1	0.18	0.00	2.37	0.03	6.7	539.5	135.3
3.5	7.0	0.17	0.00	2.35	0.03	6.7	539.5	136.5
3.3	6.9	0.17	0.00	2.33	0.03	6.7	539.5	137.7

Year	CFC-11	CFC-12	CFC-113	CFC-114	CFC-115	CCl_4	CH_3CCl_3	HCFC-22
2096	74.6	245.7	34.2	12.7	7.6	22.9	0.4	18.6
2097	73.3	243.4	33.9	12.6	7.5	22.7	0.4	18.2
2098	72.0	241.0	33.6	12.6	7.5	22.5	0.4	17.8
2099	70.8	238.6	33.3	12.6	7.5	22.4	0.4	17.4
2100	69.5	236.3	33.1	12.5	7.5	22.2	0.4	17.0

HCFC-141b	HCFC-142b	Halon-1211	Halon-1202	Halon-1301	Halon-2402	CH_3Br	CH_3Cl	HFC-23
3.2	6.8	0.16	0.00	2.31	0.03	6.7	539.5	138.9
3.1	6.7	0.15	0.00	2.29	0.03	6.7	539.5	140.1
3.0	6.6	0.15	0.00	2.28	0.02	6.7	539.5	141.3
2.9	6.5	0.14	0.00	2.26	0.02	6.7	539.5	142.5
2.8	6.4	0.13	0.00	2.24	0.02	6.7	539.5	143.7

REFERENCES

An, M., L.M. Western, D. Say, L. Chen, T. Claxton, A.L. Ganesan, R. Hossaini, P.B. Krummel, A.J. Manning, J. Mühle, S. O'Doherty, R.G. Prinn, R.F. Weiss, D. Young, J. Hu, B. Yao, and M. Rigby, Rapid increase in dichloromethane emissions from China inferred through atmospheric observations, ***Nat. Commun.***, *12*(1), 7279, doi:10.1038/s41467-021-27592-y, 2021.

Andersen, S.O., S. Gao, S. Carvalho, T. Ferris, M. Gonzalez, N.J. Sherman, Y. Wei, and D. Zaelke, Narrowing feedstock exemptions under the Montreal Protocol has multiple environmental benefits, ***Proc. Natl. Acad. Sci.***, *118*(49), e2022668118, doi:10.1073/pnas.2022668118, 2021.

Ashford, P., D. Clodic, A. McCulloch, and L. Kuijpers, Emission profiles from the foam and refrigeration sectors comparison with atmospheric concentrations. Part 1: Methodology and data, ***Int. J. Refrig.***, *27*(7), 687-700, doi:10.1016/j.ijrefrig.2004.07.025, 2004.

Boley, A.C., and M. Byers, Satellite mega-constellations create risks in Low Earth Orbit, the atmosphere and on Earth, ***Sci. Rep.***, *11*(1), 10642, doi:10.1038/s41598-021-89909-7, 2021.

Brioude, J., R.W. Portmann, J.S. Daniel, O.R. Cooper, G.J. Frost, K.H. Rosenlof, C. Granier, A.R. Ravishankara, S.A. Montzka, and A. Stohl, Variations in ozone depletion potentials of very short-lived substances with season and emission region, ***Geophys. Res. Lett.***, *37*(19), doi:10.1029/2010GL044856, 2010.

Burkholder, J.B., Ø. Hodnebrog, and V.L. Orkin, Summary of Abundances, Lifetimes, Ozone Depletion Potentials (ODPs), Radiative Efficiencies (REs), Global Warming Potentials (GWPs), and Global Temperature change Potentials (GTPs), Appendix A in ***Scientific Assessment of Ozone Depletion: 2018***, Global Ozone Research and Monitoring Project–Report No. 58, World Meteorological Organization, Geneva, Switzerland, 2018.

Carpenter, L.J., and J.S. Daniel (Lead Authors), E.L. Fleming, T. Hanaoka, J. Hu, A.R. Ravishankara, M.N. Ross, S. Tilmes, T.J. Wallington, and D.J. Wuebbles, Scenarios and Information for Policymakers, Chapter 6 in ***Scientific Assessment of Ozone Depletion: 2018***, Global Ozone Research and Monitoring Project–Report No. 58, World Meteorological Organization, Geneva, Switzerland, 2018.

Chen, D., M. Rojas, B.H. Samset, K. Cobb, A. Diongue Niang, P. Edwards, S. Emori, S.H. Faria, E. Hawkins, P. Hope, P. Huybrechts, M. Meinshausen, S.K. Mustafa, G.-K. Plattner, and A.-M. Tréguier, Framing, Context, and Methods, Chapter 1 in ***Climate Change 2021: The Physical Science Basis. Contribution of Working Group I to the Sixth Assessment Report of the Intergovernmental Panel on Climate Change***, edited by V. Masson-Delmotte, P. Zhai, A. Pirani, S.L. Connors, C. Péan, S. Berger, N. Caud, Y. Chen, L. Goldfarb, M.I. Gomis, M. Huang, K. Leitzell, E. Lonnoy, J.B.R. Matthews, T.K. Maycock, T. Waterfield, O. Yelekçi, R. Yu, and B. Zhou, Cambridge University Press, Cambridge, United Kingdom and New York, NY, USA, 139 pp., doi:10.1017/9781009157896.003, 2021.

Chipperfield, M.P., R. Hossaini, S.A. Montzka, S. Reimann, D. Sherry, and S. Tegtmeier, Renewed and emerging concerns over the production and emission of ozone-depleting substances, ***Nat. Rev. Earth Environ.***, *1*(5), 251-263, doi:10.1038/s43017-020-0048-8, 2020.

Claxton, T., R. Hossaini, O. Wild, M.P. Chipperfield, and C. Wilson, On the Regional and Seasonal Ozone Depletion Potential of Chlorinated Very Short-Lived Substances, ***Geophys. Res. Lett.***, *46*(10), 5489-5498, doi:10.1029/2018GL081455, 2019.

Claxton, T., R. Hossaini, C. Wilson, S.A. Montzka, M.P. Chipperfield, O. Wild, E.M. Bednarz, L.J. Carpenter, S.J. Andrews, S.C. Hackenberg, J. Mühle, D. Oram, S. Park, M.-K. Park, E. Atlas, M. Navarro, S. Schauffler, D. Sherry, M. Vollmer, T. Schuck, A. Engel, P.B. Krummel, M. Maione, J. Arduini, T. Saito, Y. Yokouchi, S. O'Doherty, D. Young, and C. Lunder, A Synthesis Inversion to Constrain Global Emissions of Two Very Short Lived Chlorocarbons: Dichloromethane, and Perchloroethylene, ***J. Geophys. Res.***, *125*(12), e2019JD031818, doi:10.1029/2019JD031818, 2020.

Crutzen, P.J., SST's: A Threat to the Earth's Ozone Shield, ***Ambio***, *1*(2), 41-51, 1972.

Cuevas, C.A., N. Maffezzoli, J.P. Corella, A. Spolaor, P. Vallelonga, H.A. Kjær, M. Simonsen, M. Winstrup, B. Vinther, C. Horvat, R.P. Fernandez, D. Kinnison, J.-F. Lamarque, C. Barbante, and A. Saiz-Lopez, Rapid increase in atmospheric iodine levels in the North Atlantic since the mid-20th century, ***Nat. Comm.***, *9*(1), 1452, doi:10.1038/s41467-018-03756-1, 2018.

Cui, J., J. Guo, Z. Zhai, and J. Zhang, The contribution of fluoropolymer thermolysis to trifluoroacetic acid (TFA) in environmental media, ***Chemosphere***, *222*, 637-644, doi:10.1016/j.chemosphere.2019.01.174, 2019.

Daniel, J.S., S. Solomon, and D.L. Albritton, On the evaluation of halocarbon radiative forcing and global warming potentials, ***J. Geophys. Res.***, *100*(D1), 1271-1285, doi:10.1029/94JD02516, 1995.

Danilin, M.Y., P.J. Popp, R.L. Herman, M.K.W. Ko, M.N. Ross, C.E. Kolb, D.W. Fahey, L.M. Avallone, D.W. Toohey, B.A. Ridley, O. Schmid, J.C. Wilson, D.G. Baumgardner, R.R. Friedl, T.L. Thompson, and J.M. Reeves, Quantifying uptake of HNO_3 and H_2O by alumina particles in Athena-2 rocket plume, ***J. Geophys. Res.***, *108*(D4), doi:10.1029/2002JD002601, 2003.

Danilin, M.Y., R.-L. Shia, M.K.W. Ko, D.K. Weisenstein, N.D. Sze, J.J. Lamb, T.W. Smith, P.D. Lohn, and M.J. Prather, Global stratospheric effects of the alumina emissions by solid-fueled rocket motors, ***J. Geophys. Res.***, *106*(D12), 12727-12738, doi:10.1029/2001JD900022, 2001.

David, L.M., M. Barth, L. Höglund-Isaksson, P. Purohit, G.J.M. Velders, S. Glaser, and A.R. Ravishankara, Trifluoroacetic acid deposition from emissions of HFO-1234yf in India, China and the Middle East, ***Atmos. Chem. Phys.***, *21*, 14833–14849, doi:10.5194/acp-21-14833-2021, 2021.

Dessens, O., G. Zeng, N. Warwick, and J. Pyle, Short-lived bromine compounds in the lower stratosphere; impact of climate change on ozone, ***Atmos. Sci. Lett.***, *10*(3), 201-206, doi:10.1002/asl.236, 2009.

Dupuy, E., H. Akiyoshi, and Y. Yamashita, Impact of Unmitigated HFC Emissions on Stratospheric Ozone at the End of the 21st Century as Simulated by Chemistry-Climate Models, ***J. Geophys. Res.***, *126*(21), e2021JD035307, doi:10.1029/2021JD035307, 2021.

Ebnesajjad, S., Preparation of Tetrafluoroethylene and Other Monomers, In: ***Fluoroplastics (2nd Edition)***, William Andrew Publishing, Oxford, 48–75 pp., 2015.

Ellis, D.A., S.A. Mabury, J.W. Martin, and D.C.G. Muir, Thermolysis of fluoropolymers as a potential source of halogenated organic acids in the environment, ***Nature***, *412*(6844), 321-324, doi:10.1038/35085548, 2001.

Engel, A., H. Bonisch, J. Ostermoller, M.P. Chipperfield, S. Dhomse, and P. Jöckel, A refined method for calculating equivalent effective stratospheric chlorine, ***Atmos. Chem. Phys.***, *18*(2), 601-619, doi:10.5194/acp-18-601-2018, 2017.

Falk, S., B.-M. Sinnhuber, G. Krysztofiak, P. Jocket, P. Graf, and S.T. Lennartz, Brominated VSLS and their influence on ozone under a changing climate, ***Atmos. Chem. Phys.***, *17*(18), 11313-11329, doi:10.5194/acp-2017-11313-2017, 2017.

Fang, X., S. Park, T. Saito, R. Tunnicliffe, A.L. Ganesan, M. Rigby, S. Li, Y. Yokouchi, P.J. Fraser, C.M. Harth, P.B. Krummel, J. Mühle, S. O'Doherty, P.K. Salameh, P.G. Simmonds, R.F. Weiss, D. Young, M.F. Lunt, A.J. Manning, A. Gressent, and R.G. Prinn, Rapid increase in ozone-depleting chloroform emissions from China, ***Nat. Geosci.***, *12*(2), 89-93, doi:10.1038/s41561-018-0278-2, 2019.

Feng, Y., P. Bie, Z. Wang, L. Wang, and J. Zhang, Bottom-up anthropogenic dichloromethane emission estimates from China for the period 2005–2016 and predictions of future emissions, ***Atmos. Environ.***, *186*, 241-247, doi:10.1016/j.atmosenv.2018.05.039, 2018.

Fleming, E.L., P.A. Newman, Q. Liang, J.S. Daniel, The impact of continuing CFC-11 emissions on stratospheric ozone, ***J. Geophys. Res.***, 125(3), e2019JD031849, doi:10.1029/2019JD031849, 2020.

Forster, P., T. Storelvmo, K. Armour, W. Collins, J.-L. Dufresne, D. Frame, D.J. Lunt, T. Mauritsen, M.D. Palmer, M. Watanabe, M. Wild, and H. Zhang, The Earth's Energy Budget, Climate Feedbacks, and Climate Sensitivity, Chapter 7 in ***Climate Change 2021: The Physical Science Basis, Contribution of Working Group I to the Sixth Assessment Report of the Intergovernmental Panel on Climate Change***, edited by V. Masson-Delmotte, P. Zhai, A. Pirani, S.L. Connors, C. Péan, S. Berger, N. Caud, Y. Chen, L. Goldfarb, M.I. Gomis, M. Huang, K. Leitzell, E. Lonnoy, J.B.R.

Matthews, T.K. Maycock, T. Waterfield, O. Yelekçi, R. Yu, and B. Zhou, Cambridge University Press, Cambridge, United Kingdom and New York, NY, USA, 131 pp., doi:10.1017/9781009157896.009, 2021.

Frank, H., E.H. Christoph, O. Holm-Hansen, and J.L. Bullister, Trifluoroacetate in ocean waters, ***Environ. Sci. Technol.***, ***36***(1), 12-15, doi:10.1021/es0101532, 2002.

Freeling, F., D. Behringer, F. Heydel, M. Scheurer, T.A. Ternes, and K. Nödler, Trifluoroacetate in Precipitation: Deriving a Benchmark Data Set, ***Environ. Sci. Technol.***, ***54***(18), 11210-11219, doi:10.1021/acs.est.0c02910, 2020.

Gamlen, P.H., B.C. Lane, P.M. Midgley, and J.M. Steed, The production and release to the atmosphere of CCl_3F and CCl_2F_2 (chlorofluorocarbons CFC 11 and CFC 12), ***Atmos. Environ.***, ***20***(6), 1077-1085, doi:10.1016/0004-6981(86)90139-3, 1986.

Gidden, M.J., K. Riahi, S.J. Smith, S. Fujimori, G. Luderer, E. Kriegler, D.P. van Vuuren, M. van den Berg, L. Feng, D. Klein, K. Calvin, J.C. Doelman, S. Frank, O. Fricko, M. Harmsen, T. Hasegawa, P. Havlik, J. Hilaire, R. Hoesly, J. Horing, A. Popp, E. Stehfest, and K. Takahashi, Global emissions pathways under different socioeconomic scenarios for use in CMIP6: a dataset of harmonized emissions trajectories through the end of the century, ***Geosci. Model Dev.***, ***12***(4), 1443-1475, doi:10.5194/gmd-12-1443-2019, 2019.

Ha, J.-M., D. Kim, J. Kim, B.S. Ahn, Y. Kim, and J.W. Kang, High-temperature hydrodechlorination of ozone-depleting chlorodifluoromethane (HCFC-22) on supported Pd and Ni catalysts, ***J. Environ. Sci. Health A***, ***46***(9), 989-996, doi:10.1080/10934529.2011.586262, 2011.

Harris, N.R.P., and D.J. Wuebbles (Lead Authors), J.S. Daniel, J. Hu, L.J.M. Kuijpers, K.S. Law, M.J. Prather, and R. Schofield, Scenarios and Information for Policymakers, Chapter 5 in ***Scientific Assessment of Ozone Depletion: 2014***, Global Ozone research and Monitoring Project–Report No. 55, World Meteorological Organization, Geneva, Switzerland, 2014.

Henne, S., D.E. Shallcross, S. Reimann, P. Xiao, D. Brunner, S. O'Doherty, and B. Buchmann, Future Emissions and Atmospheric Fate of HFC-1234yf from Mobile Air Conditioners in Europe, ***Environ. Sci. Technol.***, ***46***(3), 1650-1658, doi:10.1021/es2034608, 2012.

Hodnebrog, Ø., B. Aamaas, J.S. Fuglestvedt, G. Marston, G. Myhre, C.J. Nielsen, M. Sandstad, K.P. Shine, and T.J. Wallington, Updated Global Warming Potentials and Radiative Efficiencies of Halocarbons and Other Weak Atmospheric Absorbers, ***Rev. Geophys.***, ***58***(3), e2019RG000691, doi:10.1029/2019RG000691, 2020a.

Hodnebrog, Ø., G. Myhre, R.J. Kramer, K.P. Shine, T. Andrews, G. Faluvegi, M. Kasoar, A. Kirkevåg, J.-F. Lamarque, J. Mülmenstädt, D. Olivié, B.H. Samset, D. Shindell, C.J. Smith, T. Takemura, and A. Voulgarakis, The effect of rapid adjustments to halocarbons and N_2O on radiative forcing, ***NPJ Clim. Atmos. Sci.***, ***3***(1), 43, doi:10.1038/s41612-020-00150-x, 2020b.

Holland, R., M.A.H. Khan, I. Driscoll, R. Chhantyal-Pun, R.G. Derwent, C.A. Taatjes, A.J. Orr-Ewing, C.J. Percival, and D.E. Shallcross, Investigation of the Production of Trifluoroacetic Acid from Two Halocarbons, HFC-134a and HFO-1234yf and Its Fates Using a Global Three-Dimensional Chemical Transport Model, ***ACS Earth Space Chem.***, ***5***(4), 849-857, doi:10.1021/acsearthspacechem.0c00355, 2021.

Hossaini, R., E. Atlas, S.S. Dhomse, M.P. Chipperfield, P.F. Bernath, A.M. Fernando, J. Mühle, A.A. Leeson, S.A. Montzka, W. Feng, J.J. Harrison, P. Krummel, M.K. Vollmer, S. Reimann, S. O'Doherty, D. Young, M. Maione, J. Arduini, and C.R. Lunder, Recent Trends in Stratospheric Chlorine From Very Short-Lived Substances, ***J. Geophys. Res.***, ***124***(4), 2318-2335, doi:10.1029/2018JD029400, 2019.

Hossaini, R., M.P. Chipperfield, S. Dhomse, C. Ordóñez, A. Saiz-Lopez, N.L. Abraham, A. Archibald, P. Braesicke, P. Telford, N. Warwick, X. Yang, and J. Pyle, Modelling future changes to the stratospheric source gas injection of biogenic bromocarbons, ***Geophys. Res. Lett.***, ***39***(20), doi:10.1029/2012GL053401, 2012.

Hossaini, R., M.P. Chipperfield, S.A. Montzka, A.A. Leeson, S.S. Dhomse, and J.A. Pyle, The increasing threat to stratospheric ozone from dichloromethane, ***Nat. Comm.***, ***8***(15962), doi:10.1038/ncomms15962, 2017.

Hossaini, R., H. Mantle, M.P. Chipperfield, S.A. Montzka, P. Hamer, F. Ziska, B. Quack, K. Krüger, S. Tegtmeier, E. Atlas, S. Sala, A. Engel, H. Bönisch, T. Keber, D. Oram, G. Mills, C. Ordóñez, A. Saiz-Lopez, N. Warwick, Q. Liang, W. Feng, F. Moore, B.R. Miller, V. Marécal, N.A.D. Richards, M. Dorf, and K. Pfeilsticker, Evaluating global emission inventories of biogenic bromocarbons, ***Atmos. Chem. Phys.***, ***13***(23), 11819-11838, doi:10.5194/acp-13-11819-2013, 2013.

Hossaini, R., P.K. Patra, A.A. Leeson, G. Krysztofiak, N.L. Abraham, S.J. Andrews, A.T. Archibald, J. Aschmann, E.L. Atlas, D.A. Belikov, H. Bönisch, L.J. Carpenter, S. Dhomse, M. Dorf, A. Engel, W. Feng, S. Fuhlbrügge, P.T. Griffiths, N.R.P. Harris, R. Hommel, T. Keber, K. Krüger, S.T. Lennartz, S. Maksyutov, H. Mantle, G.P. Mills, B. Miller, S.A. Montzka, F. Moore, M.A. Navarro, D.E. Oram, K. Pfeilsticker, J.A. Pyle, B. Quack, A.D. Robinson, E. Saikawa, A. Saiz-Lopez, S. Sala, B.M. Sinnhuber, S. Taguchi, S. Tegtmeier, R.T. Lidster, C. Wilson, and F. Ziska, A multi-model intercomparison of halogenated very short-lived substances (TransCom-VSLS): linking oceanic emissions and tropospheric transport for a reconciled estimate of the stratospheric source gas injection of bromine, ***Atmos. Chem. Phys.***, ***16***(14), 9163-9187, doi:10.5194/acp-16-9163-2016, 2016.

Hurwitz, M.M., E.L. Fleming, P.A. Newman, F. Li, E. Mlawer, K. Cady-Pereira, and R. Bailey, Ozone depletion by hydrofluorocarbons, ***Geophys. Res. Lett.***, ***42***(20), 8686-8692, doi:10.1002/2015GL065856, 2015.

Iglesias-Suarez, F., A. Badia, R.P. Fernandez, C.A. Cuevas, D.E. Kinnison, S. Tilmes, J.-F. Lamarque, M.C. Long, R. Hossaini, and A. Saiz-Lopez, Natural halogens buffer tropospheric ozone in a changing climate, ***Nat. Clim. Change***, ***10***(2), 147-154, doi:10.1038/s41558-019-0675-6, 2020.

IPCC, (Intergovernmental Panel on Climate Change), Chemical Industry Emissions, Chapter 3 in, ***2019 Refinement to the 2006 IPCC Guidelines for National Greenhouse Gas Inventories***, 49th Session of the IPCC, Kyoto, Japan, 2019.

IPCC/TEAP (Intergovernmental Panel on Climate Change, Technology and Economic Assessment Panel), ***Special Report on Safeguarding the Ozone Layer and the Global Climate System: Issues Related to Hydrofluorocarbons and Perfluorocarbons***, 478 pp., Cambridge University Press, Cambridge, United Kingdom, doi:10.13140/2.1.4337.2161, 2005.

Johnston, H.S., D.E. Kinnison, and D.J. Wuebbles, Nitrogen oxides from high-altitude aircraft: An update of potential effects on ozone, ***J. Geophys. Res.***, ***94***(D13), 16351-16363, doi:10.1029/JD094iD13p16351, 1989.

Joudan, S., A.O. De Silva, and C.J. Young, Insufficient evidence for the existence of natural trifluoroacetic acid, ***Environ Sci Process Impacts***, ***23***(11), 1641-1649, doi:10.1039/D1EM00306B, 2021.

Jubb, A.M., M.R. McGillen, R.W. Portmann, J.S. Daniel, and J.B. Burkholder, An atmospheric photochemical source of the persistent greenhouse gas CF_4, ***Geophys. Res. Lett.***, ***42***(21), 9505-9511, doi:10.1002/2015GL06619, 2015.

Keng, F.S.-L., S.-M. Phang, N. Abd Rahman, E.C. Leedham Elvidge, G. Malin, and W.T. Sturges, The emission of volatile halocarbons by seaweeds and their response towards environmental changes, ***J. Appl. Phycol.***, ***32***(2), 1377-1394, doi:10.1007/s10811-019-02026-x, 2020.

Langematz, U., M. Tully, N. Calvo, M. Dameris, A.T.J. de Laat, A. Klekociuk, R. Müller, and P. Young, Polar Stratospheric Ozone: Past, Present, and Future, Chapter 4 in Scientific Assessment of Ozone Depletion: 2018, In Global Ozone Research and Monitoring Project–Report No. 58. Geneva, Switzerland, World Meteorological Organization, 2018.

Larson, E.J.L., R.W. Portmann, K.H. Rosenlof, D.W. Fahey, J.S. Daniel, and M.N. Ross, Global atmospheric response to emissions from a proposed reusable space launch system, ***Earths Future***, ***5***(1), 37-48, doi:10.1002/2016EF000399, 2017.

Lee, W.R., D.G. MacMartin, D. Visioni, and B. Kravitz, High-Latitude Stratospheric Aerosol Geoengineering Can Be More Effective if Injection Is Limited to Spring, ***Geophys. Res. Lett.***, ***48***(9), e2021GL092696, doi:10.1029/2021GL092696, 2021.

Legrand, M., J.R. McConnell, S. Preunkert, M. Arienzo, N. Chellman, K. Gleason, T. Sherwen, M.J. Evans, and L.J. Carpenter, Alpine ice evidence of a three-fold increase in atmospheric iodine deposition since 1950 in Europe due to increasing oceanic emissions, ***Proc. Natl. Acad. Sci.***, ***115***(48), 12136-12141, doi:10.1073/pnas.1809867115, 2018.

Lickley, M., S. Fletcher, M. Rigby, and S. Solomon, Joint inference of CFC lifetimes and banks suggests previously unidentified emissions, ***Nat. Comm.***, ***12***(1), 2920, doi:10.1038/s41467-021-23229-2, 2021.

Lickley, M., S. Solomon, S. Fletcher, G.J.M. Velders, J. Daniel, M. Rigby, S.A. Montzka, L.J.M. Kuijpers, and K. Stone, Quantifying contributions of chlorofluorocarbon banks to emissions and impacts on the ozone layer and climate, ***Nat. Comm.***, ***11***(1), 1380, doi:10.1038/s41467-020-15162-7, 2020.

Lickley, M., J.S. Daniel, E.L. Fleming, S. Reimann, and S. Solomon, Bayesian assessment of chlorofluorocarbon (CFC), hydrochlorofluorocarbon (HCFC) and halon banks suggest large reservoirs still present in old equipment, ***Atmos. Chem. Phys.***, ***22***, 11125–11136, doi: 10.5194/acp-22-11125-2022, 2022.

Maas, J., S. Tegtmeier, Y. Jia, B. Quack, J.V. Durgadoo, and A. Biastoch, Simulations of anthropogenic bromoform indicate high emissions at the coast of East Asia, ***Atmos. Chem. Phys.***, ***21***(5), 4103–4121, doi:10.5194/acp-21-4103-2021, 2021.

Maloney, C.M., R.W. Portmann, M.N. Ross, and K.H. Rosenlof, The Climate and

Ozone Impacts of Black Carbon Emissions From Global Rocket Launches, ***J. Geophys. Res., 127***(12), e2021JD036373, doi:10.1029/2021JD036373, 2022.

McCulloch, A., Chloroform in the environment: occurrence, sources, sinks and effects, ***Chemosphere***, ***50***(10), 1291-1308, doi: 10.1016/S0045-6535(02)00697-5, 2003.

McCulloch, A., and A.A. Lindley, Global emissions of HFC-23 estimated to year 2015, ***Atmos. Environ., 41***(7), 1560-1566, doi:10.1016/j.atmosenv.2006.02.021, 2007.

Meinshausen, M., Z.R.J. Nicholls, J. Lewis, M.J. Gidden, E. Vogel, M. Freund, U. Beyerle, C. Gessner, A. Nauels, N. Bauer, J.G. Canadell, J.S. Daniel, A. John, P.B. Krummel, G. Luderer, N. Meinshausen, S.A. Montzka, P.J. Rayner, S. Reimann, S.J. Smith, M. van den Berg, G.J.M. Velders, M.K. Vollmer, and R.H.J. Wang, The shared socio-economic pathway (SSP) greenhouse gas concentrations and their extensions to 2500, ***Geosci. Model Dev.***, ***13***(8), 3571-3605, doi:10.5194/gmd-13-3571-2020, 2020.

Midgley, P.M., and D.A. Fisher, The production and release to the atmosphere of chlorodifluoromethane (HCFC 22), ***Atmos. Environ.***, ***27***(14), 2215-2223, doi:10.1016/0960-1686(93)90051-Y, 1993.

Miraux, L., Environmental limits to the space sector's growth, ***Sci. Tot. Environ.***, ***806***, 150862, doi:10.1016/j.scitotenv.2021.150862, 2022.

Montzka, S.A., G.S. Dutton, R.W. Portmann, M.P. Chipperfield, S. Davis, W. Feng, A.J. Manning, E. Ray, M. Rigby, B.D. Hall, C. Siso, J.D. Nance, P.B. Krummel, J. Mühle, D. Young, S. O'Doherty, P.K. Salameh, C.M. Harth, R.G. Prinn, R.F. Weiss, J.W. Elkins, H. Walter-Terrinoni, and C. Theodoridi, A decline in global CFC-11 emissions during 2018–2019, ***Nature***, ***590***(7846), 428-432, doi:10.1038/s41586-021-03260-5, 2021.

Montzka, S.A., G.S. Dutton, P. Yu, E. Ray, R.W. Portmann, J.S. Daniel, L. Kuijpers, B.D. Hall, D. Mondeel, C. Siso, J.D. Nance, M. Rigby, A.J. Manning, L. Hu, F. Moore, B.R. Miller, and J.W. Elkins, An unexpected and persistent increase in global emissions of ozone-depleting CFC-11, ***Nature***, ***557***(7705), 413-417, doi:10.1038/s41586-018-0106-2, 2018.

Montzka, S.A., S. Reimann, (Coordinating Lead Authors) A. Engel, K. Krüger, S. O`Doherty, W.T. Sturges, D. Blake, M. Dorf, P. Fraser, L. Froidevaux, K. Jucks, K. Kreher, M.J. Kurylo, A. Mellouki, J. Miller, O.-J. Nielsen, V.L. Orkin, R.G. Prinn, R. Rhew, M.L. Santee, A. Stohl, and D. Verdonik, Ozone-Depleting Substances (ODSs) and Related Chemicals, Chapter 1 in ***Scientific Assessment of Ozone Depletion: 2010***, Global Ozone Research and Monitoring Project–Report No. 52, World Meteorological Organization, Geneva, Switzerland, 2011.

Montzka, S.A., and G.J.M. Velders (Lead Authors), P.B. Krummel, J. Mühle, V.L. Orkin, S. Park, N. Shah, H. Walter-Terrinoni, P. Bernath, C. Boone, L. Hu, M.J. Kurylo, E.L. Elvidge, M. Maione, B.R. Miller, S. O'Doherty, M. Rigby, I.J. Simpson, M.K. Vollmer, R.F. Weiss, L.J.M. Kuijpers, and W.T. Sturges, Hydrofluorocarbons (HFCs), Chapter 2 in ***Scientific Assessment of Ozone Depletion: 2018***, Global Ozone Research and Monitoring Project–Report No. 58, World Meteorological Organization, Geneva, Switzerland, 2018.

Morgenstern, O., F.M. O'Connor, B.T. Johnson, G. Zeng, J.P. Mulcahy, J. Williams, J. Teixeira, M. Michou, P. Nabat, L.W. Horowitz, V. Naik, L.T. Sentman, M. Deushi, S.E. Bauer, K. Tsigaridis, D.T. Shindell, and D.E. Kinnison, Reappraisal of the Climate Impacts of Ozone-Depleting Substances, ***Geophys. Res. Lett.***, ***47***(20), e2020GL088295, doi:10.1029/2020GL088295, 2020.

Mühle, J., L.J.M. Kuijpers, K.M. Stanley, M. Rigby, L.M. Western, J. Kim, S. Park, C.M. Harth, P.B. Krummel, P.J. Fraser, S. O'Doherty, P.K. Salameh, R. Schmidt, D. Young, R.G. Prinn, R.H.J. Wang, and R.F. Weiss, Global emissions of perfluorocyclobutane (PFC-318, c-C4F8) resulting from the use of hydrochlorofluorocarbon-22 (HCFC-22) feedstock to produce polytetrafluoroethylene (PTFE) and related fluorochemicals, ***Atmos. Chem. Phys., 22***(5), 3371-3378, doi:10.5194/acp-22-3371-2022, 2022.

Neale, R.E., P.W. Barnes, T.M. Robson, P.J. Neale, C.E. Williamson, R.G. Zepp, S.R. Wilson, S. Madronich, A.L. Andrady, A.M. Heikkilä, G.H. Bernhard, A.F. Bais, P.J. Aucamp, A.T. Banaszak, J.F. Bornman, L.S. Bruckman, S.N. Byrne, B. Foereid, D.P. Häder, L.M. Hollestein, W.C. Hou, S. Hylander, M.A.K. Jansen, A.R. Klekociuk, J.B. Liley, J. Longstreth, R.M. Lucas, J. Martinez-Abaigar, K. McNeill, C.M. Olsen, K.K. Pandey, L.E. Rhodes, S.A. Robinson, K.C. Rose, T. Schikowski, K.R. Solomon, B. Sulzberger, J.E. Ukpebor, Q.W. Wang, S.Å. Wängberg, C.C. White, S. Yazar, A.R. Young, P.J. Young, L. Zhu, and M. Zhu, Environmental effects of stratospheric ozone depletion, UV radiation, and interactions with climate change: UNEP Environmental Effects Assessment Panel, Update 2020, ***Photochem. Photobiol. Sci.***, ***20***(1), 1-67, doi:10.1007/s43630-020-00001-x, 2021.

Newman, P.A., J.S. Daniel, D.W. Waugh, and E.R. Nash, A new formulation of equivalent effective stratospheric chlorine (EESC), ***Atmos. Chem. Phys., 7***(17), 4537-4552, doi:10.5194/acp-7-4537-2007, 2007.

O'Connor, F.M., N.L. Abraham, M. Dalvi, G.A. Folberth, P.T. Griffiths, C. Hardacre, B.T. Johnson, R. Kahana, J. Keeble, B. Kim, O. Morgenstern, J.P. Mulcahy, M. Richardson, E. Robertson, J. Seo, S. Shim, J.C. Teixeira, S.T. Turnock, J. Williams, A.J. Wiltshire, S. Woodward, and G. Zeng, Assessment of pre-industrial to present-day anthropogenic climate forcing in UKESM1, ***Atmos. Chem. Phys.***, ***21***(2), 12111243, doi:10.5194/acp-21-1211-2021, 2021.

Ohneiser, K., A. Ansmann, A. Chudnovsky, R. Engelmann, C. Ritter, I. Veselovskii, H. Baars, H. Gebauer, H. Griesche, M. Radenz, J. Hofer, D. Althausen, S. Dahlke, and M. Maturilli, The unexpected smoke layer in the High Arctic winter stratosphere during MOSAiC 2019–2020, ***Atmos. Chem. Phys.***, ***21***(20), 15783-15808, doi:10.5194/acp-21-15783-2021, 2021.

Oram, D.E., M.J. Ashfold, J.C. Laube, L.J. Gooch, S. Humphrey, W.T. Sturges, E. Leedham-Elvidge, G.L. Forster, N.R.P. Harris, M.I. Mead, A.A. Samah, S.M. Phang, C.F. Ou-Yang, N.H. Lin, J.L. Wang, A.K. Baker, C.A.M. Brenninkmeijer, and D. Sherry, A growing threat to the ozone layer from short-lived anthropogenic chlorocarbons, ***Atmos. Chem. Phys., 17***(19), 11929-11941, doi:10.5194/acp-17-11929-2017, 2017.

Paulot, F., D. Paynter, V. Naik, S. Malyshev, R. Menzel, and L.W. Horowitz, Global modeling of hydrogen using GFDL-AM4.1: Sensitivity of soil removal and radiative forcing, ***Int. J. Hydrog. Energy***, ***46***(24), 13446-13460, doi:10.1016/j.ijhydene.2021.01.088, 2021.

Pisso, I., P.H. Haynes, and K.S. Law, Emission location dependent ozone depletion potentials for very short-lived halogenated species, ***Atmos. Chem. Phys., 10***(24), 12025-12036, doi:10.5194/acp-10-12025-2010, 2010.

Qian, S., D. Nasuta, A. Rhoads, Y. Wang, Y. Geng, Y. Hwang, R. Radermacher, and I. Takeuchi, Not-in-kind cooling technologies: A quantitative comparison of refrigerants and system performance, ***Int. J. Refrig., 62***, 177-192, doi:10.1016/j.ijrefrig.2015.10.019, 2016.

Quack, B., and D.W.R. Wallace, Air-sea flux of bromoform: Controls, rates, and implications, ***Global Biogeochem. Cycles***, ***17***(1), doi:10.1029/2002GB001890, 2003.

Rieger, L.A., W.J. Randel, A.E. Bourassa, and S. Solomon, Stratospheric Temperature and Ozone Anomalies Associated With the 2020 Australian New Year Fires, ***Geophys. Res. Lett., 48***(24), e2021GL095898, doi:10.1029/2021GL095898, 2021.

Rigby, M., S. Park, T. Saito, L.M. Western, A.L. Redington, X. Fang, S. Henne, A.J. Manning, R.G. Prinn, G.S. Dutton, P.J. Fraser, A.L. Ganesan, B.D. Hall, C.M. Harth, J. Kim, K.R. Kim, P.B. Krummel, T. Lee, S. Li, Q. Liang, M.F. Lunt, S.A. Montzka, J. Mühle, S. O'Doherty, M.K. Park, S. Reimann, P.K. Salameh, P. Simmonds, R.L. Tunnicliffe, R.F. Weiss, Y. Yokouchi, and D. Young, Increase in CFC-11 emissions from eastern China based on atmospheric observations, ***Nature***, ***569***(7757), 546-550, doi:10.1038/s41586-019-1193-4, 2019.

Rogelj, J., A. Popp, K.V. Calvin, G. Luderer, J. Emmerling, D. Gernaat, S. Fujimori, J. Strefler, T. Hasegawa, G. Marangoni, V. Krey, E. Kriegler, K. Riahi, D.P. van Vuuren, J. Doelman, L. Drouet, J. Edmonds, O. Fricko, M. Harmsen, P. Havlík, F. Humpenöder, E. Stehfest, and M. Tavoni, Scenarios towards limiting global mean temperature increase below 1.5 °C, ***Nat. Clim. Change***, ***8***(4), 325-332, doi:10.1038/s41558-018-0091-3, 2018.

Ross, M.N., M.Y. Danilin, D.K. Weisenstein, and M.K.W. Ko, Ozone depletion caused by NO and H2O emissions from hydrazine-fueled rockets, ***J. Geophys. Res., 109***(D21), doi:10.1029/2003JD004370, 2004.

Ross, M.N., and K.L. Jones, Implications of a growing spaceflight industry: Climate change, ***J. Space Saf. Eng.***, doi:10.1016/j.jsse.2022.04.004, 2022.

Ryan, R.G., E.A. Marais, C.J. Balhatchet, and S.D. Eastham, Impact of Rocket Launch and Space Debris Air Pollutant Emissions on Stratospheric Ozone and Global Climate, ***Earths Future***, ***10***(6), e2021EF002612, doi:https://doi.org/10.1029/2021EF002612, 2022.

Say, D., A.L. Ganesan, M.F. Lunt, M. Rigby, S. O'Doherty, C. Harth, A.J. Manning, P.B. Krummel, and S. Bauguitte, Emissions of halocarbons from India inferred through atmospheric measurements, ***Atmos. Chem. Phys.***, ***19***(15), 9865-9885, doi:10.5194/acp-19-9865-2019, 2019.

Schoenenberger, F., M.K. Vollmer, M. Rigby, M. Hill, P.J. Fraser, P.B. Krummel, R.L. Langenfelds, T.S. Rhee, T. Peter, and S. Reimann, First observations, trends, and emissions of HCFC-31 (CH2ClF) in the global atmosphere, ***Geophys. Res. Lett., 42***(18), 7817-7824, doi:10.1002/2015GL064709, 2015.

Scott, B.F., R.W. Macdonald, K. Kannan, A. Fisk, A. Witter, N. Yamashita, L. Durham, C. Spencer, and D.C.G. Muir, Trifluoroacetate Profiles in the Arctic, Atlantic,

and Pacific Oceans, ***Environ. Sci. Technol.***, ***39***(17), 6555-6560, doi:10.1021/es047975u, 2005.

Sherry, D., A. McCulloch, Q. Liang, S. Reimann, and P.A. Newman, Current sources of carbon tetrachloride (CCl_4) in our atmosphere, ***Environ. Res. Lett.***, ***13***(2), 024004, doi:10.1088/1748-9326/aa9c87, 2018.

Simmonds, P.G., M. Rigby, A. McCulloch, M.K. Vollmer, S. Henne, J. Mühle, S. O'Doherty, A.J. Manning, P.B. Krummel, P.J. Fraser, D. Young, R.F. Weiss, P.K. Salameh, C.M. Harth, S. Reimann, C.M. Trudinger, L.P. Steele, R.H.J. Wang, D.J. Ivy, R.G. Prinn, B. Mitrevski, and D.M. Etheridge, Recent increases in the atmospheric growth rate and emissions of HFC-23 (CHF_3) and the link to HCFC-22 ($CHClF_2$) production, ***Atmos. Chem. Phys.***, ***18***(6), 4153-4169, doi:10.5194/acp-18-4153-2018, 2018.

Solomon, K.R., G.J.M. Velders, S.R. Wilson, S. Madronich, J. Longstreth, P.J. Aucamp, and J.F. Bornman, Sources, fates, toxicity, and risks of trifluoroacetic acid and its salts: Relevance to substances regulated under the Montreal and Kyoto Protocols, ***J. Toxicol. Environ. Health B***, ***19***(7), 289-304, doi:10.1080/10937404.2016.1175981, 2016.

Solomon, S., K. Dube, K. Stone, P. Yu, D. Kinnison, O.B. Toon, S.E. Strahan, K.H. Rosenlof, R. Portmann, S. Davis, W. Randel, P. Bernath, C. Boone, C.G. Bardeen, A. Bourassa, D. Zawada, and D. Degenstein, On the stratospheric chemistry of midlatitude wildfire smoke, ***Proc. Natl. Acad. Sci.***, ***119***(10), e2117325119, doi:10.1073/pnas.2117325119, 2022.

SPARC (Stratosphere-troposphere Processes And their Role in Climate), ***SPARC Report on the Lifetimes of Stratospheric Ozone-Depleting Substances, Their Replacements, and Related Species***, edited by M.K.W. Ko, P.A. Newman, S. Reimann, and S.E. Strahan, SPARC Report No. 6, WCRP-15/2013, [available at: https://www.sparc-climate.org/fileadmin/customer/6_Publications/SPARC_reports_PDF/6_SPARC_LifetimeReport_Web.pdf], 2013.

SPARC (Stratosphere-troposphere Processes And their Role in Climate), ***SPARC Report on the Mystery of Carbon Tetrachloride***, edited by Q. Liang, P.A. Newman, and S. Reimann, SPARC Report No. 7, WCRP-13/2016, [available at: https://www.wcrp-climate.org/WCRP-publications/2016/SPARC_Report7_2016.pdf], 2016.

Stanley, K.M., D. Say, J. Mühle, C.M. Harth, P.B. Krummel, D. Young, S.J. O'Doherty, P.K. Salameh, P.G. Simmonds, R.F. Weiss, R.G. Prinn, P.J. Fraser, and M. Rigby, Increase in global emissions of HFC-23 despite near-total expected reductions, ***Nat. Comm.***, ***11***(1), 397, doi:10.1038/s41467-019-13899-4, 2020.

Sung, D.J., D.J. Moon, J. Kim, S. Moon, and S.-I. Hong, Production of TFE by catalytic pyrolysis of chloro-difluoromethane (CHC1F2), ***Stud. Surf. Sci. Catal.***, ***159***, 233–236, doi:10.1016/S0167-2991(06)81576-4, 2006.

Szopa, S., V. Naik, B. Adhikary, P. Artaxo, T. Berntsen, W.D. Collins, S. Fuzzi, L. Gallardo, A. Kiendler-Scharr, Z. Klimont, H. Liao, N. Unger, and P. Zanis, Short-Lived Climate Forcers. In Climate Change 2021: The Physical Science Basis. Contribution of Working Group I to the Sixth Assessment Report of the Intergovernmental Panel on Climate Change [Masson-Delmotte, V., P. Zhai, A. Pirani, S.L. Connors, C. Péan, S. Berger, N. Caud, Y. Chen, L. Goldfarb, M.I. Gomis, M. Huang, K. Leitzell, E. Lonnoy, J.B.R. Matthews, T.K. Maycock, T. Waterfield, O. Yelekçi, R. Yu, and B. Zhou (eds.)]. Cambridge University Press, Cambridge, United Kingdom and New York, NY, USA, pp. 817–922, doi:10.1017/9781009157896.008, 2021.

TEAP (Technology and Economic Assessment Panel), ***Decision XXIX/4 TEAP Task Force Report on destruction technologies for controlled substances - Addendum to the May 2018 Supplemental Report,*** United Nations Environment Programme, Vol. 1, ISBN: 978-9966-076-44-1, Nairobi, Kenya, [available at: https://ozone.unep.org/science/assessment/teap], 2018a.

TEAP (Technology and Economic Assessment Panel), ***2018 Report of the Refrigeration, Air Conditioning and Heat Pumps Technical Options Committee***, United Nations Environment Programme, ISBN: 978-9966-076-58-8, Nairobi, Kenya, [available at: https://ozone.unep.org/sites/default/files/2019-04/RTOC-assessment-report-2018_0.pdf], 2018b.

TEAP (Technology and Economic Assessment Panel), ***Report of the Halons Technical Options Committee December 2018***, United Nations Environment Programme, Vol. 1, ISBN: 978-9966-076-48-9, Nairobi, Kenya, [available at: https://ozone.unep.org/sites/default/files/assessment_panels/HTOC_assessment_2018.pdf], 2018c.

TEAP (Technology and Economic Assessment Panel), ***Report of the Technology and Economic Assessment Panel: Progress Report***, United Nations Environment Programme, Vol. 1, ISBN: 978-9966-076-83-0, Nairobi, Kenya, [available at: https://ozone.unep.org/sites/default/files/2020-06/TEAP-Progress-report-and-response-decXXXI-8-may2020_0.pdf], 2020.

TEAP (Technology and Economic Assessment Panel), ***Evaluation of 2021 Critical Use Nominations for Methyl Bromide and Related Issues: Final Report***, United Nations Environment Programme, Vol. 5, ISBN: 978-9966-076-92-2, Nairobi, Kenya, [available at: https://ozone.unep.org/system/files/documents/TEAP-CUN-final-report-september-2021.pdf], 2021a.

TEAP (Technology and Economic Assessment Panel), ***Decision XXXI/3 TEAP Task Force Report on Unexpected Emissions of Trichlorofluoromethane (CFC-11)***, United Nations Environment Programme, Vol. 3, ISBN: 978-9966-076-89-2, Nairobi, Kenya, [available at: https://ozone.unep.org/system/files/documents/Final_TEAP-DecisionXXXI-3-TF-Unexpected-Emissions-of-CFC-11-may2021.pdf], 2021b.

TEAP (Technology and Economic Assessment Panel), ***Report of the Refrigeration Technical Options Committee Vaccines Cold Chain Subcommittee***, Addendum to the TEAP 2021 Progress Report, United Nations Environment Programme, ISBN: 978-9966-076-90-8, Nairobi, Kenya, [available at: https://ozone.unep.org/system/files/documents/TEAP-RTOC-technical-note-vaccines-cold-chain.pdf], 2021c.

Thornhill, G.D., W.J. Collins, R.J. Kramer, D. Olivié, R.B. Skeie, F.M. O'Connor, N.L. Abraham, R. Checa-Garcia, S.E. Bauer, M. Deushi, L.K. Emmons, P.M. Forster, L.W. Horowitz, B. Johnson, J. Keeble, J.F. Lamarque, M. Michou, M.J. Mills, J.P. Mulcahy, G. Myhre, P. Nabat, V. Naik, N. Oshima, M. Schulz, C.J. Smith, T. Takemura, S. Tilmes, T. Wu, G. Zeng, and J. Zhang, Effective radiative forcing from emissions of reactive gases and aerosols – a multi-model comparison, ***Atmos. Chem. Phys.***, ***21***(2), 853-874, doi:10.5194/acp-21-853-2021, 2021.

Tromp, T.K., R.-L. Shia, M. Allen, J.M. Eiler, and Y.L. Yung, Potential Environmental Impact of a Hydrogen Economy on the Stratosphere, ***Science***, ***300***(5626), 1740-1742, doi:10.1126/science.1085169, 2003.

UNEP (United Nations Environment Programme), ***Assessment of Alternatives to HCFCs and HFCs and Update of the TEAP 2005 Supplement Report Data***, Report of the UNEP Technology and Economic Assessment Panel, Task Force Decision XX/8 Report, 129 pp, Nairobi, Kenya, [available at: https://ozone.unep.org/system/files/documents/teap-may-2009-decisionXX-8-task-force-report.pdf], 2009.

UNEP (United Nations Environment Programme), ***Amendment to the Montreal Protocol on Substances that Deplete the Ozone Layer***, United Nations Environment Programme, Kigali, Rwanda, [available at: https://treaties.un.org/Pages/ViewDetails.aspx?src=IND&mtdsg_no=XXVII-2-f&chapter=27&clang=_en], 2016.

UNEP, Production and consumption of ozone depleting substances under the Montreal Protocol, Nairobi, Kenya, http://ozone.unep.org/en/data-reporting/data-centre, (United Nations Environment Programme), 2020.

UNEP (United Nations Environment Programme), ***Report of the Technology and Economic Assessment Panel: Progress Report***, United Nations Environment Programme, Vol. 1, 127 pp., ISBN: 978-9966-076-91-5, Nairobi, Kenya, [available at: https://ozone.unep.org/system/files/documents/TEAP-2021-Progress-report.pdf], 2021.

van Ruijven, B., J.-F. Lamarque, D.P. van Vuuren, T. Kram, and H. Eerens, Emission scenarios for a global hydrogen economy and the consequences for global air pollution, ***Glob. Environ. Change***, ***21***(3), 983-994, doi:10.1016/j.gloenvcha.2011.03.013, 2011.

Velders, G.J.M., and J.S. Daniel, Uncertainty analysis of projections of ozone-depleting substances: Mixing ratios, EESC, ODPs, and GWPs, ***Atmos. Chem. Phys.***, ***14***(6), 2757-2776, doi:10.5194/acp-14-2757-2014, 2014.

Velders, G.J.M., J.S. Daniel, S.A. Montzka, I. Vimont, M. Rigby, P.B. Krummel, J. Muhle, S. O'Doherty, R.G. Prinn, R.F. Weiss, and D. Young, Projections of hydrofluorocarbon (HFC) emissions and the resulting global warming based on recent trends in observed abundances and current policies, ***Atmos. Chem. Phys.***, ***22***(9), 6087-6101, doi:10.5194/acp-22-6087-2022, 2022.

Vogel, B., T. Feck, and J.-U. Grooß, Impact of stratospheric water vapor enhancements caused by CH_4 and H_2O increase on polar ozone loss, ***J. Geophys. Res.***, ***116***(D5), doi:10.1029/2010JD014234, 2011.

Voigt, C., U. Schumann, K. Graf, and K.-D. Gottschaldt, Impact of rocket exhaust plumes on atmospheric composition and climate, Progres in Propulsion Physics, ***4***, 657-670, doi:10.1051/eucass/201304657, 2013.

Vollmer, M.K., J. Mühle, S. Henne, D. Young, M. Rigby, B. Mitrevski, S. Park, C.R. Lunder, T.S. Rhee, C.M. Harth, M. Hill, R.L. Langenfelds, M. Guillevic, P.M. Schlauri, O. Hermansen, J. Arduini, R.H.J. Wang, P.K. Salameh, M. Maione, P.B. Krummel, S. Reimann, S. O'Doherty, P.G. Simmonds, P.J. Fraser, R.G. Prinn, R.F. Weiss, and L.P. Steele, Unexpected nascent atmospheric emissions of three ozone-depleting hydrochlorofluorocarbons, ***Proc. Natl. Acad. Sci.***, ***118***(5), e2010914118, doi:10.1073/pnas.2010914118, 2021.

Vollmer, M.K., D. Young, C.M. Trudinger, J. Mühle, S. Henne, M. Rigby, S. Park, S.

Li, M. Guillevic, B. Mitrevski, C.M. Harth, B.R. Miller, S. Reimann, B. Yao, L.P. Steele, S.A. Wyss, C.R. Lunder, J. Arduini, A. McCulloch, S. Wu, T.S. Rhee, R.H.J. Wang, P.K. Salameh, O. Hermansen, M. Hill, R.L. Langenfelds, D. Ivy, S. O'Doherty, P.B. Krummel, M. Maione, D.M. Etheridge, L. Zhou, P.J. Fraser, R.G. Prinn, R.F. Weiss, and P.G. Simmonds, Atmospheric histories and emissions of chlorofluorocarbons CFC-13 ($CClF_3$), ΣCFC-114 (C_2Cl2F_4), and CFC-115 (C_2ClF_5), ***Atmos. Chem. Phys.***, ***18***(2), 979-1002, doi:10.5194/acp-18-979-2018, 2018.

Wallington, T.J., W.F. Schneider, D.R. Worsnop, O.J. Nielsen, J. Sehested, W. DeBruyn, and J.A. Shorter, Atmospheric chemistry and environmental impact of CFC replacements: HFCs and HCFCs, ***Environ. Sci. Technol.***, ***28***(7), 320A-326A, doi:10.1021/es00056a002, 1994.

Wang, D., W. Jia, S.C. Olsen, D.J. Wuebbles, M.K. Dubey, and A.A. Rockett, Impact of a future H_2 based road transportation sector on the composition and chemistry of the atmosphere; Part 2: Stratospheric ozone, ***Atmos. Chem. Phys., 13***(13), 6139-6150, doi:10.5194/acp-13-6139-2013, 2013.

Wang, Z., Y. Wang, J. Li, S. Henne, B. Zhang, J. Hu, and J. Zhang, Impacts of the Degradation of 2,3,3,3-Tetrafluoropropene into Trifluoroacetic Acid from Its Application in Automobile Air Conditioners in China, the United States, and Europe, ***Environ. Sci. Technol., 52***(5), 2819-2826, doi:10.1021/acs.est.7b05960, 2018.

Warwick, N.J., S. Bekki, E.G. Nisbet, and J.A. Pyle, Impact of a hydrogen economy on the stratosphere and troposphere studied in a 2-D model, ***Geophys. Res. Lett., 31***(5), doi:10.1029/2003GL019224, 2004.

Weisenstein, D.K., D.W. Keith, and J.A. Dykema, Solar geoengineering using solid aerosol in the stratosphere, ***Atmos. Chem. Phys.***, ***15***(20), 11835-11859, doi:10.5194/acp-15-11835-2015, 2015.

WMO (World Meteorological Organization), Scientific Assessment of Ozone Depletion: 2010, Global Ozone Research and Monitoring Project–Report No. 52, 516 pp., Geneva, Switzerland, 2011.

WMO (World Meteorological Organization), Scientific Assessment of Ozone Depletion: 2014, Global Ozone Research and Monitoring Project–Report No. 55, 416 pp., Geneva, Switzerland, 2014.

WMO (World Meteorological Organization), Scientific Assessment of Ozone Depletion: 2018, Global Ozone Research and Monitoring Project–Report No. 58, 588 pp., Geneva, Switzerland, 2018.

WMO (World Meteorological Organization), Report on the Unexpected Emissions of CFC-11, Ozone Re-search and Monitoring, WMO-No. 1268, 84 pp., Geneva, Switzerland, 2021.

Yokouchi, Y., Y. Nojiri, D. Toom-Sauntry, P. Fraser, Y. Inuzuka, H. Tanimoto, H. Nara, R. Murakami, and H. Mukai, Long-term variation of atmospheric methyl iodide and its link to global environmental change, ***Geophys. Res. Lett., 39***(23), doi:10.1029/2012GL053695, 2012.

Youn, D., K.O. Patten, D.J. Wuebbles, H. Lee, and C.W. So, Potential impact of iodinated replacement compounds CF_3I and CH_3I on atmospheric ozone: a three-dimensional modeling study, ***Atmos. Chem. Phys.***, ***10***(20), 10129-10144, doi:10.5194/acp-10-10129-2010, 2010.

Zeng, L., J. Dang, H. Guo, X. Lyu, I.J. Simpson, S. Meinardi, Y. Wang, L. Zhang, and D.R. Blake, Long-term temporal variations and source changes of halocarbons in the Greater Pearl River Delta region, China, ***Atmos. Environ.***, ***234***, 117550, doi:10.1016/j.atmosenv.2020.117550, 2020.

Zhang, J., D.J. Wuebbles, D.E. Kinnison, and A. Saiz-Lopez, Revising the Ozone Depletion Potentials Metric for Short-Lived Chemicals Such as CF_3I and CH_3I, ***J. Geophys. Res.***, ***125***(9), e2020JD032414, doi:10.1029/2020JD032414, 2020.

Ziska, F., B. Quack, S. Tegtmeier, I. Stemmler, and K. Krüger, Future emissions of marine halogenated very-short lived substances under climate change, ***J. of Atmos. Chem., 74***(2), 245-260, doi:10.1007/s10874-016-9355-3, 2017.